

**AGE ESTIMATION FROM ACETABULUM AND  
FEMORAL HEAD USING DIGITAL IMAGE  
PROCESSING TECHNIQUES**



**SUPACHARD KRUDTONG**

**DOCTOR OF PHILOSOPHY**

**IN BIOMEDICAL ENGINEERING**

ลิขสิทธิ์มหาวิทยาลัยเชียงใหม่  
Copyright© by Chiang Mai University  
All rights reserved

**CHIANG MAI UNIVERSITY**

**AUGUST 2024**

**AGE ESTIMATION FROM ACETABULUM AND  
FEMORAL HEAD USING DIGITAL IMAGE  
PROCESSING TECHNIQUES**

**SUPACHARD KRUDTONG**

**DOCTOR OF PHILOSOPHY**

**IN BIOMEDICAL ENGINEERING**

ลิขสิทธิ์มหาวิทยาลัยเชียงใหม่  
Copyright© by Chiang Mai University  
All rights reserved

**CHIANG MAI UNIVERSITY**

**AUGUST 2024**

**AGE ESTIMATION FROM ACETABULUM AND FEMORAL HEAD  
USING DIGITAL IMAGE PROCESSING TECHNIQUES**



**SUPACHARD KRUDTONG**

**A THESIS SUBMITTED TO CHIANG MAI UNIVERSITY IN PARTIAL  
FULFILLMENT OF THE REQUIREMENTS FOR THE DEGREE OF  
DOCTOR OF PHILOSOPHY  
IN BIOMEDICAL ENGINEERING**

ลิขสิทธิ์มหาวิทยาลัยเชียงใหม่  
Copyright© by Chiang Mai University  
All rights reserved

**CHIANG MAI UNIVERSITY**


**AUGUST 2024**


**AGE ESTIMATION FROM ACETABULUM AND FEMORAL HEAD  
USING DIGITAL IMAGE PROCESSING TECHNIQUES**

SUPACHARD KRUDTONG

THIS THESIS HAS BEEN APPROVED TO BE A PARTIAL FULFILLMENT OF  
THE REQUIREMENTS FOR THE DEGREE OF  
DOCTOR OF PHILOSOPHY  
IN BIOMEDICAL ENGINEERING

**Examination Committee:**

 ..... Chairman  
(Asst. Prof. Dr. Parkpoom Jarupoom)

 ..... Member  
(Prof. Pasuk Mahakkanukrauh, M.D.)

 ..... Member  
(Prof. Dr. Nipon Theera-Umpon)

 ..... Member  
(Assoc. Prof. Apichat Sinthubua)

 ..... Member  
(Asst. Prof. Dr. Sukon Prasitwattanaseree)

**Advisory Committee:**

 ..... Advisor  
(Prof. Pasuk Mahakkanukrauh, M.D.)

 ..... Co-advisor  
(Prof. Dr. Nipon Theera-Umpon)

 ..... Co-advisor  
(Assoc. Prof. Apichat Sinthubua)

29 August 2024

Copyright © by Chiang Mai University

## ACKNOWLEDGEMENT

I would like to express my deepest gratitude to my advisor, Professor (distinguished) Pasuk Mahakkanukrauh, MD., for her unwavering support, guidance, and encouragement throughout my journey. Her expertise and insights have been invaluable to my research.

I am also grateful to the members of my dissertation committee, Asst. Prof. Dr. Parkpoom Jarupoom, Professor Dr. Nipon Theera-Umpon, Assoc. Prof. Apichat Sinthubua and Asst. Prof. Dr. Sukon Prasitwattanaseree, for their constructive feedback and suggestions, which have significantly improved the quality of my work.

Special thanks to my colleagues and friends in the Forensic Osteology Research Center (FORC) for their camaraderie and assistance. Their support has made this journey more enjoyable and fulfilling.

Lastly, I am deeply indebted to my family for their endless love, patience, and encouragement. Their belief in me has been my greatest source of strength.

Supachard Krudtong

ลิขสิทธิ์มหาวิทยาลัยเชียงใหม่  
Copyright© by Chiang Mai University  
All rights reserved

หัวข้อคุณิพนธ์	การประเมินอายุจากอะเซตาบูลัมและฟีเมอร์อลเฮดด้วยเทคนิคการประมวลผลภาพดิจิทัล	
ผู้เขียน	นายศุภชาติ กรุดทอง	
ปริญญา	ปรัชญาคุษฎีบัณฑิต (วิศวกรรมชีวการแพทย์)	
คณะกรรมการที่ปรึกษา	ศ.(เชี่ยวชาญพิเศษ)พญ.ผาศุภ มหรรฆานุเคราะห์ ศ. ดร. นิพนธ์ ธีรอำพน รศ. อภิชาติ ลินธูปัว	อาจารย์ที่ปรึกษาหลัก อาจารย์ที่ปรึกษาร่วม อาจารย์ที่ปรึกษาร่วม

## บทคัดย่อ

การระบุตัวตนของโครงกระดูกมนุษย์เป็นเรื่องที่มีความสำคัญอย่างยิ่ง โดยเฉพาะอย่างยิ่งการประเมินอายุกระดูกเมื่อเสียชีวิตซึ่งเป็นหนึ่งในปัจจัยหลัก ข้อต่อสะโพกที่ประกอบด้วยเบ้ากระดูกสะโพก (acetabulum) และหัวกระดูกต้นขา (femoral head) เป็นส่วนสำคัญ เบ้ากระดูกสะโพกเป็นหนึ่งในองค์ประกอบของโครงกระดูกที่คงสภาพได้ดีที่สุด การวัดเปอร์เซ็นต์ความพรุนและอัตราส่วนพื้นที่ที่สามารถให้ข้อมูลเชิงลึกเกี่ยวกับอายุของกระดูกได้ การประมาณอายุของกระดูกแบบดั้งเดิมมักดำเนินการโดยผู้เชี่ยวชาญ แต่การส่งตัวอย่างกระดูกไปยังผู้เชี่ยวชาญนั้นมีข้อจำกัด ปัจจุบันเทคนิคการประมวลผลภาพถูกใช้อย่างแพร่หลาย ทำให้การส่งภาพเพื่อการวิเคราะห์จากผู้เชี่ยวชาญเป็นเรื่องง่ายขึ้น งานวิจัยนี้ใช้เทคนิคการประมวลผลภาพเพื่อช่วยในการประมาณอายุของกระดูก โดยใช้ภาพของเบ้ากระดูกสะโพกและหัวกระดูกต้นขาจากประชากรไทย

เก็บตัวอย่างจากโครงกระดูกจำนวน 167 ร่าง ประกอบด้วยผู้หญิง 59 คน อายุระหว่าง 26 ถึง 100 ปี และผู้ชาย 108 คน อายุระหว่าง 26 ถึง 97 ปี โครงกระดูกที่รับบริจาคอยู่ระหว่างปี พ.ศ. 2554 ถึง พ.ศ. 2562 ภาพถ่ายสีถูกแปลงเป็นภาพเฉดสีเทา โดยค่าพิกเซลอยู่ในช่วง 0 ถึง 255 พิกเซลที่มีค่าความเข้มต่ำกว่าค่าที่กำหนดจะถูกจัดเป็นพิกเซลของรูพรุน ในขณะที่พิกเซลที่มีค่าความเข้มสูงกว่าค่าที่กำหนดจะถูกจัดเป็นเนื้อกระดูก เปอร์เซ็นต์ความพรุนของ acetabular fossa ถูกคำนวณจากภาพของเบ้ากระดูกสะโพก และเปอร์เซ็นต์ความพรุนของ fovea capitis ถูกคำนวณจากภาพของหัวกระดูกต้นขา นอกจากนี้ยังมีการคำนวณอัตราส่วนพื้นที่ โดยอัตราส่วนพื้นที่ของเบ้ากระดูกสะโพกถูกคำนวณ

จากอัตราส่วนพื้นที่ของ acetabular fossa ต่อพื้นที่รวมของเบ้ากระดูกสะโพก และอัตราส่วนพื้นที่ของ หัวกระดูกต้นขาถูกคำนวณจากอัตราส่วนพื้นที่ของ fovea capitis ต่อพื้นที่รวมของหัวกระดูกต้นขา ความสัมพันธ์ระหว่างตัวแปรหลักสองตัวนี้และอายุถูกวิเคราะห์โดยใช้วิธีการทางสถิติ

ที่ระดับความเชื่อมั่น 90% หรือระดับนัยสำคัญ  $\alpha = 0.10$  พบความสัมพันธ์ระหว่างเปอร์เซ็นต์ ความพรุนและอายุประเมินในผู้ชาย สมการอายุประเมินสำหรับเบ้ากระดูกสะโพกด้านซ้ายในผู้ชายคือ  $A = 2.2776P - 25.2553$  ( $R^2 = 0.3317$ ) โดยที่ A แทนอายุประเมิน และ P แทนเปอร์เซ็นต์ความพรุน ของกระดูก นอกจากนี้ยังพบความสัมพันธ์ระหว่างอัตราส่วนพื้นที่และอายุประเมินในหัวกระดูกต้นขาทั้งผู้หญิงและผู้ชายทั้งด้านซ้ายและขวา สำหรับหัวกระดูกต้นขาด้านขวาในผู้หญิง สมการประมาณ อายุคือ  $A = 2.6049R + 33.7348$  ( $R^2 = 0.2023$ ) โดยที่ A แทนอายุประเมิน และ R แทนอัตราส่วนพื้นที่ ความคลาดเคลื่อนของสมการเปอร์เซ็นต์ความพรุนและอายุประเมินอยู่ในช่วง 0 ถึง 16 ปี โดยมีความ คลาดเคลื่อนเฉลี่ยอยู่ระหว่าง 5 ถึง 9 ปี ส่วนความคลาดเคลื่อนของสมการอัตราส่วนพื้นที่และอายุ ประเมินอยู่ในช่วง 0 ถึง 36 ปี โดยมีความคลาดเคลื่อนเฉลี่ยอยู่ระหว่าง 8 ถึง 17 ปี ข้อจำกัดที่สำคัญใน กระบวนการนี้คือความสะอาดของกระดูก เนื่องจากมีผลโดยตรงต่อค่าความเข้มของฟิสิกเซล อาจ นำไปสู่อายุประเมินที่คลาดเคลื่อนอย่างมากได้

ลิขสิทธิ์มหาวิทยาลัยเชียงใหม่  
Copyright© by Chiang Mai University  
All rights reserved

<b>Dissertation Title</b>	Age Estimation from Acetabulum and Femoral Head Using Digital Image Processing Techniques	
<b>Author</b>	Mr.Supachard Krudtong	
<b>Degree</b>	Doctor of Philosophy (Biomedical Engineering)	
<b>Advisory Committee</b>	Prof. Pasuk Mahakkanukrauh, M.D.	Advisor
	Prof. Dr. Nipon Theera-Umpon	Co-advisor
	Assoc. Prof. Apichat Sinthubua	Co-advisor

## ABSTRACT

The personal identification of human skeletal remains is of great importance, with age at death being one of the key parameters. The hip joint, which includes the acetabulum and femoral head, is a crucial part of skeletal remains. The acetabulum, in particular, is one of the most well-preserved skeletal elements. Percent porosity and area ratio can provide insights into the age of the bone. Traditionally, age estimation of bones has been conducted by experts, but sending bone samples to specialists has its limitations. Nowadays, image processing techniques are widely used, making it much easier to send images for expert analysis. This research employs image processing techniques to assist in estimating the age of bones, using images of the acetabulum and femoral head from the Thai population.

Samples were collected from 167 skeletons, comprising 59 females aged 26 to 100 years and 108 males aged 26 to 97 years. The skeleton donations were made between 2011 and 2019. Color images were converted to grayscale, with pixel values ranging from 0 to 255. Dark gray pixels with values below a certain threshold were classified as porous pixels, while light gray pixels with values above the threshold were classified as bone pixels. Percent porosity of the acetabular fossa was calculated from acetabulum images, and percent porosity of the fovea capitis was calculated from femoral head images. Area



ratios were also determined. The area ratio of the acetabulum was calculated as the ratio of the acetabular fossa area to the total acetabulum area. The area ratio of the femoral head was calculated as the ratio of the fovea capitis area to the total femoral head area. The interrelationships between these two main variables and age were analyzed using statistical methods.

At a confidence level of 90% or a significance level of  $\alpha = 0.10$ , a relationship exists between percent porosity and estimated age in males. The estimated age equation for the left side of the male acetabulum is  $A = 2.2776P - 25.2553$  ( $R^2 = 0.3317$ ), where A represents the estimated age and P represents percent porosity. There is also a relationship between area ratio and estimated age in the femoral head for both females and males, on both the left and right sides. For the right side of the female femoral head, the estimated age equation is  $A = 2.6049R + 33.7348$  ( $R^2 = 0.2023$ ), where A is the estimated age and R is the area ratio. The errors for percent porosity to estimated age equations range from 0 to 16 years, with average errors between 5 and 9 years. For area ratio to estimated age equations, errors range from 0 to 36 years, with average errors between 8 and 17 years. A significant challenge in this process is the cleanliness of the bones, as it directly affects pixel values, leading to potential inaccuracies.

## CONTENTS

	Page
Acknowledgement	c
Abstract in Thai	d
Abstract in English	f
Contents	h
List of Tables	j
List of Figures	l
Statement of Originality in Thai	o
Statement of Originality in English	p
Chapter 1 Introduction	1
1.1 Objectives and outcomes	3
1.2 Scope of study	3
Chapter 2 Literature Review	4
Chapter 3 Methodology	21
3.1 Introduction	21
3.2 Hip joint	23
3.3 Sample	24

	Page
3.4 Recording images and photography	25
3.5 Digital image processing	27
3.6 Statistics process	32
3.7 Equation audit	33
Chapter 4 Results	35
4.1 Solutions in each group	35
4.1.1 Percent porosity and age	35
4.1.2 Area ratio and age	48
4.2 Solutions of every group	61
4.3 Solution of equations audit	62
Chapter 5 Conclusion and Suggestion	64
5.1 Percent porosity and age relationship	64
5.2 Area ratio and age relationship	65
5.3 Solution of equations audit	66
5.4 Suggestion	66
References	70
Curriculum Vitae	73

## LIST OF TABLES

	Page
Table 2.1 p-Values obtained from pair-wise comparisons of acetabular shape across age groups	13
Table 4.1 Percent porosity and age of female acetabulum left side.	36
Table 4.2 Percent porosity and age of female acetabulum right side.	37
Table 4.3 Percent porosity and age of female acetabulum both sides.	38
Table 4.4 Percent porosity and age of male acetabulum left side.	39
Table 4.5 Percent porosity and age of male acetabulum right side.	40
Table 4.6 Percent porosity and age of male acetabulum both sides.	41
Table 4.7 Percent porosity and age of female femoral head left side.	42
Table 4.8 Percent porosity and age of female femoral head right side.	43
Table 4.9 Percent porosity and age of female femoral head both sides.	44
Table 4.10 Percent porosity and age of male femoral head left side.	45
Table 4.11 Percent porosity and age of male femoral head right side.	46
Table 4.12 Percent porosity and age of male femoral head both sides.	47
Table 4.13 Area ratio and age of female acetabulum left side.	49
Table 4.14 Area ratio and age of female acetabulum right side.	50
Table 4.15 Area ratio and age of female acetabulum both sides.	51
Table 4.16 Area ratio and age of male acetabulum left side.	52
Table 4.17 Area ratio and age of male acetabulum right side.	53
Table 4.18 Area ratio and age of male acetabulum both sides.	54

	Page
Table 4.19 Area ratio and age of female femoral head left side.	55
Table 4.20 Area ratio and age of female femoral head right side.	56
Table 4.21 Area ratio and age of female femoral head both sides.	57
Table 4.22 Area ratio and age of male femoral head left side.	58
Table 4.23 Area ratio and age of male femoral head right side.	59
Table 4.24 Area ratio and age of male femoral head both sides.	60
Table 4.25 Percent porosity and age relationship.	61
Table 4.26 Area ratio and age relationship.	62
Table 4.27 Equations audit of percent porosity and age relationship.	63
Table 4.28 Equations audit of area ratio and age relationship.	63
Table 5.1 Percent porosity and age relationship.	65
Table 5.2 Percent porosity and age non-relationship.	65
Table 5.3 Area ratio and age relationship.	66
Table 5.4 Area ratio and age non-relationship.	66

## LIST OF FIGURES

	Page
Figure 1.1 Acetabulum, acetabular fossa and lunate surface (left), femoral head and fovea capitis (right)	1
Figure 2.1 Histomorphometry determination of the porosity and pore size distribution in bone: (A and C) the photographic image of a bone cross-section, (B and D) the image after process	5
Figure 2.2 Age-related changes and porosity determined by NMR and bone histomorphometry	5
Figure 2.3 Box plot of age relate to porosities of the acetabular fossa at each states	7
Figure 2.4 Reference system in which the sacrum is positioned (left). Example of the profile of the sacral base, with the four variables (right).	8
Figure 2.5 Scanned and cleaned image of the core (pores are shown as black) (left). Relationship between REA and porosity (right).	9
Figure 2.6 Box plot of the actual age of subjects according to overall score (left). Scatter graph showing distribution of scores for subjects aged over 50 (right).	10
Figure 2.7 Histograms (circles) of sample I (a) and II (b) and their approximations (solid lines)	11
Figure 2.8 PCA plot for visualizing shape variation among all female age groups	14
Figure 2.9 Anteroposterior view of the left hip joint	15
Figure 2.10 The fovea capitis femoris (FCF) photographed in face with a reference scale (left). The fovea capitis maximum diameter and the polyline outlining the boundary edges of the FCF (right).	17
Figure 2.11 Image processing workflow employed.	19

	Page
Figure 3.1 Captured image of acetabulum (left). Captured image of femoral head (right).	21
Figure 3.2 Work flow.	22
Figure 3.3 Cropped grayscale image of acetabulum (left). Cropped grayscale image of femoral head (right).	23
Figure 3.4 Right os coxae and acetabulum (left). Right Femur and femoral head.	24
Figure 3.5 Dirty bones.	25
Figure 3.6 Acetabulum photo (left). Femoral head photo (right).	27
Figure 3.7 Grayscale image (left). Grayscale variation (right).	28
Figure 3.8 Edge detection and segmentation.	29
Figure 3.9 Acetabular fossa (left). Lunate surface (right).	30
Figure 3.10 Histogram and statistic values.	31
Figure 3.11 Femoral head and histogram.	32
Figure 4.1 Percent porosity and age of female acetabulum left side.	36
Figure 4.2 Percent porosity and age of female acetabulum right side.	37
Figure 4.3 Percent porosity and age of female acetabulum both sides.	38
Figure 4.4 Percent porosity and age of male acetabulum left side.	39
Figure 4.5 Percent porosity and age of male acetabulum right side.	40
Figure 4.6 Percent porosity and age of male acetabulum both sides.	41
Figure 4.7 Percent porosity and age of female femoral head left side.	42
Figure 4.8 Percent porosity and age of female femoral head right side.	43
Figure 4.9 Percent porosity and age of female femoral head both sides.	44

	Page
Figure 4.10 Percent porosity and age of male femoral head left side.	45
Figure 4.11 Percent porosity and age of male femoral head right side.	46
Figure 4.12 Percent porosity and age of male femoral head both sides.	47
Figure 4.13 Area ratio and age of female acetabulum left side.	49
Figure 4.14 Area ratio and age of female acetabulum right side.	50
Figure 4.15 Area ratio and age of female acetabulum both sides.	51
Figure 4.16 Area ratio and age of male acetabulum left side.	52
Figure 4.17 Area ratio and age of male acetabulum right side.	53
Figure 4.18 Area ratio and age of male acetabulum both sides.	54
Figure 4.19 Area ratio and age of female femoral head left side.	55
Figure 4.20 Area ratio and age of female femoral head right side.	56
Figure 4.21 Area ratio and age of female femoral head both sides.	57
Figure 4.22 Area ratio and age of male femoral head left side.	58
Figure 4.23 Area ratio and age of male femoral head right side.	59
Figure 4.24 Area ratio and age of male femoral head both sides.	60
Figure 5.1 Clear acetabular fossa (left), Unclear acetabular fossa (right).	68



## ข้อความแห่งการริเริ่ม

- 1) วิทยานิพนธ์นี้ได้เสนอวิธีการใหม่ในการประเมินอายุกระดูก โดยใช้เทคนิคการประมวลผลภาพดิจิทัล โดยพิจารณาจากค่าความเข้มแสงของฟิสิกเซลจากภาพถ่ายของกระดูกข้อต่อสะโพก
- 2) กระประเมินความพรุนของกระดูกจากความเข้มแสงของฟิสิกเซล ทำให้ได้ผลประเมินจากมาตรฐานเดียวกัน โดยไม่ขึ้นกับการสังเกตของผู้ประเมินที่อาจให้ผลลัพธ์ที่ขัดแย้งกันได้
- 3) การส่งภาพถ่ายของกระดูกให้ผู้เชี่ยวชาญประเมินอายุ สามารถทำได้ง่ายและรวดเร็วกว่าการส่งกระดูกจริงให้ผู้เชี่ยวชาญมาก ช่วยลดเวลาและค่าใช้จ่ายได้เป็นอย่างมาก

ลิขสิทธิ์มหาวิทยาลัยเชียงใหม่  
Copyright© by Chiang Mai University  
All rights reserved

## STATEMENTS OF ORIGINALITY

1. This thesis proposes a novel method for estimating bone age using digital image processing techniques, focusing on the pixel intensity values from the images of the hip joint bones.
2. The assessment of bone porosity based on pixel intensity values provides a standardized evaluation, eliminating potential discrepancies that may arise from subjective observations by evaluators.
3. Sending bone images for age estimation by experts is significantly easier and faster than sending the actual bones, greatly reducing both time and costs.



ลิขสิทธิ์มหาวิทยาลัยเชียงใหม่  
Copyright© by Chiang Mai University  
All rights reserved

## CHAPTER 1

### Introduction

The personal identification of human skeletal remains is a crucial process performed in every case. To determine if the remains belong to an individual person, various pieces of information need to be assessed, including ethnic background, sex, age, and stature at the time of death. Age at death is particularly significant and can be estimated using different parts of the skeletal remains. Common methods for estimating the age of adult remains include analyzing the pubic symphysis surface, auricular surface of the ilium, sternal rib end, cranial suture closure, and dental wear. The pubic symphysis surface is widely used for estimating adult age [Evison, 2009]. Additionally, the region of the acetabulum (as shown in figure 1.1) is another useful area for estimating age at death in adults [Rissech, 2006]. This region comprises the lunate surface (outer area) and the acetabular fossa (inner area).



Figure 1.1 Acetabulum, acetabular fossa and lunate surface (left), femoral head and fovea capitis (right)

Rissech (2006) conducted a study on the acetabulum to estimate the age at death in adult males from Portugal. In this study, the acetabulum was classified into seven variables. Similarly, Khomkham (2017) also examined the same seven variables as Rissech (2006), but in Thai individuals. One of the variables they both investigated was the porosity of the acetabular fossa. Rissech (2006) categorized the porosities of the acetabular fossa into seven states, ranging from state 0 to state 6, with each state being described. To determine the porosity state of each acetabular fossa, careful observation of the acetabular fossa area is necessary. A team-based approach, as outlined by Evison (2009), is employed to investigate and analyze the skeletal remains. A specialist focuses on the acetabular fossa area and determines the level of porosity. It is worth noting that different specialists may have varying judgments and responses to different states of porosity levels. This variability among specialists can sometimes lead to disagreements regarding the estimated age at death.

A computer program based on image processing is a valuable tool utilized in various medical fields. It aids specialists in working more efficiently and expeditiously. Consistency in using the same image processing approach yields consistent outcomes and reduces discrepancies. The objective of this study is to develop an algorithm based on image processing to calculate the porosity of the acetabular fossa and its correlation with age at death. The program is capable of extracting the lunate surface and acetabular fossa (as depicted in figure 1.1) and calculating the area ratio between them. This area ratio is then analyzed in relation to the age at death. Additionally, the femoral head (also shown in figure 1.1), which is connected to the acetabulum, is considered in this study. The program can extract the femoral head and fovea capitis, calculate the area ratio of the fovea capitis and femoral head, and determine the porosity of the fovea capitis. All calculations are performed with respect to the age at death. The outcome of this study is an image processing program that focuses on the acetabulum and femoral head. The porosity and area ratio obtained from the program are utilized to estimate the age at death.

## **1.1 Objectives and outcomes**

1. A computer program based on image processing to analyze the acetabulum and femoral head.
2. Relationship of porosity and area ratio relate to age at death.

## **1.2 Scope of study**

1. Focus on acetabulum and femoral head both left and right side.
2. The skeletons are from the Forensic Osteology Research Center (FORC) of the Faculty of Medicine, Chiang Mai University, Thailand.
3. The 2D images are taken by digital SLR camera. 55 mm lens, ISO 100, use the electronic flash to record bones in laboratory settings [Buikstra, 1994].
4. Porosity and area ratio are found by using image processing technique.
5. Conduct the mathematic equation to estimate the age at death from 4.

## CHAPTER 2

### Literature Review

In 2003, Xiaodu Wang and their team conducted a study where they utilized low field pulsed nuclear magnetic resonance (NMR) to measure the porosity and pore size distribution in cortical bone [Wang, 2003]. They also applied this technique to detect age-related changes. The efficacy of this technique was compared to data obtained from bone histomorphometry. The study involved collecting samples from 19 mid-diaphysis cadaver femurs ranging from 16 to 89 years of age, including 12 male and 7 female samples. A custom-built 0.5-40 MHz broadband NMR system was used for the measurements, followed by histomorphometry analysis. An image processing software called NIH image was utilized to determine the cross-sectional area of individual pores. The boundaries of each pore in the images were manually outlined using a drawing tool, and the threshold function was applied to remove background noise from the images (see figure 2.1). The cross-sectional area of individual pores was then determined to estimate pore size and a nominal pore size. The results (see figure 2.2) indicated that both NMR and histomorphometry measurements exhibited similar age-dependent changes in bone porosity. However, the porosity results obtained from NMR were greater than those from histomorphometry (see figure 2.2), with a relationship described by the equation  $P_{ohisto} = 0.89P_{oNMR}$ . The results showed that cortical porosity increased from approximately 8% to 28% from young to elderly individuals. The discussion highlighted the applicability of the NMR technique in quantifying cortical porosity and pore size distribution, while also acknowledging certain limitations of the NMR technique. In histomorphometry measurements, errors may occur due to variations in pore orientations.

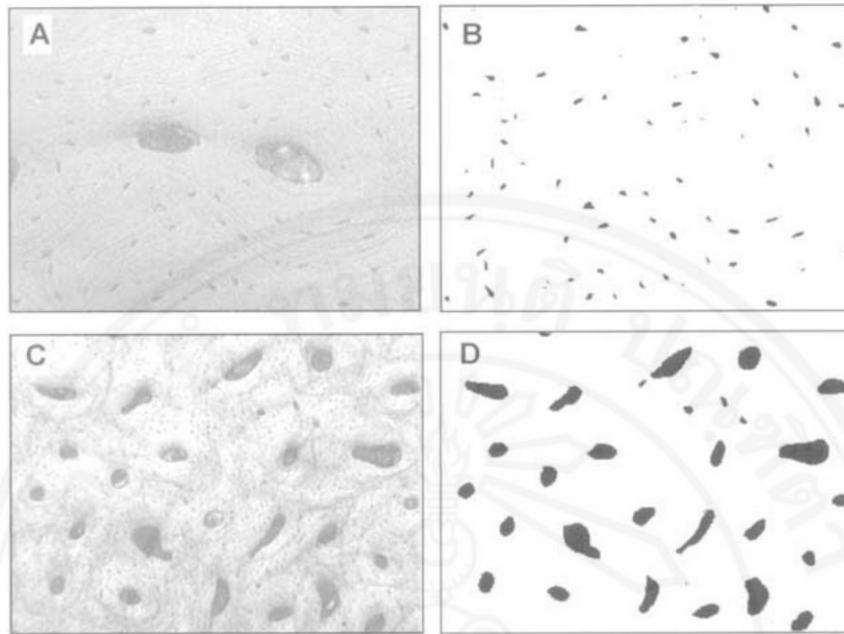


Figure 2.1 Histomorphometry determination of the porosity and pore size distribution in bone: (A and C) the photographic image of a bone cross-section, (B and D) the image after process [Wang, 2003].

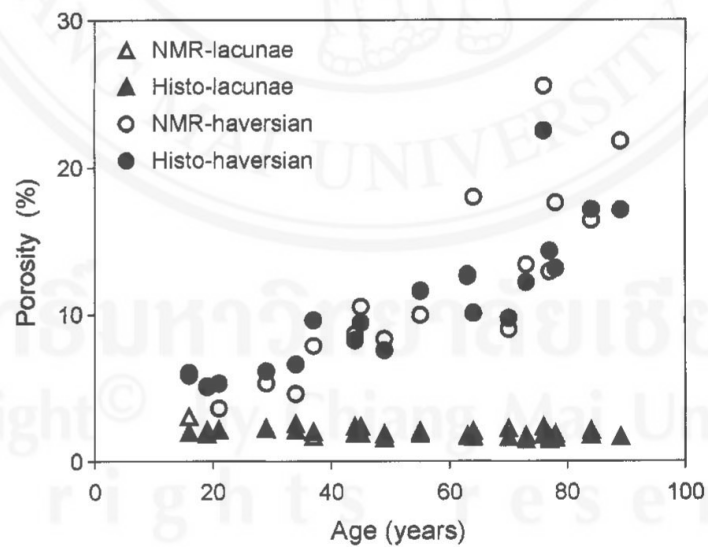


Figure 2.2 Age-related changes and porosity determined by NMR and bone histomorphometry [Wang, 2003].

In 2006, Carme Rissech and a team conducted a study on the acetabulum of adult males to estimate age at death [Rissech, 2006]. They analyzed 242 male individuals ranging in age from 16 to 96 years old, using only the left os coxa. The study focused on the examination of the acetabular region, specifically seven variables including acetabular rim shape, apex activity, and activity of the acetabular fossa. One of the variables studied was the porosities of the acetabular fossa, which were categorized into seven states represented by codes 0 to 6.

The states of porosities were described as follows:

Code 0: dense acetabular fossa

Code 1: acetabular fossa with microporosities

Code 2: microporosities or peripheral trabecular bone

Code 3: macroporosities on the three lobes

Code 4: macroporosities with destruction

Code 5: bone destruction on most of the fossa

Code 6: bone proliferation

To determine the state of each acetabular fossa, a close morphological examination was conducted and the results were correlated with the age at death using box plots (refer to Figure 2.3). The study provided information on the number of specimens, mean, and variance for each state of porosity. Based on the analysis of seven age indicators, the study found that age at death for male specimens could be estimated with an accuracy of 89% in a 10-year interval or 67% in a 5-year interval. The results were also compared to other research studies. It is important to note that the study only included the left os coxa of male individuals, with no inclusion of the right os coxa or female individuals. Additionally, the porosities variable was determined through a close morphological examination of the acetabulum. The presented results are based on observations made during the examination. To evaluate the consistency of the observations, both intra- and interobserver consistencies were quantified. The



appropriateness of the variables and their correlation with age were further examined using the Kruskal-Wallis and Kendal range tests.

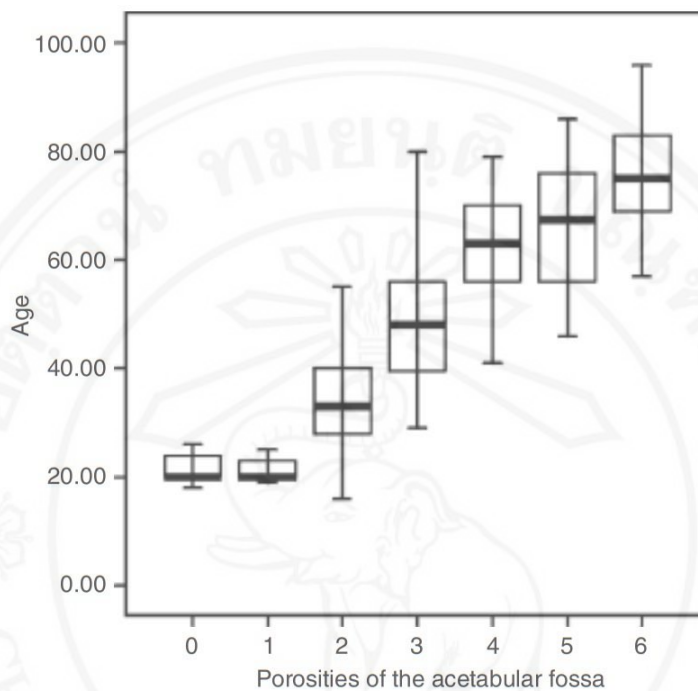


Figure 2.3 Box plot of age relate to porosities of the acetabular fossa at each state [Rissech, 2006].

In 2009, Stefano Benazzi and a team conducted a study on the sacral base to improve sex assessment through image processing techniques [Benazzi, 2009]. The study included samples with an age range of 19 to 70 years old, comprising a total of 114 sacra, with 57 from males and 57 from females. The sacra were obtained from two different Italian populations: Bologna, northern Italy (76 sacra), and Sassari, Sardinia (38 sacra). Photographs of the sacra were taken using a 4.0 megapixels digital camera, fixed at a distance of 300 mm without using zoom. To ensure accurate measurements, a technical drawing software called AutoCAD LT 2.0 was used to create a grid of analogous dimensions. Four metric data points were collected for analysis, including the maximum transverse diameter (m.t.d.), maximum superior breadth (m.s.b.), area of the upper face, and perimeter of the body. The values of m.t.d. and m.s.b. were compared with the 200 mm Mitutoyo digimatic absolute caliper to assess measurement accuracy. Discriminant

analysis was performed using SPSS version 11.5 to analyze the data. Initially, the data from the two different populations were considered separately, and then both intra- and inter-population comparisons were made. The results demonstrated a sex prediction success rate of 88.3%. Additionally, the sex diagnoses determined through the proposed method were compared with those made using the traditional anthropological method, which relies on sexual traits of the skull and pelvis. The discriminant function produced concordant results with the traditional method in 10 out of 12 cases (83.3%). In the discussion, the authors clarified that the proposed method is not intended to replace the traditional anthropological procedures based on sexual traits of the skull and pelvis. Rather, it serves as an additional tool that can be used in conjunction with the traditional approach to enhance sex assessment accuracy.

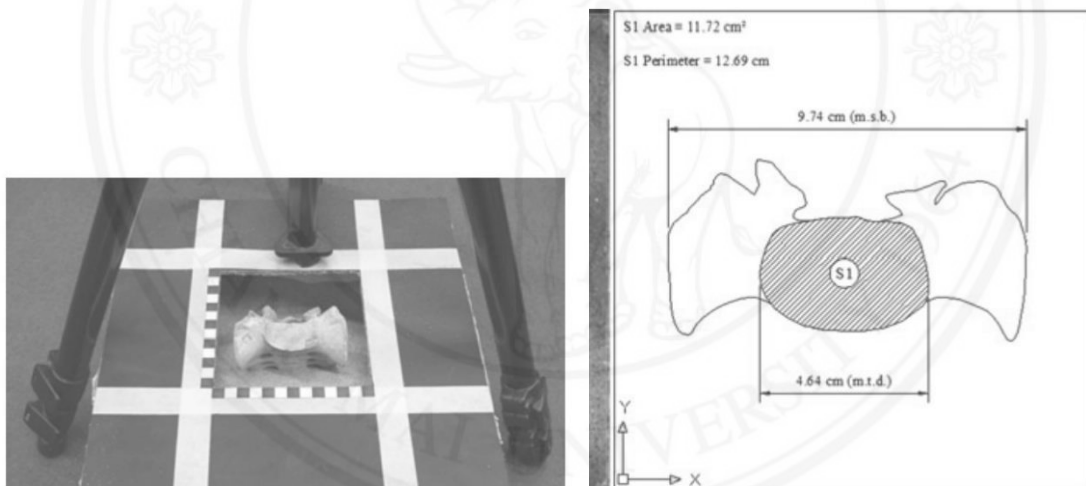


Figure 2.4 Reference system in which the sacrum is positioned (left).

Example of the profile of the sacral base, with the four variables (right). [Benazzi, 2009]

In 2013, William D. Martin III and their team study about Using image analysis to measure the porosity distribution of a porous pavement [Martin III, 2013]. Their study was talked about A method was developed and assessed for determining the distribution of porosity across a porous pavement sample using image analysis. The measured average porosity obtained through this method showed favorable comparisons with other porosity measurement techniques, including two volumetric-based methods and the ASTM D7063 standard, which employs a vacuum sealing device. The study also examined the impact

of the representative elemental area (REA), defined as the minimum pavement cross-sectional area required for a statistically significant measure of porosity. Experimentally, the REA was determined to be 83.9 cm<sup>2</sup> (13 in<sup>2</sup>) for various gradations of porous pavements, specifically ASTM standard gradations No. 89, No. 78, No. 7, and No. 67. While the method is capable of measuring one-dimensional porosity distribution in different orientations (vertical, horizontal, or radial in cylinders), this research focused on its application to vertical porosity distributions. The image analysis results and REA were used to create a smoothed profile of the porosity distribution, revealing that in a porous pavement sample compacted in a single lift, porosity is highest at the surface due to surface texture, decreases sharply to a minimum at a depth of approximately 2–3 cm (1 in), and then increases linearly until about two centimeters from the bottom, where it rises sharply due to wall effects. This porosity distribution aligns with previously proposed distributions.

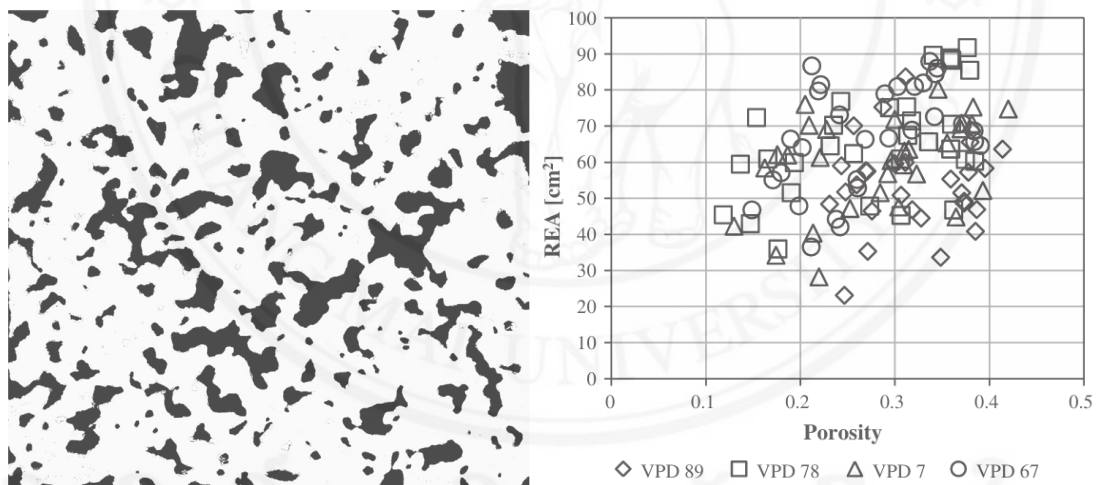


Figure 2.5 Scanned and cleaned image of the core (pores are shown as black) (left). Relationship between REA and porosity (right). [Martin III, 2013]

In 2013, Venara, A. and their team studied about estimation of skeletal age at death in adults using the acetabulum and the auricular surface [Venara, 2013]. The study was conducted on 210 bones (108 male and 102 female) from the Terry Collection. Two observers, one a novice and the other experienced with the technique, analyzed the bones. Age estimation was based on the method described by Rougé-Maillart et al., focusing on the auricular surface and acetabulum. Intra- and inter-observer correlations were

conducted to assess the reliability and reproducibility of this technique in the overall population, followed by an analysis of subjects over 50 years of age. For both observers, the data showed a moderate to strong correlation between the estimated scores and actual ages (overall correlations of 0.648 and 0.773) in the general population. The consistency between the observers' results improved when total scores were used. However, the inter-observer correlation was lower than in the previous study, as some criteria were more challenging for the novice observer to classify. For subjects over 50, the results were less reliable than anticipated, with greater inter-observer variability compared to the general population. This study confirms the reproducibility and effectiveness of the method. However, certain criteria require redefinition, and others may need to be weighted differently. Additionally, a modification to the Bayesian approach, including adjustments to the intervals, should be considered.

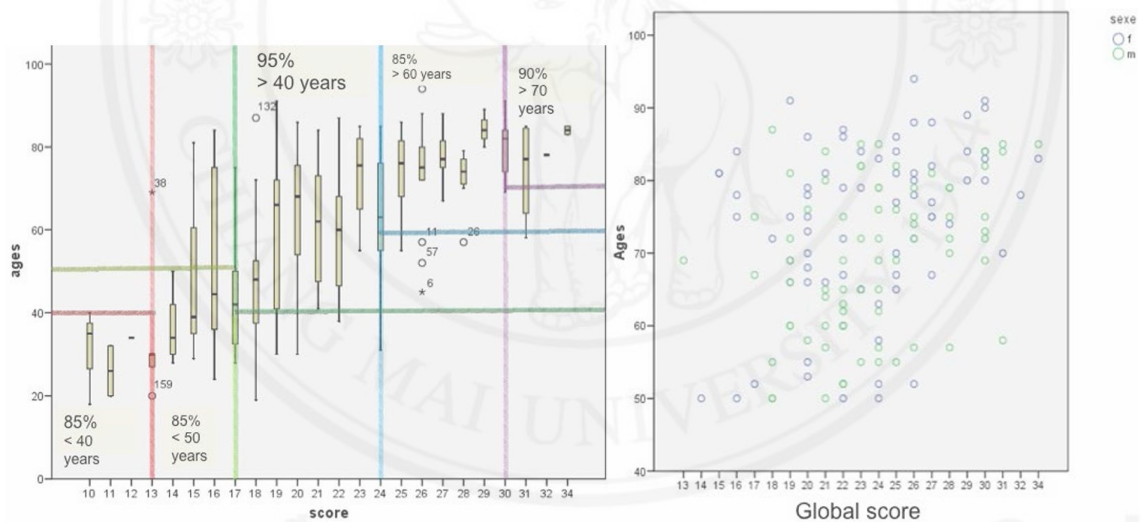


Figure 2.6 Box plot of the actual age of subjects according to overall score (left). Scatter graph showing distribution of scores for subjects aged over 50 (right). [Venara, 2013]

In 2015, M. Cieszko, and their team conducted a study on bone porosity using histograms of 3D  $\mu$ CT images [Cieszko, 2015]. The aim of the study was to present a new method for determining bone porosity and the global image segmentation threshold. Two area samples from the same CT image were selected, and information from the normed histogram was obtained from the CT scan. The results obtained from this new method were compared with the standard method and Otsu's method. The new method

first determined the bone porosity from the histogram of the 3D  $\mu$ CT image. Then, the binarization threshold was calculated to produce a reconstructed binary image of the bone sample. Optimization methods from numerical mathematical computing were used to determine the porosity parameter and the density distribution parameters of pores. In order to optimize the implementation, the mathematical model of the histogram was matched with the histogram of the bone sample scan. The porosity parameter was then calculated using this optimization process, and the approximation error was obtained. Once the porosity parameter was obtained, the binarization threshold was immediately determined. The mathematic model results were presented in Figure 2.4, showing that the approximation error was lower as the voxel density increased. The porosities and binarization thresholds were given at a confidence level of 0.99. In comparison with the standard method and Otsu's method, the proposed method showed very close results for sample I, but the results were not clear for sample II. In sample I, the new method, standard method, and Otsu's method yielded porosity values of 89, 91, and 89, respectively. In sample II, the new method, standard method, and Otsu's method yielded porosity values of 47, 112, and 65, respectively. The lack of clarity in the results was attributed to the difficulties in establishing the position of the histogram's minimum. In order to achieve better precision, other macroscopic parameters such as tortuosity and permeability could also be identified.

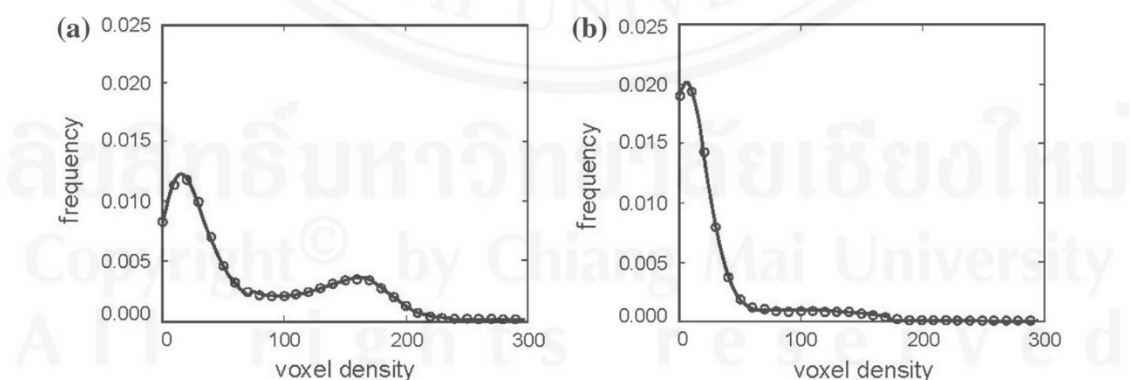


Figure 2.7 Histograms (circles) of sample I (a) and II (b) and their approximations (solid lines) [Cieszko, 2015].

In 2017, Pandaree Khomkham and their team validated the evaluation methods introduced by Rissech [Rissech, 2006] for estimating the age at death in the Thai population [Khomkham, 2017]. The study utilized 48 Thai skeletal remains, consisting of 34 males and 14 females. The age range of the sample varied from 20 to 89 years at the time of death, with age intervals of 10 years. Age intervals for males were categorized from 20-29 years to 80-89 years, while age intervals for females started from 50-59 years to 80-89 years. The evaluation focused on both the left and right sides of the acetabulum, excluding any individuals with pathological bone diseases. The study specifically examined the seventh variable, which relates to the porosities of the acetabular fossa. To analyze the correlation between the actual age at death and the predicted age, the statistical method, Spearman's rho, was employed. The results indicated that there were no significant differences in evaluation scores between the left and right acetabulum, nor between male and female specimens. The correlation between evaluation scores and age at death in the Thai population showed a strong Spearman's rho score of  $r = 0.75$  for right-side male specimens. The study did not encounter intra and inter-observer errors, prompting suggestions for further research to enhance the validity and reliability of the findings. In conclusion, based on the study's results, five out of the seven variables identified by Rissech [Rissech, 2006] can be utilized to estimate the age at death in Thai dry bone acetabula.

In 2017, Marta San-Millan and their team conducted a study on the shape variability of the acetabulum and acetabular fossa in adult humans, exploring their relationship with sex and age. The study aimed to provide implications for adult age estimation using geometric morphometrics [San-Millan, 2017]. A total of 682 individuals were analyzed, comprising 327 females and 355 males. To analyze the shape and size variation of the acetabulum and its fossa, a two-dimensional geometric morphometric analysis was performed, which also considered their association with sex and age. The photography technique used was discussed, with fixed positions and inclinations of both the camera and the acetabulum to ensure the acetabular rim remained parallel to the camera lens. The camera was consistently positioned 320 mm above the acetabular fossa. Landmarks and semi-landmarks were utilized to capture the shape of the lunate surface of the acetabulum, with the first and second landmarks located at the apex of the anterior

and posterior acetabular horns, respectively. The landmarks were identified using a clockwise orientation. A total of 2 bi-dimensional landmarks and 32 sliding semi-landmarks were employed in the analysis. Age groups were divided into three categories: 15-39 years old, 40-64 years old, and those over 65 years old. Each age group represented a range of approximately 25 years. The resulting shape visualization was presented in Figure 2.5, and p-values from pair-wise comparisons of acetabular shape across age groups were displayed in Table 2.1. These results were subsequently discussed and compared to previous studies. In conclusion, the study suggests that 3D shape-data would provide more accuracy than the 2D procedures employed in this research.

Table 2.1 p-Values obtained from pair-wise comparisons of acetabular shape across age groups [San-Millan, 2017].

	Females 15-39	Females 60-64	Female >65		Males 15-39	Males 40-64	Males >65
Females 15-39	1.000			Males 15-39	1.000		
Females 40-64	0.005	1.000		Males 40-64	0.019	1.000	
Females >65	0.002	0.002	1.000	Males >65	0.004	0.004	1.000



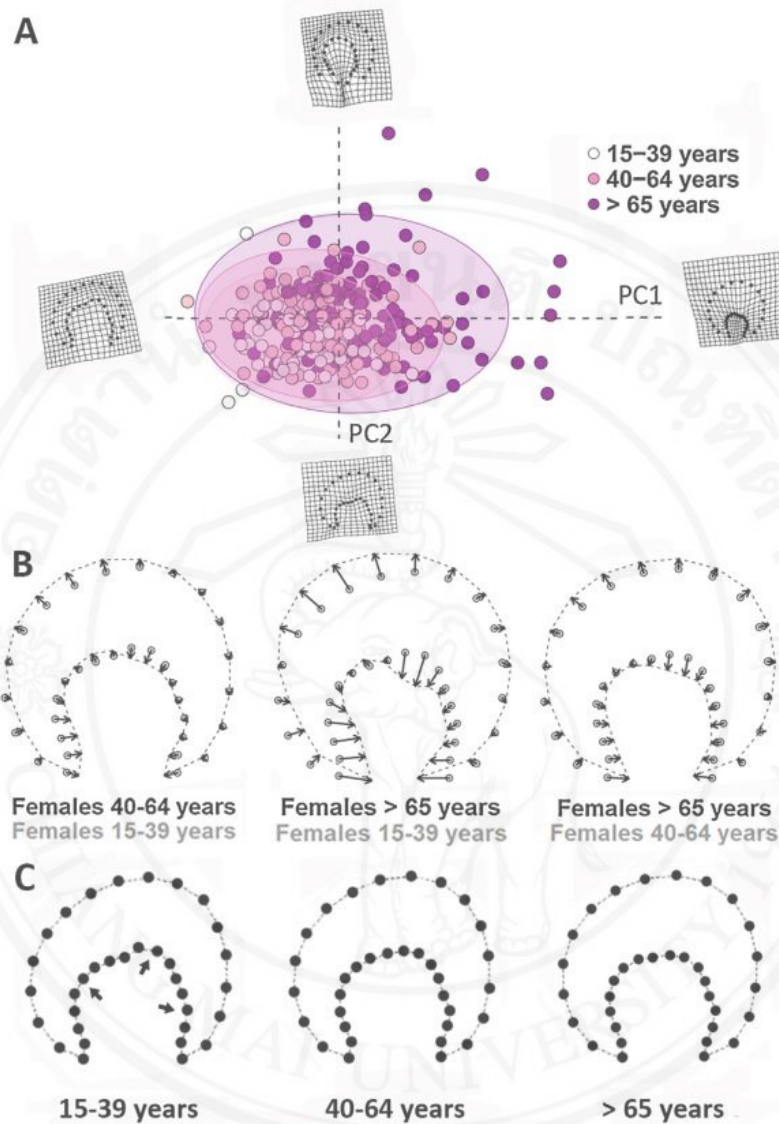


Figure 2.8 PCA plot for visualizing shape variation among all female age groups [San-Millan, 2017].

In 2017, Nihat Acar and his team conducted a study on the variant configurations of the femoral head fovea capitis and their relation to age groups [Acar, 2017]. The study utilized 600 true pelvis anteroposterior radiographs. The patients, ranging from 20 to 80 years old, were divided into three groups. The first group consisted of individuals aged 20 to 39 years, with 100 males and 100 females. The second group consisted of individuals aged 40 to 59 years, with 100 males and 100 females. The third group



consisted of individuals aged 60 to 80 years, with 100 males and 100 females. The study introduced the fovea capitis index (FCI), which is the ratio of the fovea capitis diameter (FCD) to the femoral head diameter (FHD), expressed as a percentage (%), as shown in figure 2.6. The depth of each fovea capitis was also measured and recorded. The results of the study revealed that the average FCI value for both genders on both sides in the first group (age 20 to 39 years) was  $26.08\% \pm 4.46\%$ . In the second group (age 40 to 59 years), the average FCI value was  $26.78\% \pm 4.93\%$ . In the third group (age 60 to 80 years), the average FCI value was  $28.93\% \pm 4.40\%$ . The results indicated that the size of the fovea capitis increases with the aging process. Although there was no statistical significance between the first and second group, the FCI average value in the second group was larger than that of the first group. The third group had the highest FCI average value, showing a significant statistical difference compared to the first and second group's average values ( $P=0.016$  and  $0.032$ , respectively). A total of 1200 hip joints were analyzed in the study. Of these, 97% (1164 out of 1200 hip joints) had FCI values ranging between 18% and 35%. Additionally, 95.75% (1149 out of 1200 hip joints) had fovea depths ranging between 2 mm and 4 mm. It was observed that the average FCI value of the left hip was larger than that of the right hip.

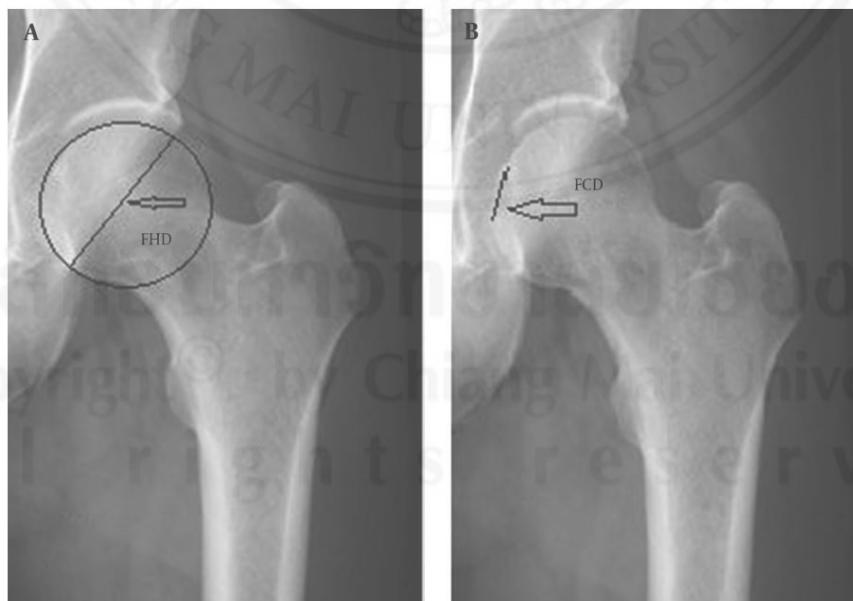


Figure 2.9 Anteroposterior view of the left hip joint [Acar, 2017].

In 2018, Yuan Li and their team conducted a study using pelvic x-ray images to develop a deep learning bone age assessment for forensic age estimation [Li, 2018]. A total of 1875 conventional pelvic anteroposterior radiography images were collected from subjects aged 10 to 25 years. Among the subjects, 1072 (57.2%) were females and 803 (42.8%) were males. The radiography images were obtained from the West China Hospital of Sichuan University between January 2010 and March 2017. The deep learning system utilized a fine-tuned convolutional neural network (CNN) to automatically estimate the age, while the cubic regression model was used to calculate the bone age. Several statistical analyses, including Mann-Whitney U test, t-tests, and F tests, were performed. The CNN model's estimated bone age exhibited a mean absolute error (MAE) of 0.94 years and a root-mean-squared error (RMSE) of 1.30 years when compared to the actual chronological ages. The estimated bone ages generated by the CNN model showed a significant correlation ( $R^2=0.9288$ ) with the actual chronological ages. There were no statistically significant differences observed between the sexes ( $p=0.873$ ). The CNN model's results were compared to the ground truth ages, resulting in an MAE of 0.91 years and an RMSE of 1.23 years. Furthermore, the cubic regression model's results were compared to the ground truth ages, yielding an MAE of 1.05 years and an RMSE of 1.61 years. The errors obtained from the CNN model were lower than those of the cubic regression model. In conclusion, the CNN model effectively handles samples within the age range of 19-21 years, but not for ages over 22 years.

In 2018, Andreas Bertsatos and his team studied about Morphological variation of the femoral head fovea capitis [Bertsatos, 2018]. The study was said about the fovea capitis femoris serves as the distal attachment site for the ligamentum teres femoris. While recent studies suggest that this ligament may play a role in providing mechanical stability to the hip joint, there is limited published research on the morphological variation of the fovea capitis femoris. This study examines the morphological variation of the fovea capitis femoris with respect to sex and age. Morphometric measurements were taken from both the left and right femurs of 212 individuals from the Athens skeletal collection. The fovea capitis femoris was photographed directly with a reference scale, and a polyline outlining its boundary edges was extracted. Two shape variables and three size variables of the fovea capitis femoris were calculated for morphological analysis. The results

indicated bilateral asymmetry in one size variable and one shape variable. Sexual dimorphism in the fovea capitis femoris is linked to size variables, while age-related changes are observed in its shape. Males generally have a larger fovea capitis area and greater maximum diameter, whereas older individuals tend to have a more irregular fovea capitis perimeter. However, the fovea capitis femoris cannot be reliably used for age estimation or sex determination in human skeletal remains.

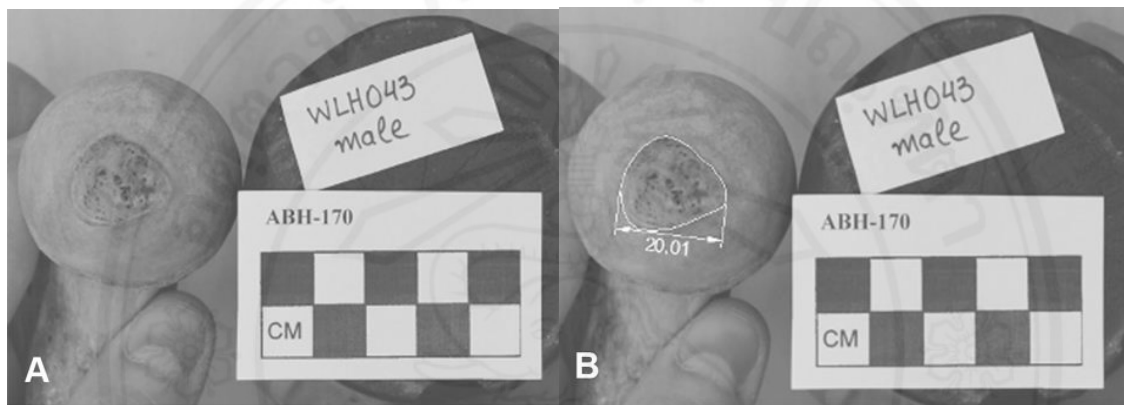


Figure 2.10 The fovea capitis femoris (FCF) photographed in face with a reference scale (left). The fovea capitis maximum diameter and the polyline outlining the boundary edges of the FCF (right). [Bertsatos, 2018]

In 2019, Tristan Whitmarsh and their team conducted a cross-sectional study on age-related cortical and trabecular bone changes in elderly females, specifically focusing on the femoral head [Whitmarsh, 2019]. The study included female patients aged 70 and above. A total of 37 femoral head specimens were scanned, and they were divided into three age groups. Group one consisted of individuals aged 70 to 79, with 6 scans. Group two consisted of individuals aged 80 to 89, with 22 scans. Group three consisted of individuals aged 90 to 99, with 9 scans. The specimens were acquired through micro-CT scans, and the average CT values were used to measure bone mineral density in  $\text{mg}/\text{cm}^3$ . Otsu's method, a clustering-based image thresholding technique, was used to differentiate bone and marrow volume pixels. The degree of anisotropy (DA) was also assessed, ranging from 0 to 1, where a DA value of 0 indicated isotropic bone and a DA value of 1 indicated anisotropic trabecular bone. The study focused on the superior medial hemisphere of the femoral head. Statistical analyses, such as T-tests and the Shapiro-Wilk

test, were performed. The results showed a decrease in average trabecular bone mineral density (Tb, BMD) and cortical thickness (Ct.Th) between age groups two and three, but no significant difference was found between groups one and two. Additionally, there was no significant change in the degree of anisotropy (DA) across any age group. The study suggested that the population may have impaired functional adaptation since the femoral head specimens were collected from patients with hip fractures. In conclusion, age-related bone degradation continues throughout old age, but the distribution of bone does not change significantly.

In 2019, Arnab Kumar Pal and their team study about porosity estimation by digital image analysis [Kumar Pal, 2019]. The study said that porosity and permeability are critical rock properties that significantly influence decision-making during the planning and execution phases of petroleum exploration and development. With advancements in image analysis and processing techniques, Digital Image Analysis (DIA) has become increasingly important for pore structure analysis and characterization. In this study, both 2D and 3D image analysis techniques were employed using FESEM backscattered images to estimate porosity. Traditional porosity estimation methods rely on physical measurements that produce a single representative porosity value for the entire rock core sample. However, in reality, porosity varies from the micro to macro level, introducing substantial uncertainty in porosity estimation. Therefore, digital image analysis is seen as an alternative method, as it can capture both micro- and macro-pores in a rock sample.

In this study, porosity was estimated by applying image thresholding to the backscattered electron microscope images obtained from rock core samples provided by KDMIPE, ONGC, from two different petroleum-producing basins. Carbonate core samples were sourced from the Bombay Offshore Basin, while sandstone core samples were obtained from the A&AA basin. Representative rock chips from each core sample were used to acquire BSE images through the FESEM technique. These images were processed and analyzed using ImageJ software to determine 2D porosity. A minimum of three images were stacked to calculate 3D porosity.

The porosity values derived through digital image analysis were compared with those obtained using a helium gas porosimeter. The 2D porosity values ranged from 14.54% to 45.33% for carbonates and 3.90% to 35.56% for sandstones, while the 3D porosity values ranged from 7.80% to 9.89% for carbonates and 3.52% to 9.75% for sandstones. The 2D porosity values were found to be within the expected range, whereas the 3D porosity values were underestimated when compared to those obtained through conventional techniques. The study concludes that image analysis is a valuable tool for porosity estimation, revealing significant heterogeneity at the micro level. This heterogeneity requires further investigation to better understand its impact on reservoir quality.

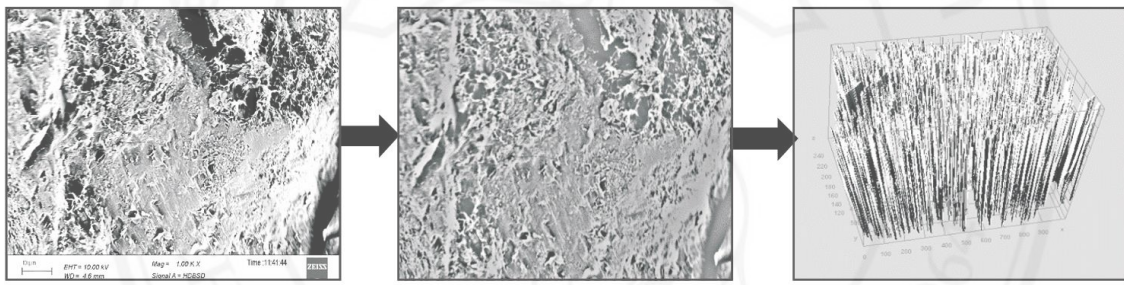
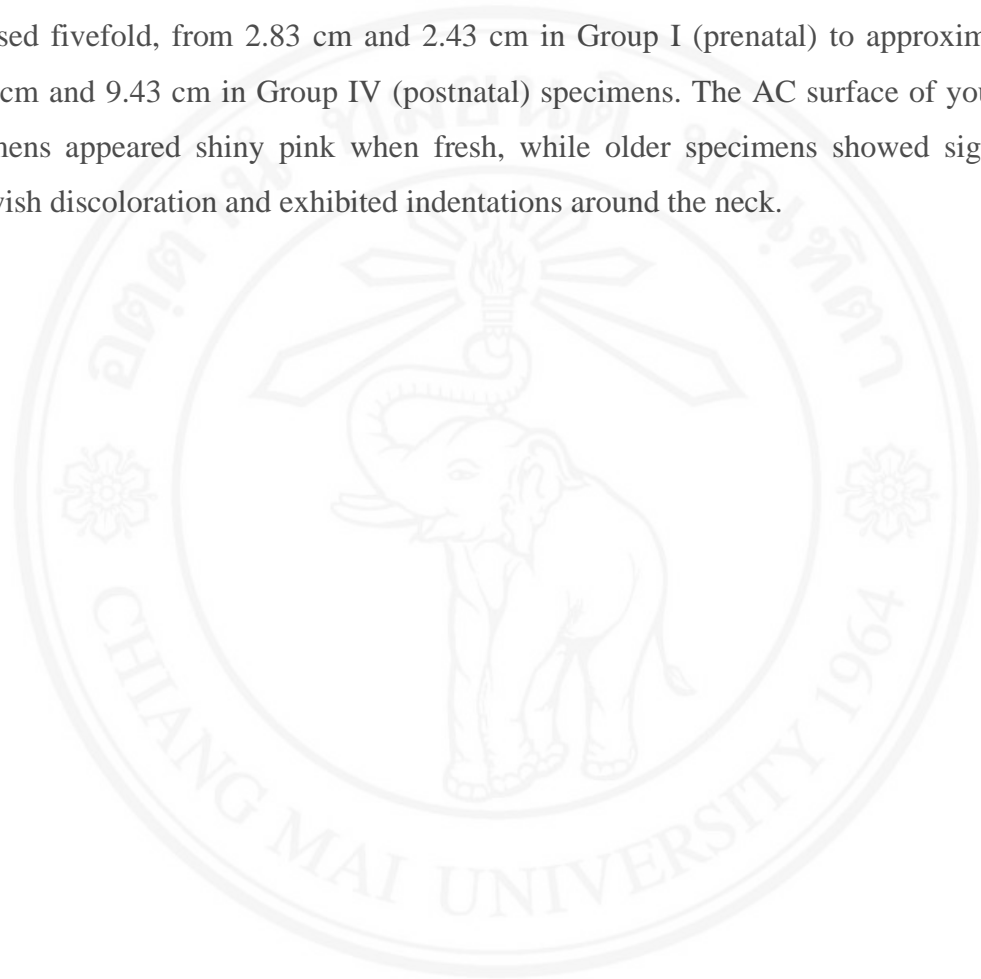


Figure 2.11 Image processing workflow employed. [Kumar Pal, 2019]

In 2021, Ranjith Kumar Sundari and their team studied about age related anatomical changes in articular cartilage of femoral head in buffalo (*bubalus bubalis*) [Sundari, 2021]. They investigate the anatomical characteristics of the femoral head articular cartilage (AC) in twenty-four intact hip joints from apparently healthy buffaloes, obtained from the GHMC Abattoir in Hyderabad. The samples were categorized into four groups: Group I (prenatal), Group II (birth to 3 years), Group III (3 to 6 years), and Group IV (6 years and above). The morphological examination of the femoral head AC revealed that in the postnatal groups, the articular surface was covered by a strip of AC composed of hyaline cartilage adjacent to the subchondral bone. In contrast, during the prenatal stage, the entire proximal epiphysis of the femoral head consisted solely of hyaline cartilage, as the AC had not yet differentiated. In the postnatal groups (II, III, and IV), a layer of mature AC covered the hemispherical femoral head, blending peripherally with the epiphyseal cartilage. The thickness of the femoral head AC decreased slightly with

advancing age at various points on the articular surface, including the lateral surface, neck, and midpoint. Specifically, the thickness was 1.89 mm, 1.38 mm, and 1.49 mm in Group II, reducing to 1.64 mm, 1.37 mm, and 1.36 mm in Group IV, respectively. Additionally, as age progressed, the average length and width of the femoral head increased fivefold, from 2.83 cm and 2.43 cm in Group I (prenatal) to approximately 10.77 cm and 9.43 cm in Group IV (postnatal) specimens. The AC surface of younger specimens appeared shiny pink when fresh, while older specimens showed signs of yellowish discoloration and exhibited indentations around the neck.



ลิขสิทธิ์มหาวิทยาลัยเชียงใหม่  
Copyright© by Chiang Mai University  
All rights reserved



## CHAPTER 3

### Methodology

#### 3.1 Introduction

The assessment of bone age using digital image processing techniques begins with capturing images of the bone, focusing on specific areas of interest: the acetabulum and the femoral head. Both female and male bones, from both the left and right sides, are utilized in this process. The obtained images undergo digital image processing to determine the porosity and area ratio of the bone in the specified regions. Subsequently, statistical methods are employed to derive equations that relate these parameters to the actual known age of the bones.

All images are captured using standardized imaging methods under lighting conditions that are as consistent as possible, to minimize variations in results that could arise from the imaging process. Although the imaging is conducted in a laboratory setting, careful consideration is given to ensure that the procedure closely resembles typical field conditions. This approach is intended to enable practitioners to smoothly apply these principles and procedures in their ongoing work.



Figure 3.1 Captured image of acetabulum (left). Captured image of femoral head (right).

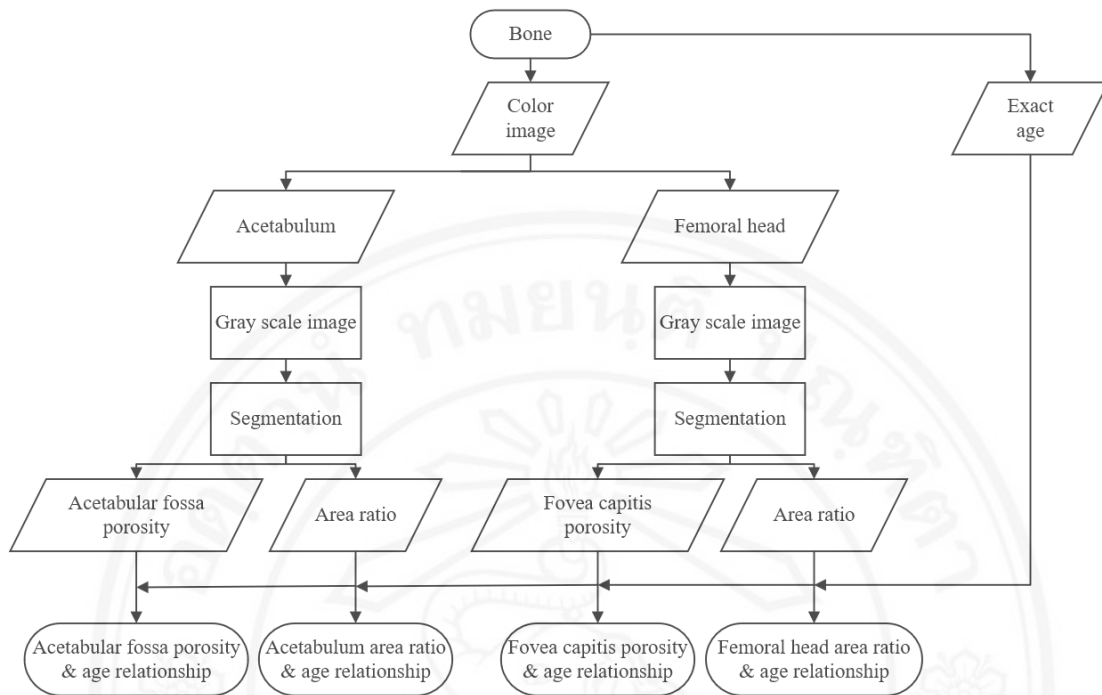


Figure 3.2 Work flow

In the digital image processing procedure, color images of bones are first converted into grayscale images. The resulting bone images are then cropped to retain only the regions of interest, specifically the acetabulum or the femoral head. This cropping reduces the image size and processing requirements, thereby decreasing the overall processing time. In each image, two primary metrics are calculated: percent porosity and area ratio. Percent porosity refers to the ratio of pixels identified as porous to the total number of pixels. The area ratio represents the ratio of one region's area to another region's area. These metrics are then compared with the known age of the bone.

Copyright© by Chiang Mai University  
All rights reserved



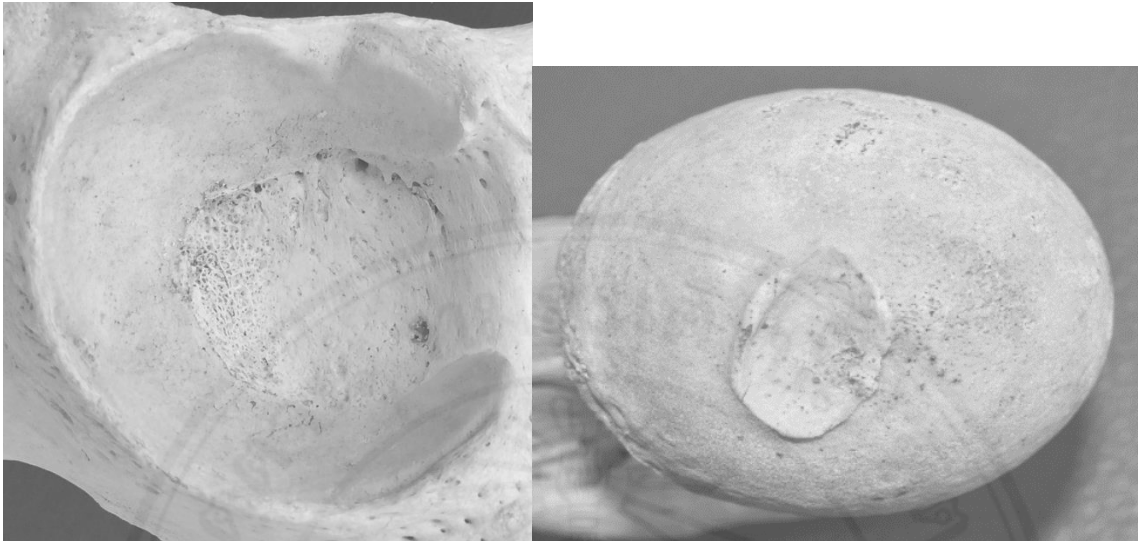


Figure 3.3 Cropped grayscale image of acetabulum (left). Cropped grayscale image of femoral head (right).

Statistical methods are employed to derive the results. The data on percent porosity, area ratio, and bone age are subjected to statistical analysis to establish equations that relate these variables to the bone's age. Specifically, the equation  $A = f(P)$  is derived when age ( $A$ ) is related to percent porosity ( $P$ ), and  $A = f(R)$  is derived when age ( $A$ ) is related to area ratio ( $R$ ). Once these equations are obtained, they are tested using a new set of bone data, which will be conducted by external individuals. This testing aims to evaluate the results and determine the accuracy of the equations in practical application.

### 3.2 Hip joint

The hip joint serves as the connection between the pelvis and the upper leg, functioning as a ball-and-socket joint. In this joint, the socket is known as the acetabulum, while the ball is referred to as the femoral head.

The acetabulum is a concave surface within the pelvis, acting as a cup or socket to support the femoral head of the upper leg. Within the acetabulum, there are several areas of interest. The particular focus is on the acetabular fossa, which is located inside the acetabulum. The porosity within the acetabular fossa, as well as the area ratio between the acetabular fossa and the entire acetabulum, are key areas of study.

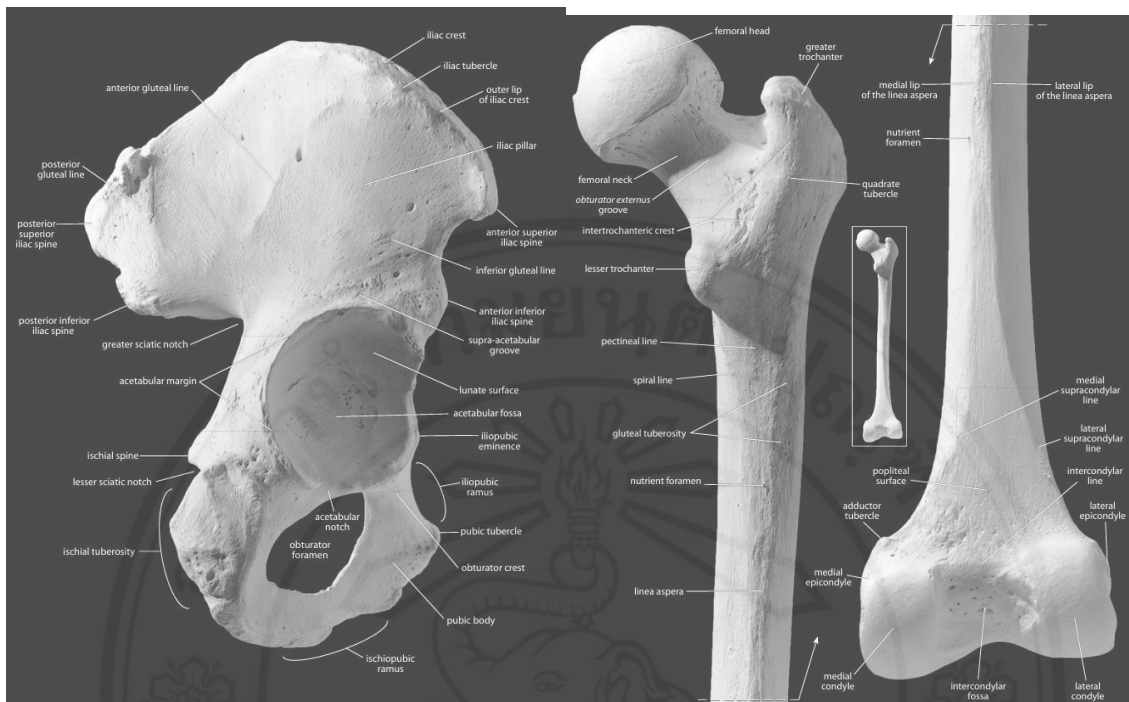


Figure 3.4 Right os coxae and acetabulum (left). Right Femur and femoral head (right) [White, 2012].

The femoral head is the uppermost part of the leg and articulates with the pelvis at the acetabulum to form the hip joint. The femoral head is a round, ball-like structure, and within it lies the fovea capitis. The porosity of the fovea capitis, along with the area ratio between the fovea capitis and the circular area of the femoral head, are also of particular interest.

### 3.3 Sample

The bone samples used for data collection were obtained from the Forensic Osteology Research Center (FORC) and were donated human remains. These bones had all soft tissues removed, leaving only the bone structure. Images of the hip joint, including both the acetabulum and femoral head on both the left and right sides, were captured from 205 skeletons, resulting in approximately 800 images. The donations spanned from 2011 to 2019, with donor ages ranging from 19 to 100 years. Upon reviewing the images, it was observed that many of the bones were not adequately cleaned, which could affect the pixel values and potentially lead to misinterpretations of porosity. Consequently, images

of bones that were not sufficiently clean were excluded, leaving a final dataset consisting of images from 167 skeletons, divided into 59 females aged 26 to 100 years and 108 males aged 26 to 97 years.

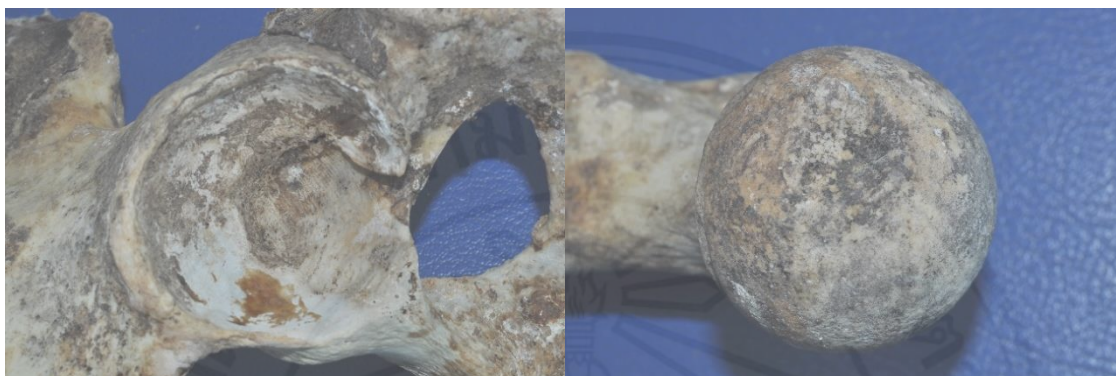


Figure 3.5 Dirty bones.

### 3.4 Recording images and photography

The imaging of bone specimens has been examined in terms of the standards employed for capturing images. This investigation aims to determine the optimal imaging practices to ensure that the images adhere to standardized quality. To achieve consistency, it is essential that all images be captured under identical environmental conditions, thereby ensuring uniformity in the imaging results. This approach minimizes discrepancies due to variations in the imaging process itself, ensuring that any observed deviations in the results are attributable to the bone specimens rather than the imaging procedure. This is crucial for maintaining accuracy and reliability in subsequent steps of the process.

In 1994, Jane E. Buikstra and Douglas H. Ubelaker developed the "Standards for Data Collection from Human Skeletal Remains," derived from the proceedings of a seminar held at the Field Museum of Natural History. These standards address the recording of images and photography, specifying that systematically captured black-and-white photographs should serve as the primary record. Black-and-white negative films are noted for their long-term stability if stored under optimal conditions, specifically at temperatures below 20 degrees Celsius and 30% humidity. In contrast, color slides are subject to deterioration over time and should be replaced every 10 years. The standards

also provide detailed guidance on photographic equipment and techniques for documenting both unburned bones and cremated remains.

For photographing unburned bones, 35 mm single-lens reflex (SLR) cameras are widely utilized. A 55 mm lens with macro close-up capabilities generally yields satisfactory results, while a 105 mm lens with similar macro close-up features is also recommended. The systematic photography discussed here should employ black-and-white film with an ISO rating of 80 to 125. Color photography may be used for illustrative purposes in presentations, but should be adapted to the lighting conditions. Incandescent and fluorescent lighting can cause color distortion; therefore, electronic flash is generally recommended for photographing bones in the laboratory. When using color photography, placing the bones against a black background enhances color accuracy and minimizes shadows.

Building upon the aforementioned color photography standards, these principles were adapted to establish a standardized approach for photographing bones for sample collection in this research. A single-lens reflex digital camera was used, initially with a 55 mm lens. However, since all cameras have a minimum focus distance of 50 centimeters—referring to the distance between the subject and the camera's sensor plane—the use of the 55 mm lens resulted in images that captured only a small portion of the bone, specifically the acetabulum, which is a very small structure. Enlarging these images from the original would lead to significant pixel distortion and an altered pixel ratio, resulting in highly inaccurate outcomes. Therefore, a 105 mm lens was used instead, which allowed for full and accurate capture of the acetabulum within the frame. The ISO setting for the photography was maintained at 100, as per the established standard.

An electronic flash was employed in conjunction with ambient lighting to minimize shadows and reduce color distortion. The use of flash does not alter the results; while it may brighten the image, the camera and flash exposure measurements are still calibrated according to the 18% gray scale standard, which is a general photography standard and not one from image processing techniques. The porosity ratio was calculated based on the pixel ratio of porosity to bone tissue. Thus, any increase in brightness due to

the flash would affect both the porosity pixels and the bone tissue pixels equally, ensuring that the porosity ratio remains unchanged.

For the photography setup in the laboratory, the camera was mounted on a tripod, and a shutter release cable was used to minimize camera shake. When using an electronic flash, the camera's shutter speed was set to 1/60 of a second, which is fast enough to prevent motion blur. The aperture was set to f/16 to ensure that the entire image remains sharp. The bones were positioned at a sufficient distance from the camera to fully capture the acetabulum within the frame, with the distance always exceeding 50 centimeters. The camera was aligned so that its plane was parallel to the plane of the acetabulum. Photographs were taken of the acetabulum and femoral head on both the left and right sides, resulting in a total of four images per skeleton.



Figure 3.6 Acetabulum photo (left). Femoral head photo (right).

### 3.5 Digital image processing

Digital images of the bone will be processed using image processing techniques to achieve the desired outcomes. The final outputs of the digital image processing will include the total number of pixels, the number of pixels within the region of interest, the mean pixel value, the standard deviation of pixel values, and the number of pixels with values below the threshold. These results will then be subjected to further statistical analysis.

The process of image processing begins with cropping out the extraneous parts of the image, retaining only the area of interest, specifically the acetabulum and femoral

head. Standard cropping tools from image viewing software are utilized at this stage. Removing the unwanted portions reduces the image size, decreasing the number of pixels to be processed, which in turn minimizes processing resources and accelerates the processing time. Subsequently, the color image is converted into a grayscale image. This step involves transforming an RGB (red, green, blue) image into a grayscale one. The pixel values of the grayscale image range from 0 to 255, where a pixel value of 0 represents black, while a value of 255 represents white. The values between 0 and 255 represent varying shades of gray, progressing from dark to light.

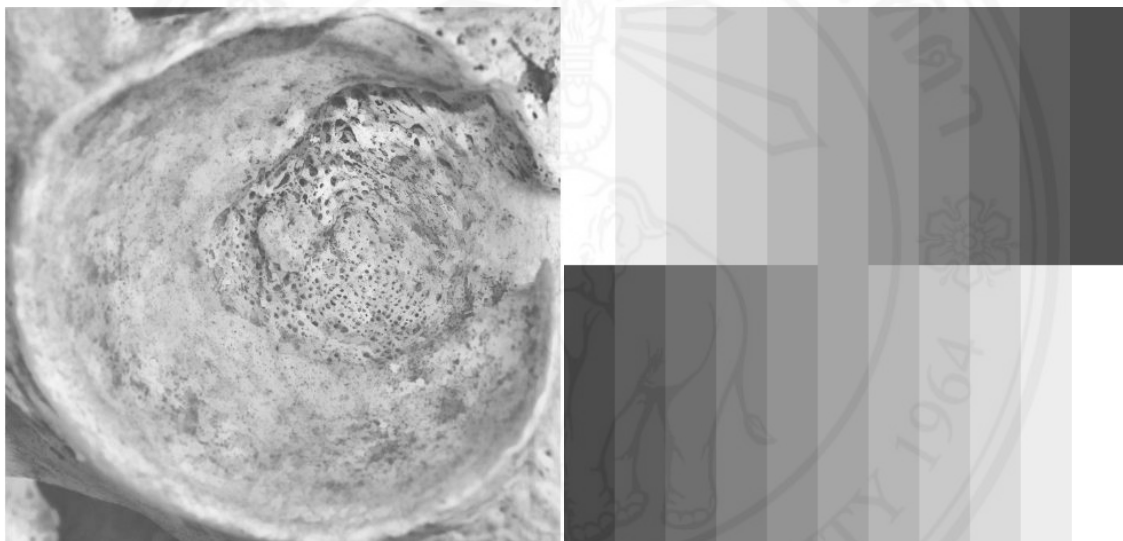


Figure 3.7 Grayscale image (left). Grayscale variation (right).

The grayscale image of the acetabulum undergoes edge detection or segmentation processes to identify the acetabular margin. The region of interest (ROI) is defined using the acetabular margin as a boundary. The ROI is specifically designated to include only the acetabulum area, which is considered the foreground in this context. Conversely, the area outside the ROI, which lies beyond the acetabulum, is classified as the background. The pixel values within the background region, which are not of interest, can be altered to either black or white.



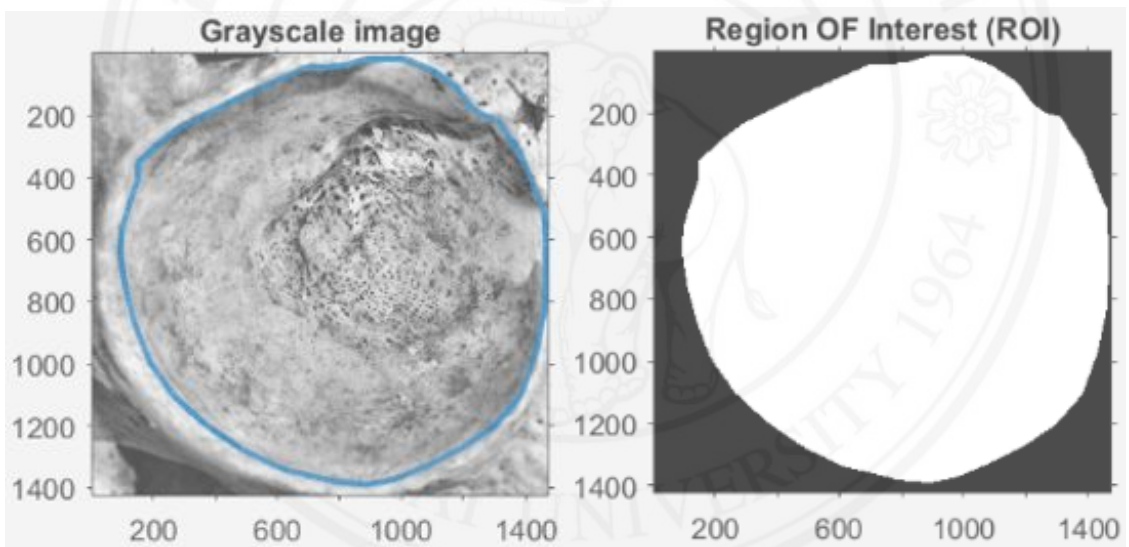
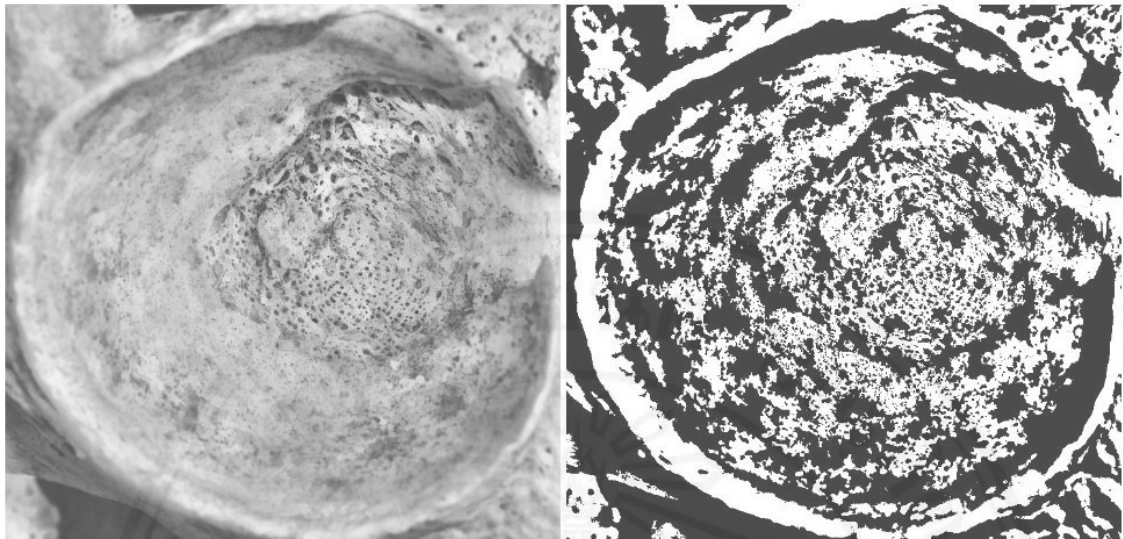


Figure 3.8 Edge detection and segmentation.

ลิขสิทธิ์มหาวิทยาลัยเชียงใหม่  
Copyright© by Chiang Mai University  
All rights reserved

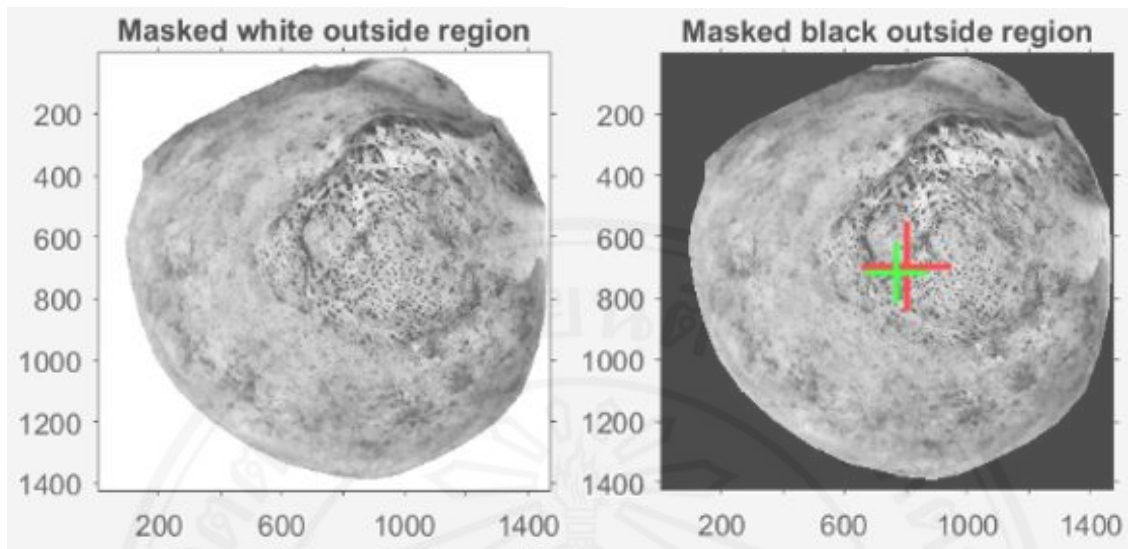


Figure 3.8 Edge detection and segmentation (Cont.).

The acetabulum consists of two primary regions: the acetabular fossa and the lunate surface. The segmentation process is repeated to differentiate and separate these two areas.

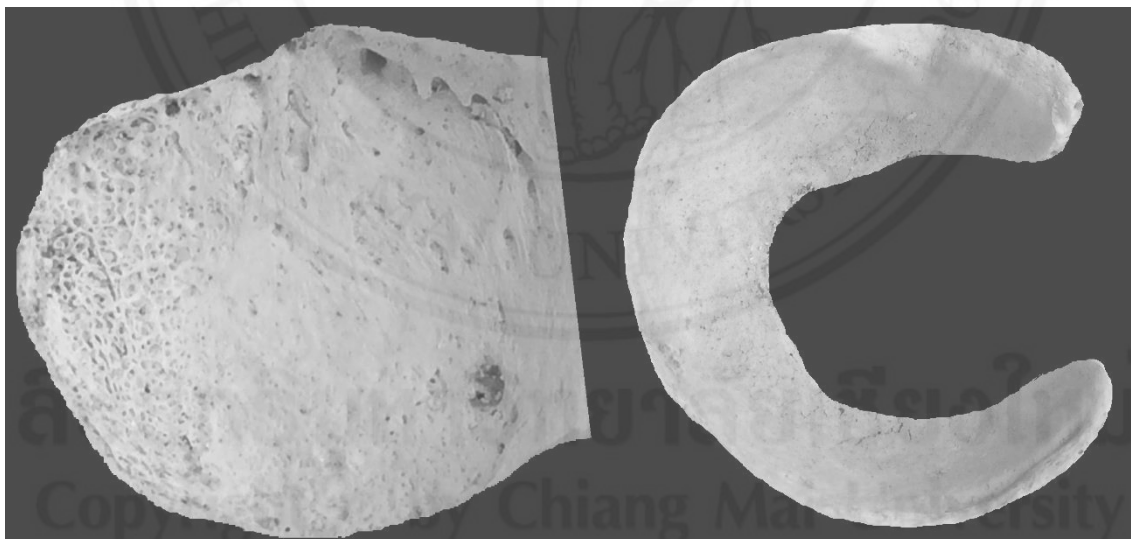


Figure 3.9 Acetabular fossa (left). Lunate surface (right).

The histogram of the acetabular fossa was generated. An image histogram is a graphical representation that depicts the distribution of pixel intensities in an image. The x-axis of the histogram represents pixel intensity values, ranging from 0 to 255, where 0 corresponds to dark pixels and 255 to light pixels. The y-axis indicates the number of



pixels corresponding to each intensity value. A high peak in the histogram indicates a large number of pixels at a particular intensity value. A symmetric bell-shaped curve in the histogram suggests a normal distribution of pixel intensities. However, the histogram of the bone did not exhibit a normal distribution, as it did not display a symmetric bell curve. Statistical values, including the mean, standard deviation, maximum intensity, minimum intensity, number of pixels within the acetabular fossa, and total pixel count, were calculated.

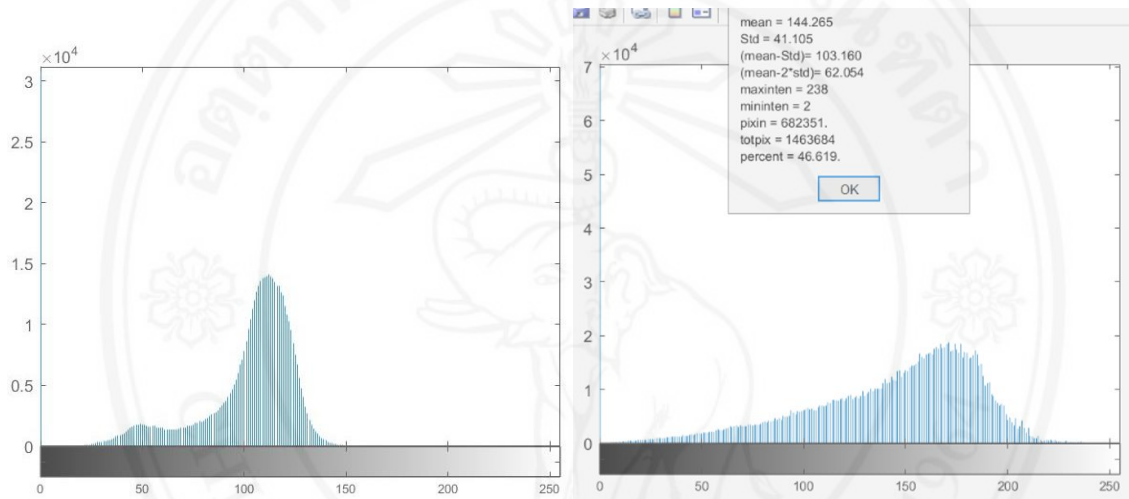


Figure 3.10 Histogram and statistic values.

After obtaining the statistical values from the histogram, the two primary variables required for analysis are the area ratio and percent porosity. The area ratio refers to the proportion of the acetabular fossa area relative to the total acetabulum area, which is calculated as the number of pixels representing the acetabular fossa divided by the total number of pixels. Percent porosity represents the porosity within the acetabular fossa area. It is determined by the ratio of pixels identified as porosity to the total pixels within the acetabular fossa. The mean and standard deviation derived from the histogram are used to define the porosity pixels. A threshold is established as the mean minus the standard deviation, and pixels with values below this threshold are classified as porosity pixels. The number of porosity pixels is then divided by the total number of acetabular fossa pixels to calculate the percent porosity. These two main variables, percent porosity

and area ratio, are then refined. Along with the exact age, these three variables are utilized to explore their interrelationships.

After processing the acetabulum, the femoral head was subjected to the same procedure. The same three primary variables—area ratio, percent porosity, and the exact age of the femoral head—were adjusted. The area ratio is defined as the ratio of the fovea capitis area to the femoral head area. Percent porosity is calculated as the ratio of porosity pixels within the fovea capitis to the total pixels of the fovea capitis.

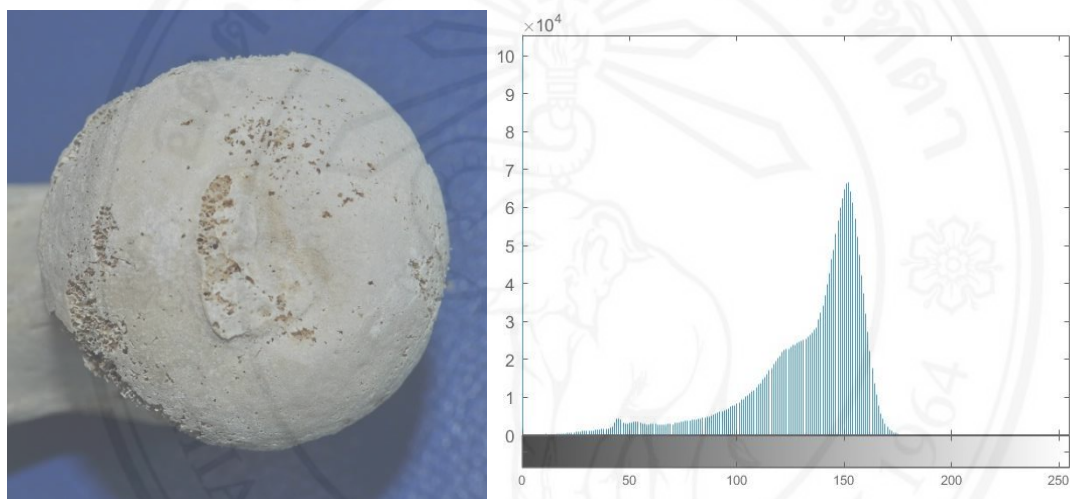


Figure 3.11 Femoral head and histogram.

Digital image processing techniques were applied to all images. Upon completion of the digital image processing, the variables—percent porosity, area ratio, and age—were

adjusted for both the acetabulum and femoral head. These three variables were then analyzed using statistical methods to explore their interrelationships.

### 3.6 Statistics process

After obtaining the three main variables—percent porosity, area ratio, and age—from image processing, their relationships were analyzed using statistical methods. The analysis is divided into two equations: one describing the relationship between percent porosity and age, and the other describing the relationship between area ratio and age. In this analysis, age is assumed to have a linear relationship with the other variables.

Regression analysis, F-tests, and ANOVA tables were employed to determine these relationships, with a significance level of  $\alpha = 0.10$ , equivalent to a confidence level of 90% (0.90). The use of statistics, specifically F-tests or ANOVA tables, serves to assess whether the variables x and y are related, where y represents bone age and x represents either percent porosity or area ratio.

The final outcome will yield a linear equation relating either percent porosity or area ratio to estimated age. The equation will take the form  $A = aP + b$  or  $A = aR + b$ , where A represents the estimated age, P is the percent porosity, and R is the area ratio. The coefficients a and b correspond to the linear equation's slope and intercept, respectively. Regression analysis, including the  $R^2$  value and the P-value, will be reported to indicate whether there is a statistically significant relationship between the variables x and y.

The  $R^2$  value ranges from 0 to 1 ( $0 \leq R^2 \leq 1$ ), and it is interpreted as a percentage. Specifically,  $100R^2\%$  of the variation in the dependent variable y can be explained by its linear relationship with the independent variable x. For instance, if  $R = 0.80$  (or  $R^2 = 0.64$ ), this indicates that 64% of the variation in y is due to its linear relationship with x. In simpler terms, the closer the  $R^2$  value is to 1, the better the equation fits the data.

The P-value is used to report the relationship between the variables x and y by comparing it to the significance level. If the P-value is less than the significance level ( $\alpha = 0.10$ ), the null hypothesis is rejected, indicating that there is a statistically significant relationship between the variables x and y.

### **3.7 Equation audit**

After deriving the estimated age equations through statistical analysis, these equations undergo a validation process. Equations that establish a relationship between two parameters are subjected to external testing. An independent party will conduct these tests. A separate set of bone samples, which had been previously set aside, will be used for this validation. The 10 samples are allocated for each equation. This process serves to assess the practical applicability of the equations. The error values associated with each

equation will be determined. The results, along with the error metrics, will be compared to findings from previous research studies.



ลิขสิทธิ์มหาวิทยาลัยเชียงใหม่  
Copyright© by Chiang Mai University  
All rights reserved

## CHAPTER 4

### Results

The analysis is conducted separately for each group, with results categorized by gender (female or male), anatomical region (acetabulum or femoral head), and side (left or right). The two primary outcomes assessed are percent porosity and area ratio. The results for each group are presented as follows.

#### 4.1 Solutions in each group

##### 4.1.1 Percent porosity and age

##### Acetabulum

ลิขสิทธิ์มหาวิทยาลัยเชียงใหม่  
Copyright© by Chiang Mai University  
All rights reserved

Female acetabulum left side, the results of percent porosity and age have shown as figure and table below. Number of bone sample (observations) is 17. The relationship equation is  $A = 0.2316P + 67.072$  which A is age and P is percent porosity. Regression ( $R^2$ ) = 0.0069. P-value is 0.7184.

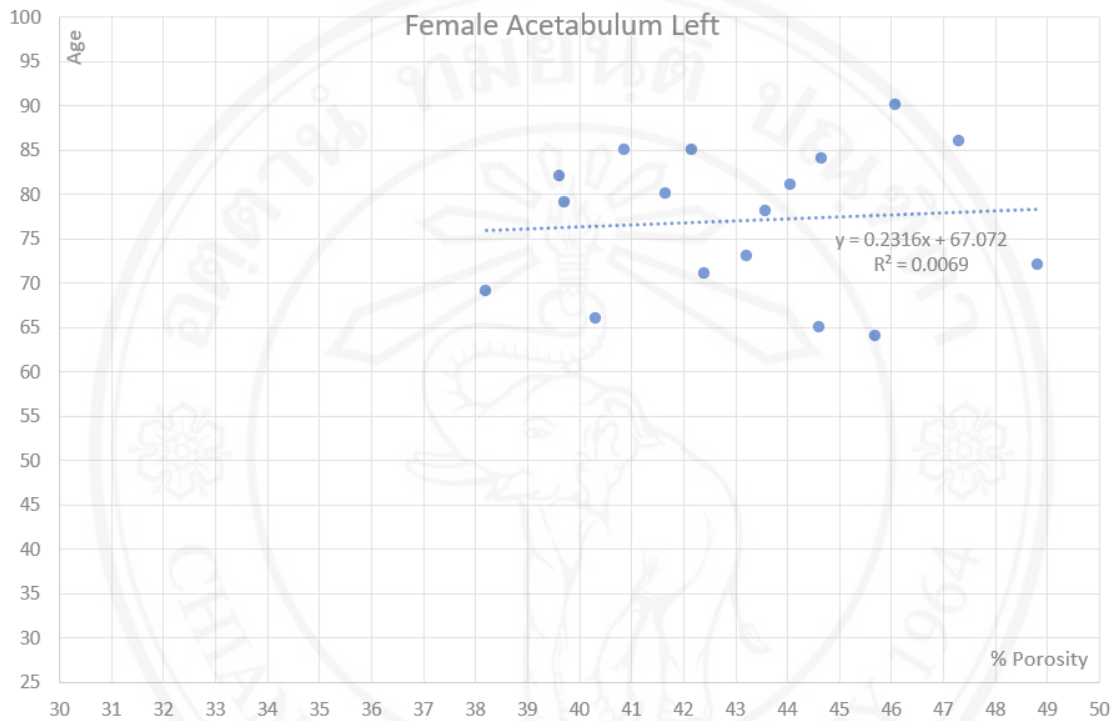


Figure 4.1 Percent porosity and age of female acetabulum left side.

Table 4.1 Percent porosity and age of female acetabulum left side.

SUMMARY OUTPUT								
<i>Regression Statistics</i>								
Multiple R	0.082942247							
R Square	0.006879416							
Adjusted R Square	-0.059328623							
Standard Error	8.365285562							
Observations	17							
<i>ANOVA</i>								
	<i>df</i>	<i>SS</i>	<i>MS</i>	<i>F</i>	<i>Significance F</i>			
Regression	1	7.271138444	7.271138444	0.103906059	0.751640626			
Residual	15	1049.670038	69.97800254					
Total	16	1056.941176						
	<i>Coefficients</i>	<i>Standard Error</i>	<i>t Stat</i>	<i>P-value</i>	<i>Lower 95%</i>	<i>Upper 95%</i>	<i>Lower 90.0%</i>	<i>Upper 90.0%</i>
Intercept	67.07154047	31.04960418	2.160141562	0.047355143	0.890875757	133.2522052	12.64002082	121.5030601
%poro	0.231591384	0.718458954	0.322344627	0.751640626	-1.299767627	1.762950394	-1.027903341	1.491086108

Female acetabulum right side, the results of percent porosity and age have shown as figure and table below. Number of bone sample (observations) is 23. The relationship equation is  $A = 0.7801P + 36.292$  which A is age and P is percent porosity. Regression ( $R^2$ ) = 0.0336. P-value is 0.4022.

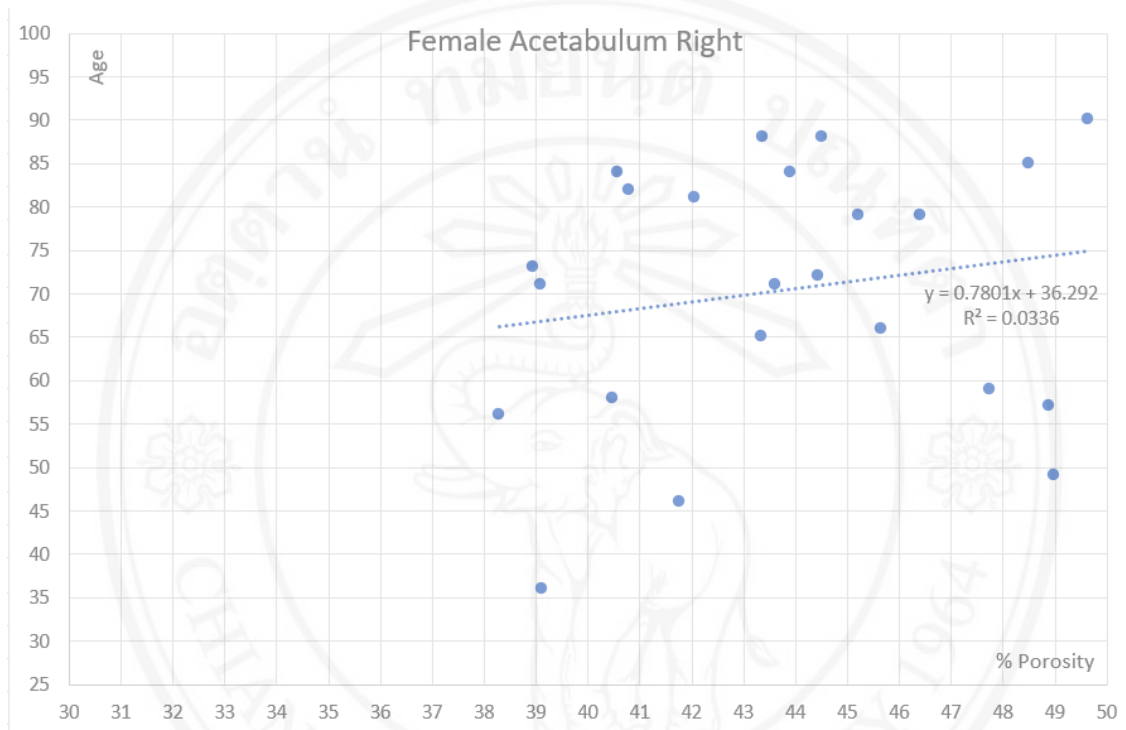


Figure 4.2 Percent porosity and age of female acetabulum right side.

Table 4.2 Percent porosity and age of female acetabulum right side.

SUMMARY OUTPUT								
<i>Regression Statistics</i>								
Multiple R	0.183417378							
R Square	0.033641935							
Adjusted R Square	-0.012375116							
Standard Error	15.08868311							
Observations	23							
<i>ANOVA</i>								
	<i>df</i>	<i>SS</i>	<i>MS</i>	<i>F</i>	<i>Significance F</i>			
Regression	1	166.4427404	166.4427404	0.73107542	0.40218474			
Residual	21	4781.03552	227.6683581					
Total	22	4947.478261						
	<i>Coefficients</i>	<i>Standard Error</i>	<i>t Stat</i>	<i>P-value</i>	<i>Lower 95%</i>	<i>Upper 95%</i>	<i>Lower 90.0%</i>	<i>Upper 90.0%</i>
Intercept	36.2922674	40.00445022	0.907205753	0.37459104	-46.90154112	119.4860759	-32.54510639	105.1296412
%poro	0.780066272	0.912326751	0.855029485	0.40218474	-1.117221071	2.677353615	-0.78981351	2.349946054

Female acetabulum both sides, the results of percent porosity and age have shown as figure and table below. Number of bone sample (observations) is 40. The relationship equation is  $A = 0.5004P + 51.475$  which A is age and P is percent porosity. Regression ( $R^2$ ) = 0.0160. P-value is 0.4361.

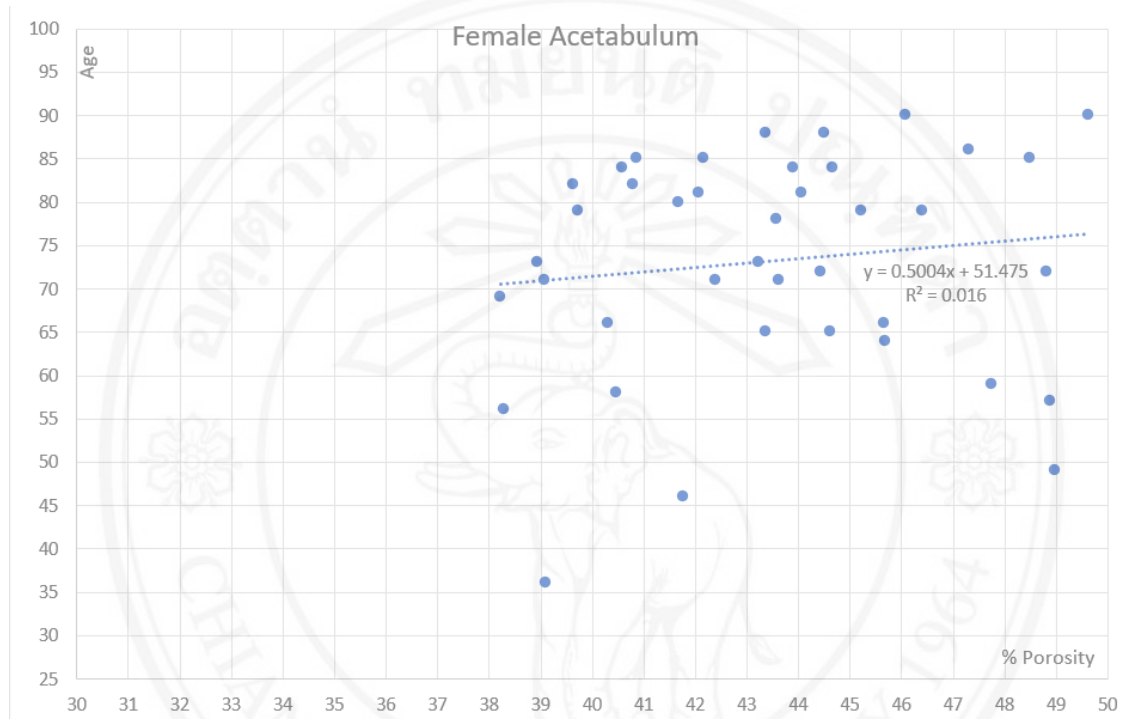


Figure 4.3 Percent porosity and age of female acetabulum both sides.

Table 4.3 Percent porosity and age of female acetabulum both sides.

SUMMARY OUTPUT								
Regression Statistics								
Multiple R	0.126658595							
R Square	0.0160424							
Adjusted R Square	-0.009851221							
Standard Error	12.91233436							
Observations	40							
ANOVA								
	df	SS	MS	F	Significance F			
Regression	1	103.2966107	103.2966107	0.619550262	0.436096387			
Residual	38	6335.678389	166.7283787					
Total	39	6438.975						
	Coefficients	Standard Error	t Stat	P-value	Lower 95%	Upper 95%	Lower 90.0%	Upper 90.0%
Intercept	51.47495076	27.70793336	1.857769401	0.070963091	-4.616827834	107.5667294	4.760636925	98.18926459
%poro	0.500427646	0.635774378	0.787115152	0.436096387	-0.786630294	1.787485586	-0.571459002	1.572314294



Male acetabulum left side, the results of percent porosity and age have shown as figure and table below. Number of bone sample (observations) is 35. The relationship equation is  $A = 2.2776P - 25.2553$  which A is age and P is percent porosity. Regression ( $R^2$ ) = 0.3317. P-value is 0.0003.

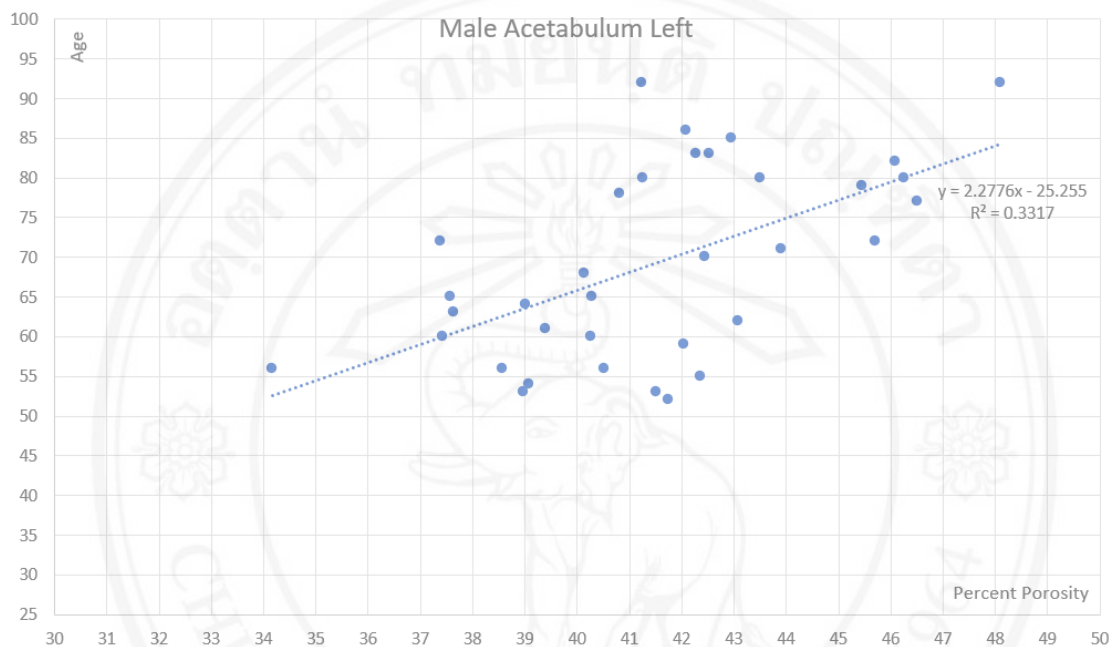


Figure 4.4 Percent porosity and age of male acetabulum left side.

Table 4.4 Percent porosity and age of male acetabulum left side.

SUMMARY OUTPUT								
<i>Regression Statistics</i>								
Multiple R	0.5759691							
R Square	0.331740404							
Adjusted R Square	0.311490113							
Standard Error	10.05300139							
Observations	35							
<i>ANOVA</i>								
	<i>df</i>	<i>SS</i>	<i>MS</i>	<i>F</i>	<i>Significance F</i>			
Regression	1	1655.612095	1655.612095	16.38200692	0.000293982			
Residual	33	3335.07362	101.062837					
Total	34	4990.685714						
	<i>Coefficients</i>	<i>Standard Error</i>	<i>t Stat</i>	<i>P-value</i>	<i>Lower 95%</i>	<i>Upper 95%</i>	<i>Lower 90.0%</i>	<i>Upper 90.0%</i>
Intercept	-25.2553103	23.41274673	-1.078699163	0.288543648	-72.88890168	22.37828107	-64.87811359	14.36749298
%poro	2.2775512	0.562709952	4.047469199	0.000293982	1.132709194	3.422393206	1.325243211	3.229859189

Male acetabulum right side, the results of percent porosity and age have shown as figure and table below. Number of bone sample (observations) is 48. The relationship equation is  $A = 2.4259P - 35.2704$  which A is age and P is percent porosity. Regression ( $R^2$ ) = 0.2118. P-value is 0.0010.

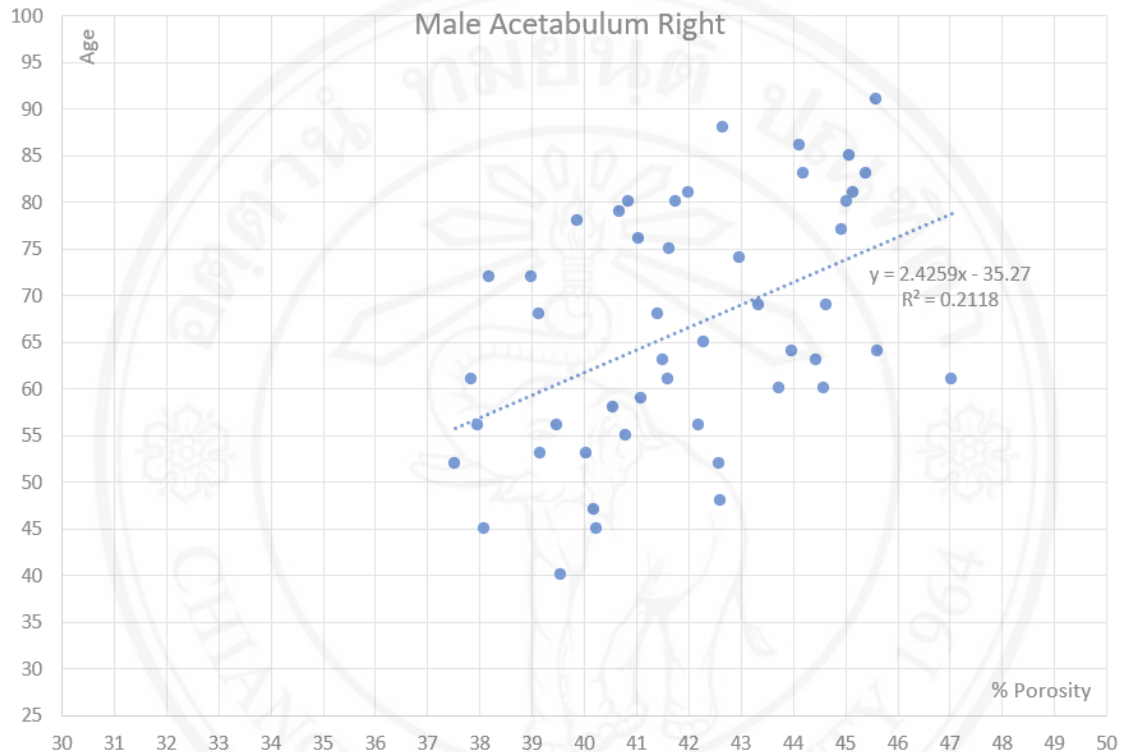


Figure 4.5 Percent porosity and age of male acetabulum right side.

Table 4.5 Percent porosity and age of male acetabulum right side.

SUMMARY OUTPUT								
Regression Statistics								
Multiple R	0.460262274							
R Square	0.211841361							
Adjusted R Square	0.194707477							
Standard Error	11.65787132							
Observations	48							
ANOVA								
	df	SS	MS	F	Significance F			
Regression	1	1680.325673	1680.325673	12.36388477	0.000996232			
Residual	46	6251.674327	135.9059636					
Total	47	7932						
	Coefficients	Standard Error	t Stat	P-value	Lower 95%	Upper 95%	Lower 90.0%	Upper 90.0%
Intercept	-35.27036623	28.99189286	-1.216559622	0.229977308	-93.62801977	23.08728731	-83.93790909	13.39717663
%poro	2.425911324	0.689917955	3.516231614	0.000996232	1.037178509	3.81464414	1.267773365	3.584049284

Male acetabulum both sides, the results of percent porosity and age have shown as figure and table below. Number of bone sample (observations) is 83. The relationship equation is  $A = 2.2899P - 27.964$  which A is age and P is percent porosity. Regression ( $R^2$ ) = 0.2442. P-value is  $2.0612 \times 10^{-6}$ .

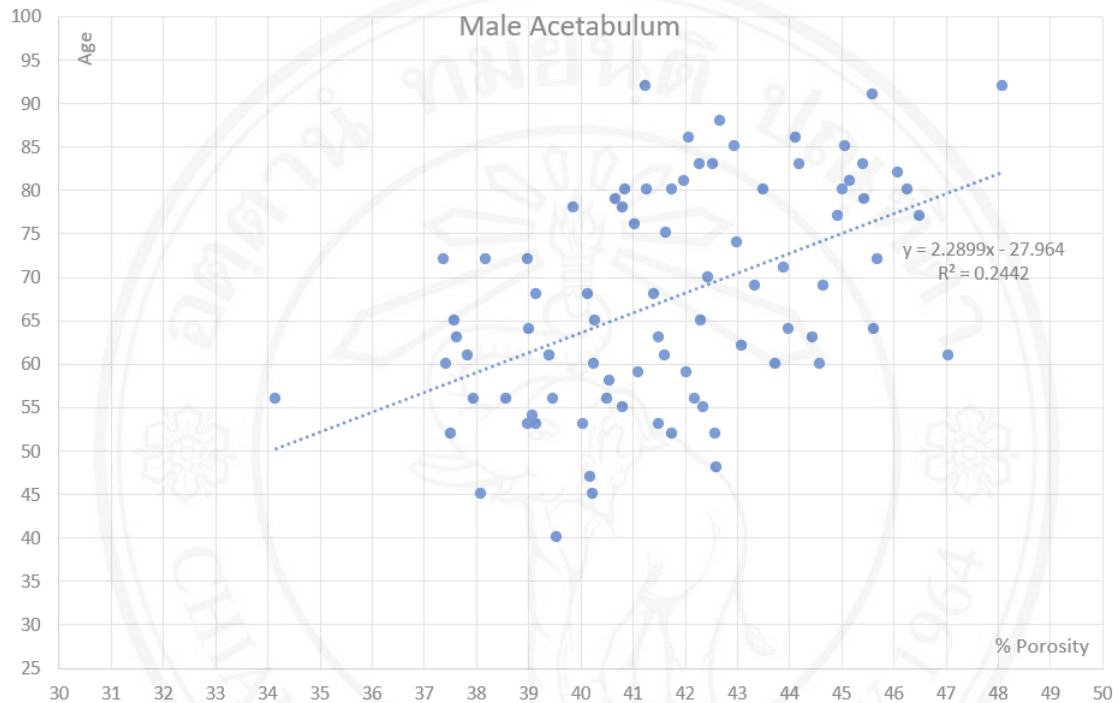


Figure 4.6 Percent porosity and age of male acetabulum both sides.

Table 4.6 Percent porosity and age of male acetabulum both sides.

SUMMARY OUTPUT								
<i>Regression Statistics</i>								
Multiple R	0.494119665							
R Square	0.244154243							
Adjusted R Square	0.234822814							
Standard Error	11.04639935							
Observations	83							
<i>ANOVA</i>								
	<i>df</i>	<i>SS</i>	<i>MS</i>	<i>F</i>	<i>Significance F</i>			
Regression	1	3192.696196	3192.696196	26.16472144	2.06125E-06			
Residual	81	9883.858021	122.0229385					
Total	82	13076.55422						
	<i>Coefficients</i>	<i>Standard Error</i>	<i>t Stat</i>	<i>P-value</i>	<i>Lower 95%</i>	<i>Upper 95%</i>	<i>Lower 90.0%</i>	<i>Upper 90.0%</i>
Intercept	-27.96371765	18.7340263	-1.492669926	0.139408541	-65.23855356	9.311118251	-59.13496263	3.207527325
%poro	2.289906097	0.447671674	5.115146277	2.06125E-06	1.39917989	3.180632304	1.5450324	3.034779794

## Femoral head

Female femoral head left side, the results of percent porosity and age have shown as figure and table below. Number of bone sample (observations) is 25. The relationship equation is  $A = 2.7106P - 50.054$  which A is age and P is percent porosity. Regression ( $R^2$ ) = 0.0452. P-value is 0.3077.

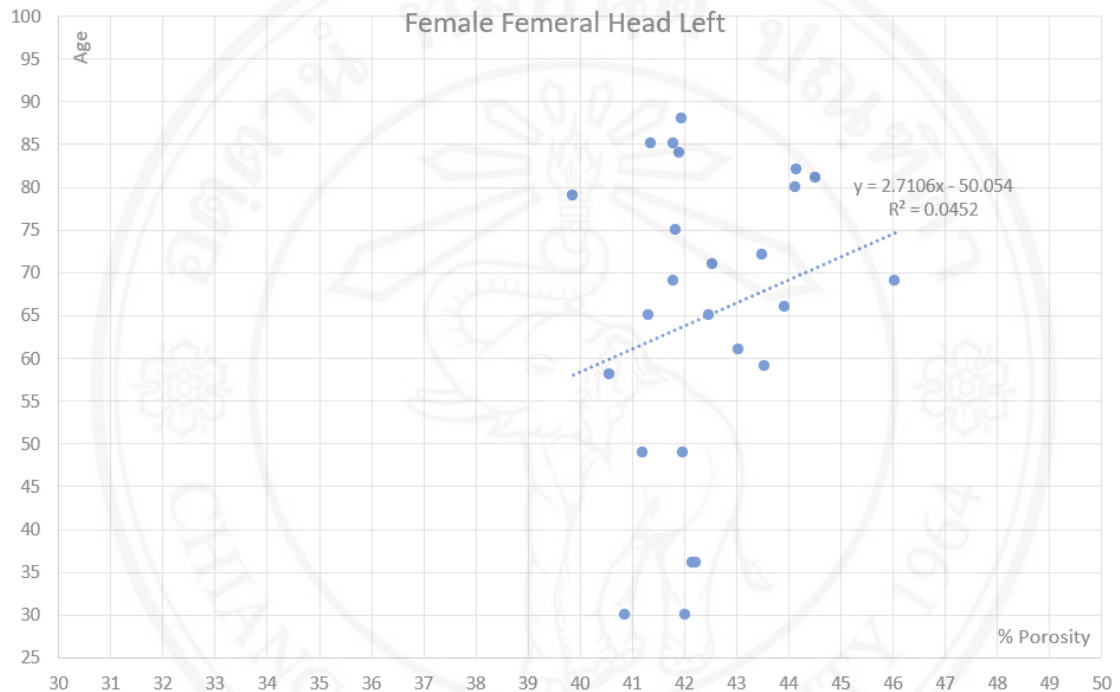


Figure 4.7 Percent porosity and age of female femoral head left side.

Table 4.7 Percent porosity and age of female femoral head left side.

SUMMARY OUTPUT								
Regression Statistics								
Multiple R	0.212550617							
R Square	0.045177765							
Adjusted R Square	0.003663755							
Standard Error	17.78464459							
Observations	25							
ANOVA								
	df	SS	MS	F	Significance F			
Regression	1	344.2075827	344.2075827	1.088253448	0.307699938			
Residual	23	7274.752417	316.2935834					
Total	24	7618.96						
	Coefficients	Standard Error	t Stat	P-value	Lower 95%	Upper 95%	Lower 90.0%	Upper 90.0%
Intercept	-50.05357324	110.3087511	-0.453758861	0.654255009	-278.2446106	178.1374642	-239.108601	139.0014545
%poro	2.710622909	2.598388459	1.043193869	0.307699938	-2.664553151	8.085798968	-1.742681088	7.163926906

Female femoral head right side, the results of percent porosity and age have shown as figure and table below. Number of bone sample (observations) is 34. The relationship equation is  $A = 3.7040P - 91.5155$  which A is age and P is percent porosity. Regression ( $R^2$ ) = 0.0746. P-value is 0.1180.

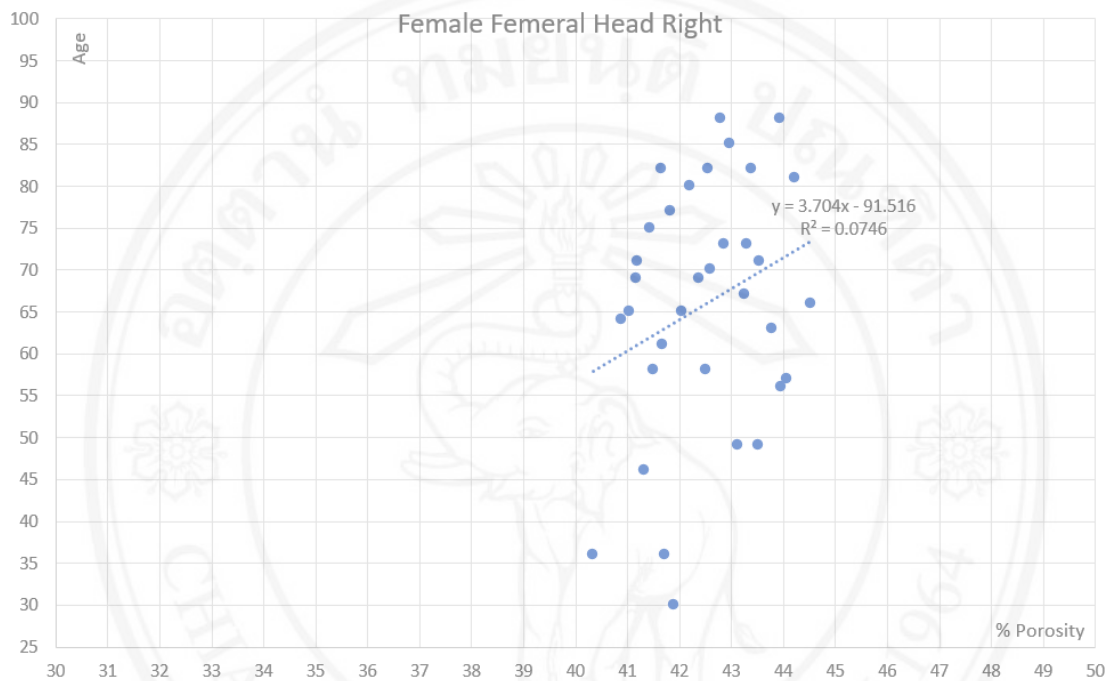


Figure 4.8 Percent porosity and age of female femoral head right side.

Table 4.8 Percent porosity and age of female femoral head right side.

SUMMARY OUTPUT								
Regression Statistics								
Multiple R	0.273161888							
R Square	0.074617417							
Adjusted R Square	0.045699211							
Standard Error	14.55511501							
Observations	34							
ANOVA								
	df	SS	MS	F	Significance F			
Regression	1	546.6384196	546.6384196	2.58029208	0.118026133			
Residual	32	6779.243933	211.8513729					
Total	33	7325.882353						
	Coefficients	Standard Error	t Stat	P-value	Lower 95%	Upper 95%	Lower 90.0%	Upper 90.0%
Intercept	-91.5153993	98.05449934	-0.93331301	0.357647675	-291.2460191	108.2149392	-257.6089531	74.57787322
%poro	3.7039847	2.30586963	1.606328758	0.118026133	-0.992918036	8.400887435	-0.201901922	7.609871321

Female femoral head both sides, the results of percent porosity and age have shown as figure and table below. Number of bone sample (observations) is 59. The relationship equation is  $A = 3.1768P - 69.4137$  which A is age and P is percent porosity. Regression ( $R^2$ ) = 0.0585. P-value is 0.0648.

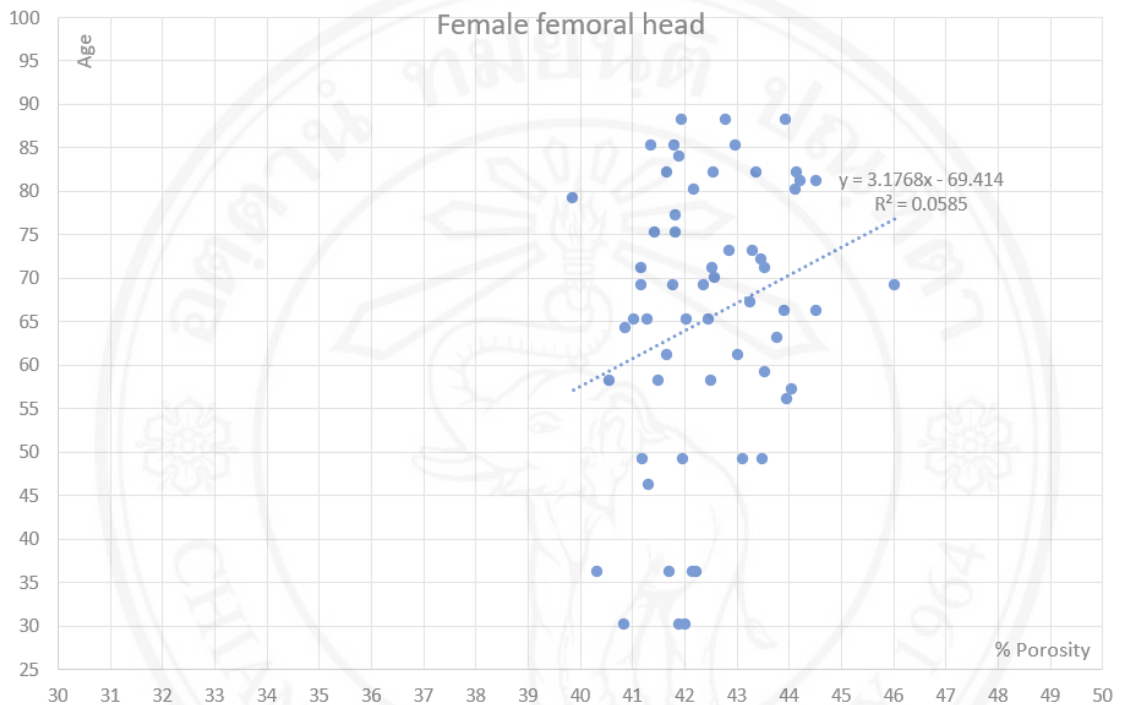


Figure 4.9 Percent porosity and age of female femoral head both sides.

Table 4.9 Percent porosity and age of female femoral head both sides.

SUMMARY OUTPUT								
<b>Regression Statistics</b>								
Multiple R	0.241967482							
R Square	0.058548262							
Adjusted R Square	0.042031565							
Standard Error	15.7184132							
Observations	59							
<b>ANOVA</b>								
	<i>df</i>	<i>SS</i>	<i>MS</i>	<i>F</i>	<i>Significance F</i>			
Regression	1	875.8065866	875.8065866	3.544792388	0.064839607			
Residual	57	14082.90528	247.0685136					
Total	58	14958.71186						
	<i>Coefficients</i>	<i>Standard Error</i>	<i>t Stat</i>	<i>P-value</i>	<i>Lower 95%</i>	<i>Upper 95%</i>	<i>Lower 90.0%</i>	<i>Upper 90.0%</i>
Intercept	-69.41371319	71.70005333	-0.968112435	0.337078213	-212.9905934	74.16316704	-189.2982737	50.47084728
%poro	3.176799533	1.687308165	1.882761904	0.064839607	-0.201976786	6.555575852	0.355571538	5.998027528

Male femoral head left side, the results of percent porosity and age have shown as figure and table below. Number of bone sample (observations) is 49. The relationship equation is  $A = 3.1073P - 65.1583$  which A is age and P is percent porosity. Regression ( $R^2$ ) = 0.0985. P-value is 0.0281.

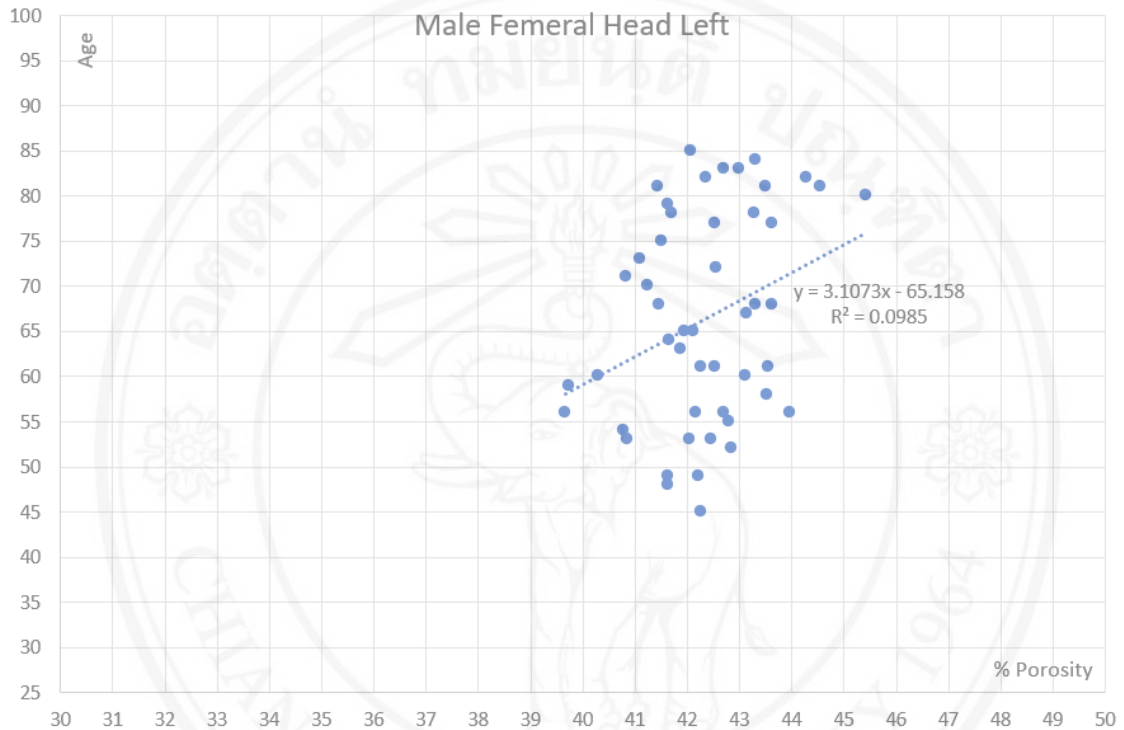


Figure 4.10 Percent porosity and age of male femoral head left side.

Table 4.10 Percent porosity and age of male femoral head left side.

SUMMARY OUTPUT								
<i>Regression Statistics</i>								
Multiple R	0.313879036							
R Square	0.09852005							
Adjusted R Square	0.079339625							
Standard Error	11.20171134							
Observations	49							
<i>ANOVA</i>								
	<i>df</i>	<i>SS</i>	<i>MS</i>	<i>F</i>	<i>Significance F</i>			
Regression	1	644.5181642	644.5181642	5.136489532	0.028072827			
Residual	47	5897.481836	125.4783369					
Total	48	6542						
	<i>Coefficients</i>	<i>Standard Error</i>	<i>t Stat</i>	<i>P-value</i>	<i>Lower 95%</i>	<i>Upper 95%</i>	<i>Lower 90.0%</i>	<i>Upper 90.0%</i>
Intercept	-65.15826422	58.0823438	-1.12182567	0.267635339	-182.0048684	51.68833993	-162.6161809	32.29965249
%poro	3.107320334	1.371048517	2.266382477	0.028072827	0.349126486	5.865514182	0.806801391	5.407839277



Male femoral head right side, the results of percent porosity and age have shown as figure and table below. Number of bone sample (observations) is 59. The relationship equation is  $A = 4.9079P - 138.2524$  which A is age and P is percent porosity. Regression ( $R^2$ ) = 0.1118. P-value is 0.0096.

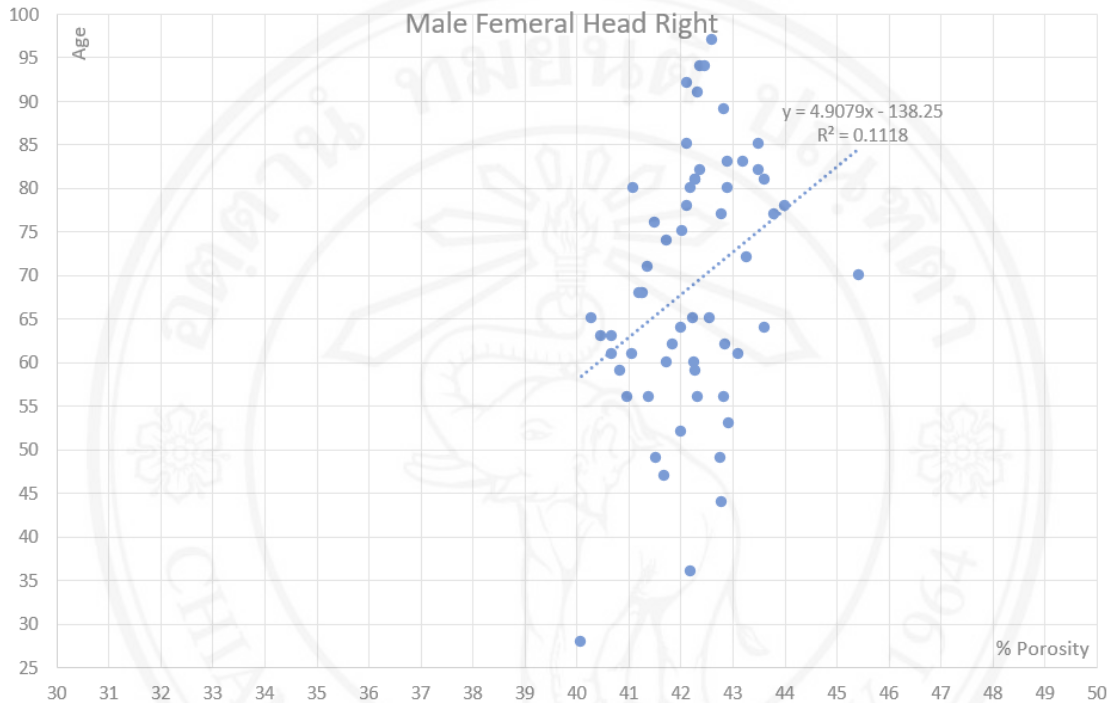


Figure 4.11 Percent porosity and age of male femoral head right side.

Table 4.11 Percent porosity and age of male femoral head right side.

SUMMARY OUTPUT								
<i>Regression Statistics</i>								
Multiple R	0.334329752							
R Square	0.111776383							
Adjusted R Square	0.096193513							
Standard Error	14.02498474							
Observations	59							
<i>ANOVA</i>								
	<i>df</i>	<i>SS</i>	<i>MS</i>	<i>F</i>	<i>Significance F</i>			
Regression	1	1410.936234	1410.936234	7.17302909	0.009652702			
Residual	57	11211.91122	196.7001969					
Total	58	12622.84746						
	<i>Coefficients</i>	<i>Standard Error</i>	<i>t Stat</i>	<i>P-value</i>	<i>Lower 95%</i>	<i>Upper 95%</i>	<i>Lower 90.0%</i>	<i>Upper 90.0%</i>
Intercept	-138.2523601	77.38602635	-1.78652874	0.079332154	-293.2152049	16.71048468	-267.6440317	-8.860688494
%poro	4.907924592	1.832510979	2.678251125	0.009652702	1.238384652	8.577464532	1.843913296	7.971935888



Male femoral head both sides, the results of percent porosity and age have shown as figure and table below. Number of bone sample (observations) is 108. The relationship equation is  $A = 3.8652P - 95.6029$  which A is age and P is percent porosity. Regression ( $R^2$ ) = 0.0972. P-value is 0.0010.

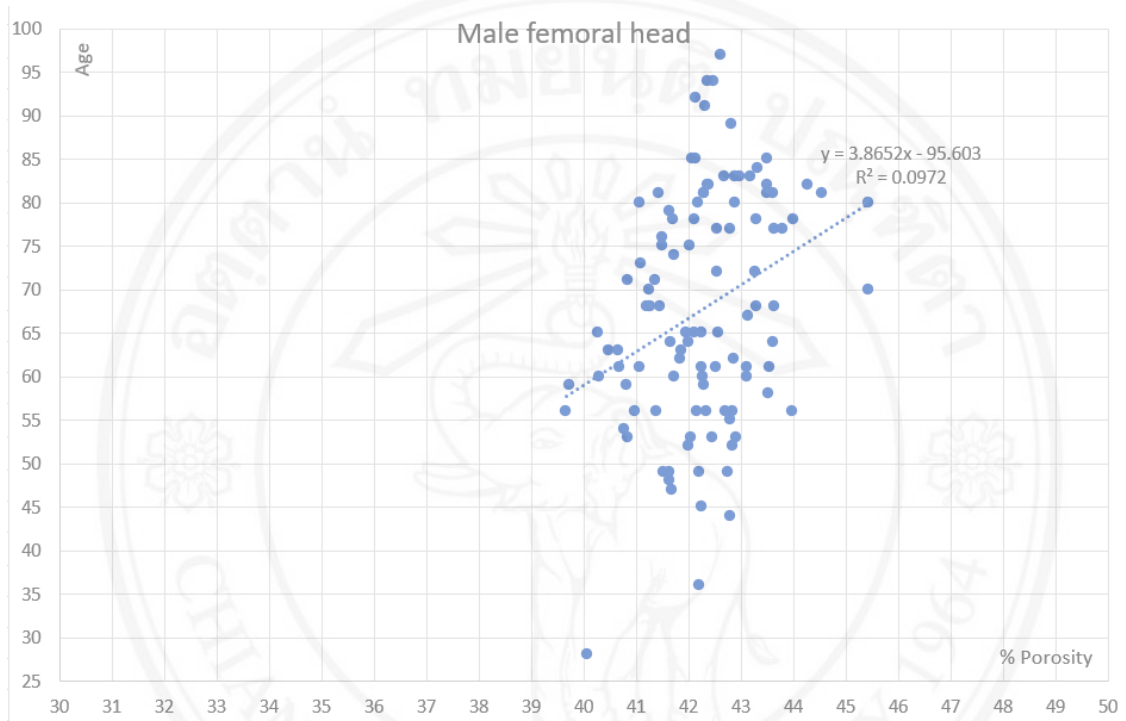


Figure 4.12 Percent porosity and age of male femoral head both sides.

Table 4.12 Percent porosity and age of male femoral head both sides.

SUMMARY OUTPUT								
Regression Statistics								
Multiple R	0.311747929							
R Square	0.097186771							
Adjusted R Square	0.088669665							
Standard Error	12.83267445							
Observations	108							
ANOVA								
	df	SS	MS	F	Significance F			
Regression	1	1879.098122	1879.098122	11.41077403	0.001022247			
Residual	106	17455.81854	164.6775334					
Total	107	19334.91667						
	Coefficients	Standard Error	t Stat	P-value	Lower 95%	Upper 95%	Lower 90.0%	Upper 90.0%
Intercept	-95.60292658	48.39031943	-1.975662234	0.050792263	-191.5414414	0.335588224	-175.8996951	-15.30615804
%poro	3.865226956	1.144240847	3.377983723	0.001022247	1.596658186	6.133795726	1.966524002	5.763929909

#### 4.1.2 Area ratio and age

##### Acetabulum



ลิขสิทธิ์มหาวิทยาลัยเชียงใหม่  
Copyright© by Chiang Mai University  
All rights reserved

Female acetabulum left side, the results of area ratio and age have shown as figure and table below. Number of bone sample (observations) is 21. The relationship equation is  $A = -0.5687R + 94.4611$  which A is age and R is area ratio. Regression ( $R^2$ ) = 0.0354. P-value is 0.4144.

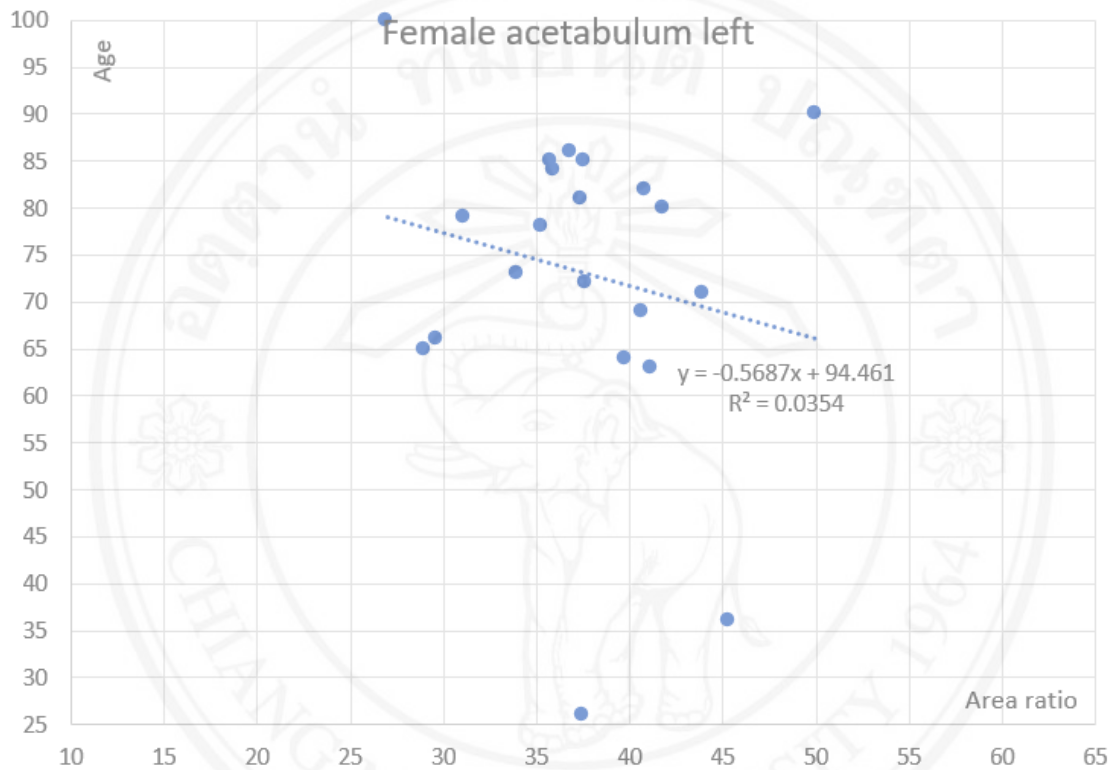


Figure 4.13 Area ratio and age of female acetabulum left side.

Table 4.13 Area ratio and age of female acetabulum left side.

SUMMARY OUTPUT								
Regression Statistics								
Multiple R	0.18802265							
R Square	0.035352517							
Adjusted R Square	-0.015418403							
Standard Error	17.07684089							
Observations	21							
ANOVA								
	df	SS	MS	F	Significance F			
Regression	1	203.0581233	203.0581233	0.696314284	0.414394033			
Residual	19	5540.7514	291.6184948					
Total	20	5743.809524						
	Coefficients	Standard Error	t Stat	P-value	Lower 95%	Upper 95%	Lower 90.0%	Upper 90.0%
Intercept	94.46108572	25.87432247	3.650765573	0.001700167	40.30550639	148.616665	49.72094575	139.2012257
Percent	-0.568724256	0.681552161	-0.834454483	0.414394033	-1.995229325	0.857780812	-1.747218462	0.609769949

Female acetabulum left side, the results of area ratio and age have shown as figure and table below. Number of bone sample (observations) is 28. The relationship equation is  $A = -1.0374R + 104.5570$  which A is age and R is area ratio. Regression ( $R^2$ ) = 0.0642. P-value is 0.1933.

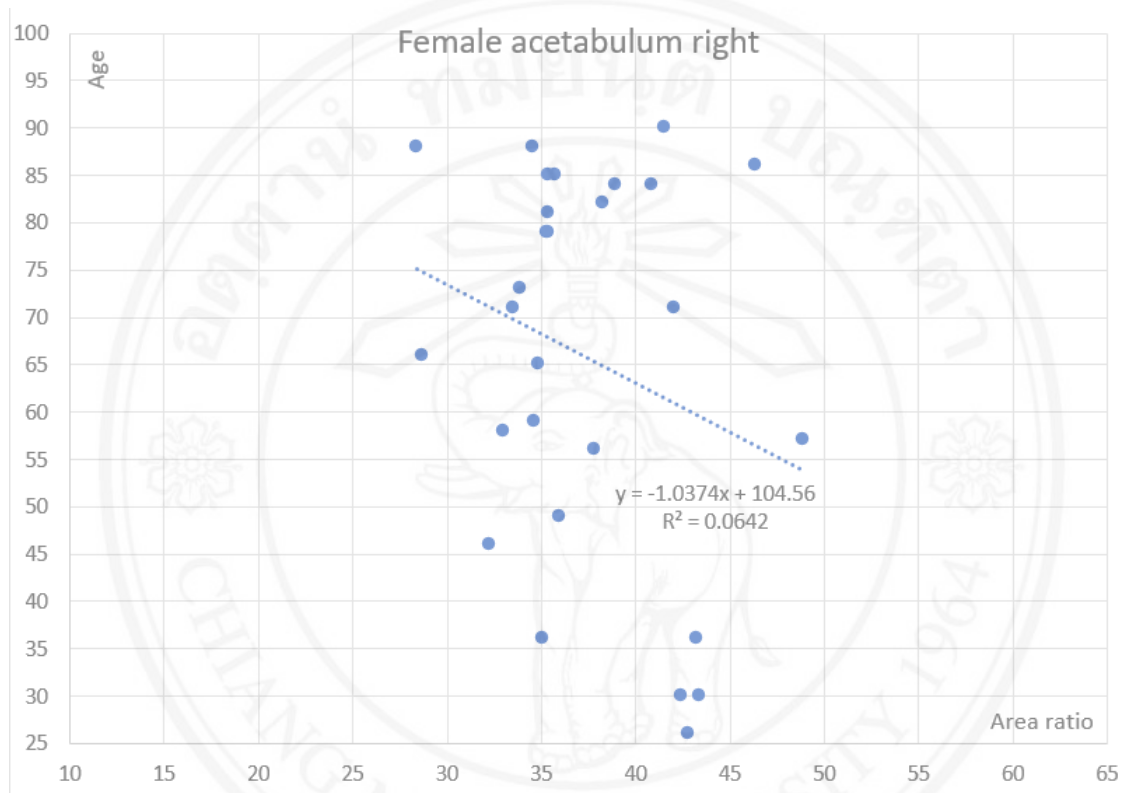


Figure 4.14 Area ratio and age of female acetabulum right side.

Table 4.14 Area ratio and age of female acetabulum right side.

SUMMARY OUTPUT								
Regression Statistics								
Multiple R	0.253374754							
R Square	0.064198766							
Adjusted R Square	-0.028206411							
Standard Error	20.08282969							
Observations	28							
ANOVA								
	df	SS	MS	F	Significance F			
Regression	1	719.3930305	719.3930305	1.783677835	0.193273202			
Residual	26	10486.32126	403.3200483					
Total	27	11205.71429						
	Coefficients	Standard Error	t Stat	P-value	Lower 95%	Upper 95%	Lower 90.0%	Upper 90.0%
Intercept	104.5570131	29.33041272	3.564798562	0.001438239	44.2674863	164.8465399	54.53053557	154.5834906
Percent	-1.037378517	0.77674603	-1.335544022	0.193273202	-2.634002848	0.559245814	-2.362210465	0.287453431

Female acetabulum both sides, the results of area ratio and age have shown as figure and table below. Number of bone sample (observations) is 49. The relationship equation is  $A = -0.8018R + 98.9409$  which A is age and R is area ratio. Regression ( $R^2$ ) = 0.0473. P-value is 0.1331.

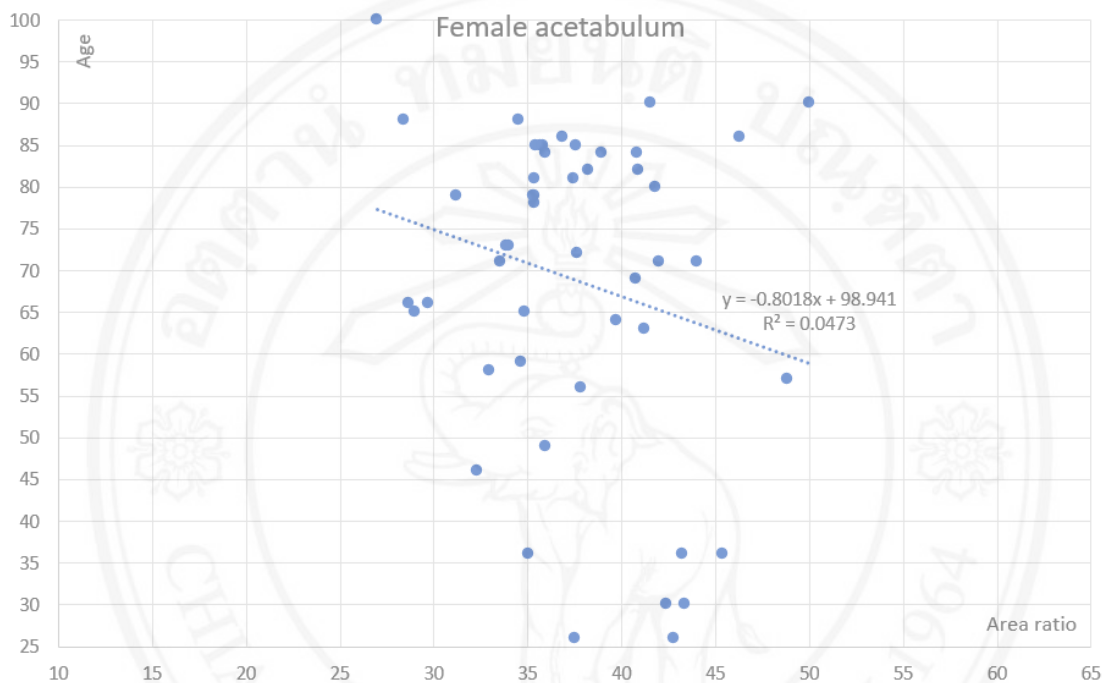


Figure 4.15 Area ratio and age of female acetabulum both sides.

Table 4.15 Area ratio and age of female acetabulum both sides.

SUMMARY OUTPUT								
<i>Regression Statistics</i>								
Multiple R	0.217584535							
R Square	0.04734303							
Adjusted R Square	0.027073732							
Standard Error	18.8893043							
Observations	49							
<i>ANOVA</i>								
	<i>df</i>	<i>SS</i>	<i>MS</i>	<i>F</i>	<i>Significance F</i>			
Regression	1	833.3919125	833.3919125	2.335701586	0.133140761			
Residual	47	16769.87339	356.8058169					
Total	48	17603.26531						
	<i>Coefficients</i>	<i>Standard Error</i>	<i>t Stat</i>	<i>P-value</i>	<i>Lower 95%</i>	<i>Upper 95%</i>	<i>Lower 90.0%</i>	<i>Upper 90.0%</i>
Intercept	98.94086447	19.8553034	4.98309507	8.90685E-06	58.99714622	138.8845827	65.62512034	132.2566086
Percent	-0.801759498	0.524608636	-1.528300228	0.133140761	-1.857135945	0.253616949	-1.682014347	0.078495351

Male acetabulum left side, the results of area ratio and age have shown as figure and table below. Number of bone sample (observations) is 44. The relationship equation is  $A = 0.1324R + 63.7569$  which A is age and R is area ratio. Regression ( $R^2$ ) = 0.0033. P-value is 0.7124.

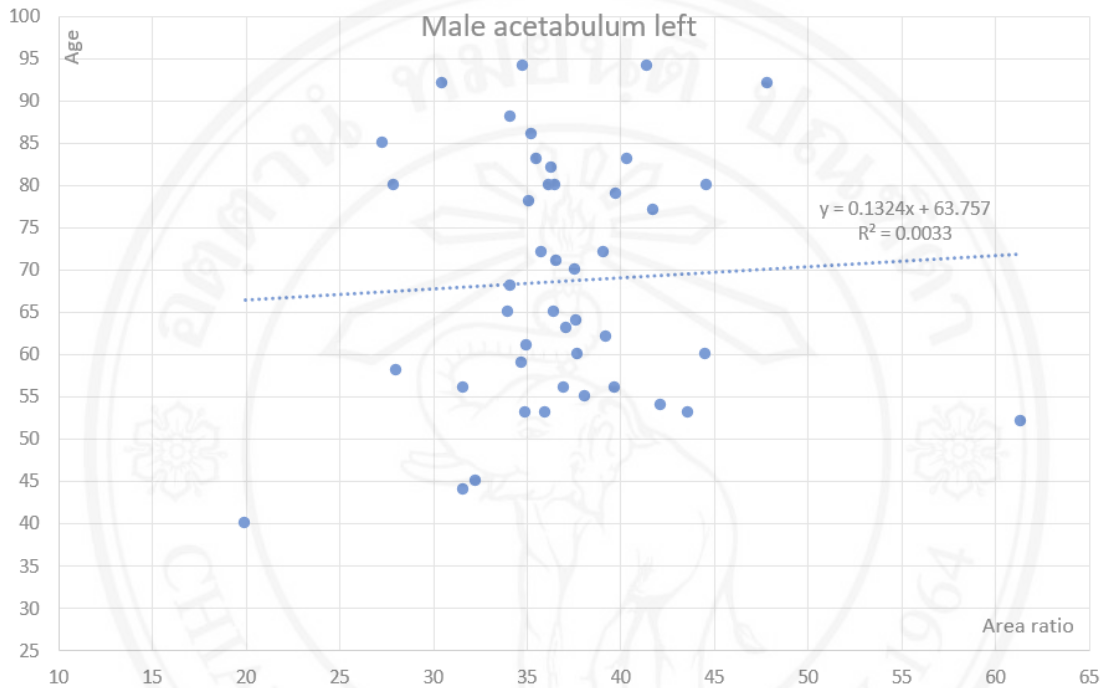


Figure 4.16 Area ratio and age of male acetabulum left side.

Table 4.16 Area ratio and age of male acetabulum left side.

SUMMARY OUTPUT								
<i>Regression Statistics</i>								
Multiple R	0.057175121							
R Square	0.003268994							
Adjusted R Square	-0.020462696							
Standard Error	14.7263201							
Observations	44							
<i>ANOVA</i>								
	<i>df</i>	<i>SS</i>	<i>MS</i>	<i>F</i>	<i>Significance F</i>			
Regression	1	29.87266558	29.87266558	0.137748064	0.712395721			
Residual	42	9108.309153	216.8645036					
Total	43	9138.181818						
	<i>Coefficients</i>	<i>Standard Error</i>	<i>t Stat</i>	<i>P-value</i>	<i>Lower 95%</i>	<i>Upper 95%</i>	<i>Lower 90.0%</i>	<i>Upper 90.0%</i>
Intercept	63.75688911	13.33323834	4.781800751	2.15511E-05	36.84932478	90.66445345	41.33101745	86.18276078
Percent	0.132389038	0.356705062	0.371144263	0.712395721	-0.587470922	0.852248997	-0.467571883	0.732349958

Male acetabulum right side, the results of area ratio and age have shown as figure and table below. Number of bone sample (observations) is 57. The relationship equation is  $A = -0.6275R + 88.4590$  which A is age and R is area ratio. Regression ( $R^2$ ) = 0.0306. P-value is 0.1928.

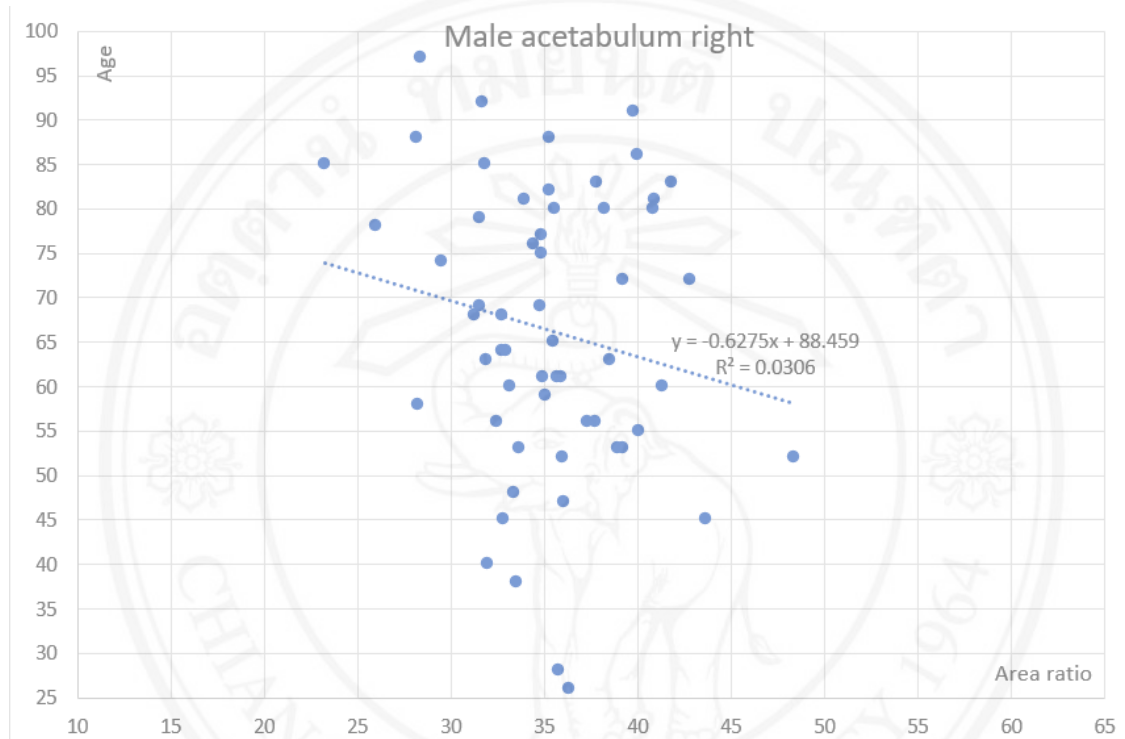


Figure 4.17 Area ratio and age of male acetabulum right side.

Table 4.17 Area ratio and age of male acetabulum right side.

SUMMARY OUTPUT								
<i>Regression Statistics</i>								
Multiple R	0.175042456							
R Square	0.030639861							
Adjusted R Square	0.013015132							
Standard Error	16.08110025							
Observations	57							
<i>ANOVA</i>								
	<i>df</i>	<i>SS</i>	<i>MS</i>	<i>F</i>	<i>Significance F</i>			
Regression	1	449.5684731	449.5684731	1.738458505	0.192798626			
Residual	55	14223.09819	258.6017853					
Total	56	14672.66667						
	<i>Coefficients</i>	<i>Standard Error</i>	<i>t Stat</i>	<i>P-value</i>	<i>Lower 95%</i>	<i>Upper 95%</i>	<i>Lower 90.0%</i>	<i>Upper 90.0%</i>
Intercept	88.45895347	16.91546435	5.229472373	2.71993E-06	54.55960539	122.3583015	60.15880708	116.7590999
Percent	-0.627486951	0.475907484	-1.318506164	0.192798626	-1.581226861	0.326252959	-1.423696336	0.168722434

Male acetabulum both sides, the results of area ratio and age have shown as figure and table below. Number of bone sample (observations) is 101. The relationship equation is  $A = -0.1373R + 72.2740$  which A is age and R is area ratio. Regression ( $R^2$ ) = 0.0023. P-value is 0.6345.

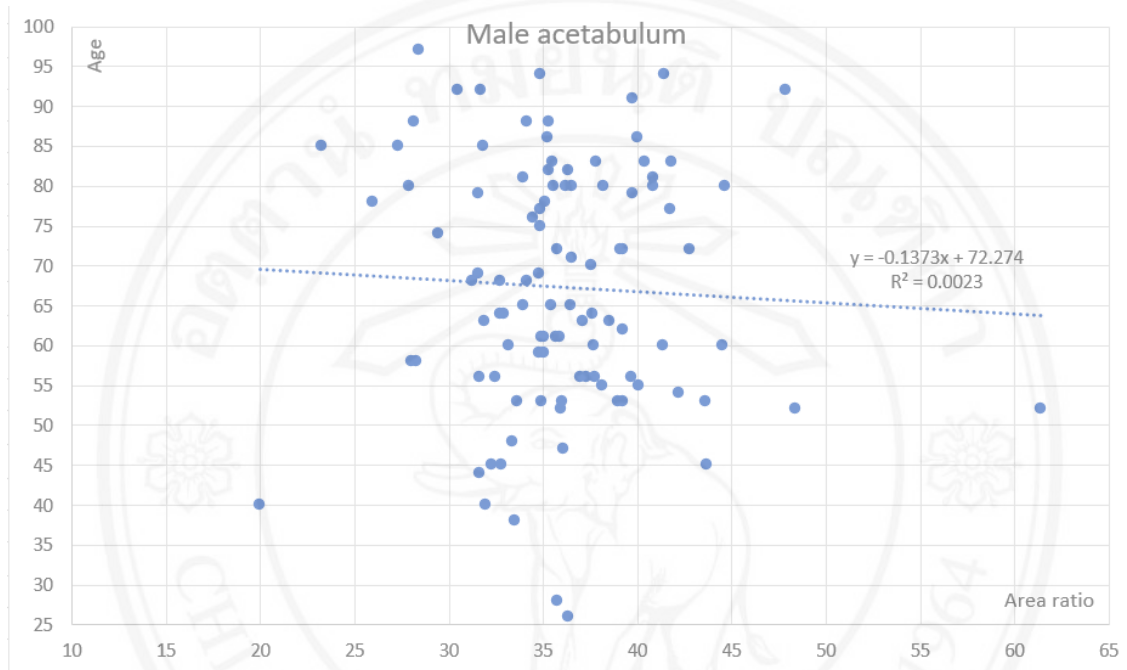


Figure 4.18 Area ratio and age of male acetabulum both sides.

Table 4.18 Area ratio and age of male acetabulum both sides.

SUMMARY OUTPUT								
<i>Regression Statistics</i>								
Multiple R	0.047868175							
R Square	0.002291362							
Adjusted R Square	-0.007786503							
Standard Error	15.53350676							
Observations	101							
<i>ANOVA</i>								
	<i>df</i>	<i>SS</i>	<i>MS</i>	<i>F</i>	<i>Significance F</i>			
Regression	1	54.86106312	54.86106312	0.227365831	0.634534787			
Residual	99	23887.69339	241.2898322					
Total	100	23942.55446						
	<i>Coefficients</i>	<i>Standard Error</i>	<i>t Stat</i>	<i>P-value</i>	<i>Lower 95%</i>	<i>Upper 95%</i>	<i>Lower 90.0%</i>	<i>Upper 90.0%</i>
Intercept	72.27403566	10.46938464	6.903369982	4.90476E-10	51.50050518	93.04756614	54.89076199	89.65730933
Percent	-0.137317322	0.287980264	-0.476828932	0.634534787	-0.708732642	0.434097999	-0.615477204	0.340842561



### Femoral head

Female femoral head left side, the results of area ratio and age have shown as figure and table below. Number of bone sample (observations) is 21. The relationship equation is  $A = 2.5970R + 28.8814$  which A is age and R is area ratio. Regression ( $R^2$ ) = 0.1877. P-value is 0.0497.

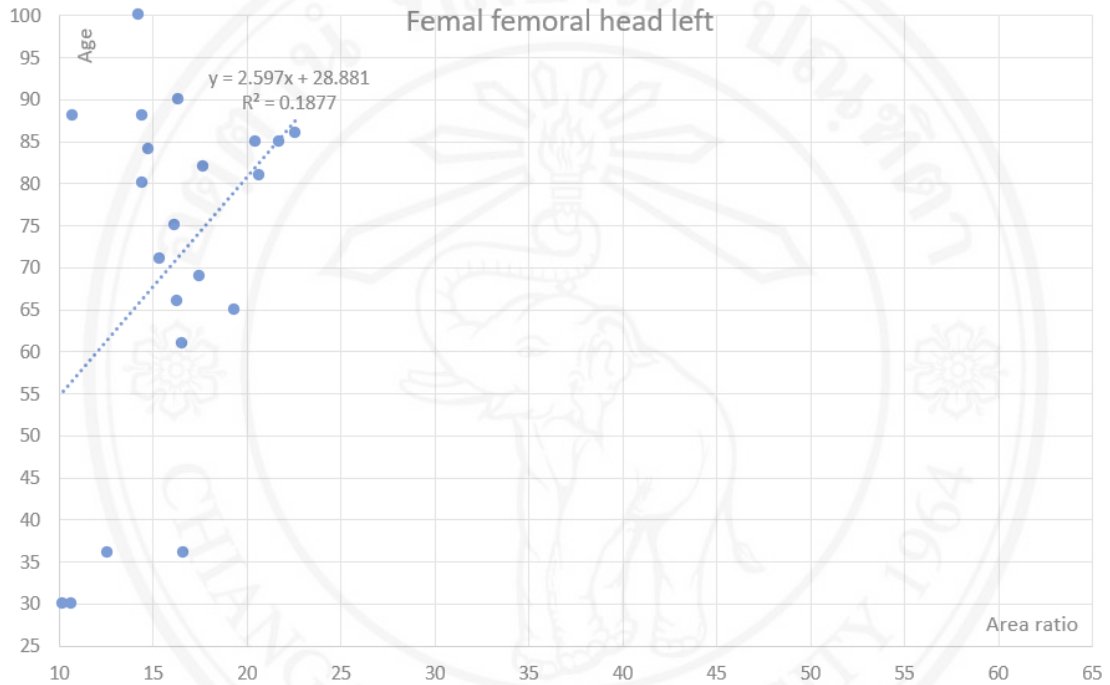


Figure 4.19 Area ratio and age of female femoral head left side.

Table 4.19 Area ratio and age of female femoral head left side.

SUMMARY OUTPUT								
<i>Regression Statistics</i>								
Multiple R	0.43328487							
R Square	0.187735778							
Adjusted R Square	0.14498503							
Standard Error	19.4626838							
Observations	21							
<i>ANOVA</i>								
	<i>df</i>	<i>SS</i>	<i>MS</i>	<i>F</i>	<i>Significance F</i>			
Regression	1	1663.446273	1663.446273	4.391403304	0.049749031			
Residual	19	7197.125155	378.7960608					
Total	20	8860.571429						
	<i>Coefficients</i>	<i>Standard Error</i>	<i>t Stat</i>	<i>P-value</i>	<i>Lower 95%</i>	<i>Upper 95%</i>	<i>Lower 90.0%</i>	<i>Upper 90.0%</i>
Intercept	28.8814546	20.47600837	1.410502188	0.174554087	-13.97532345	71.73823265	-6.524283319	64.28719252
Percent	2.597038155	1.239300623	2.095567538	0.049749031	0.00315214	5.190924169	0.454122784	4.739953525

Female femoral head right side, the results of area ratio and age have shown as figure and table below. Number of bone sample (observations) is 31. The relationship equation is  $A = 2.6049R + 33.7348$  which A is age and R is area ratio. Regression ( $R^2$ ) = 0.2023. P-value is 0.0111.

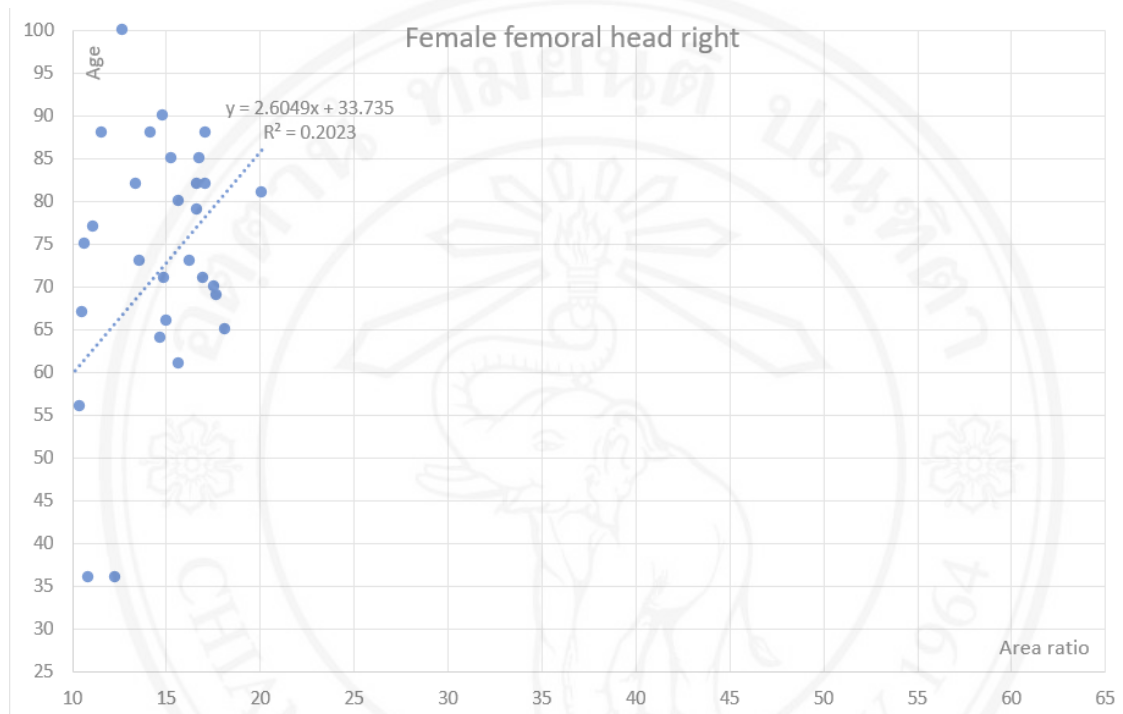


Figure 4.20 Area ratio and age of female femoral head right side.

Table 4.20 Area ratio and age of female femoral head right side.

SUMMARY OUTPUT								
<b>Regression Statistics</b>								
Multiple R	0.449738508							
R Square	0.202264725							
Adjusted R Square	0.174756613							
Standard Error	15.14085579							
Observations	31							
<b>ANOVA</b>								
	<i>df</i>	<i>SS</i>	<i>MS</i>	<i>F</i>	<i>Significance F</i>			
Regression	1	1685.622024	1685.622024	7.352911704	0.011135892			
Residual	29	6648.119911	229.2455142					
Total	30	8333.741935						
	<i>Coefficients</i>	<i>Standard Error</i>	<i>t Stat</i>	<i>P-value</i>	<i>Lower 95%</i>	<i>Upper 95%</i>	<i>Lower 90.0%</i>	<i>Upper 90.0%</i>
Intercept	33.73481597	14.18430789	2.378319495	0.024197466	4.724649031	62.74498291	9.633875091	57.83575685
Percent	2.604860544	0.960627029	2.711625288	0.011135892	0.64015767	4.569563419	0.972633197	4.237087891

Female femoral head both sides, the results of area ratio and age have shown as figure and table below. Number of bone sample (observations) is 52. The relationship equation is  $A = 2.4047R + 34.7602$  which A is age and R is area ratio. Regression ( $R^2$ ) = 0.1782. P-value is 0.0018.

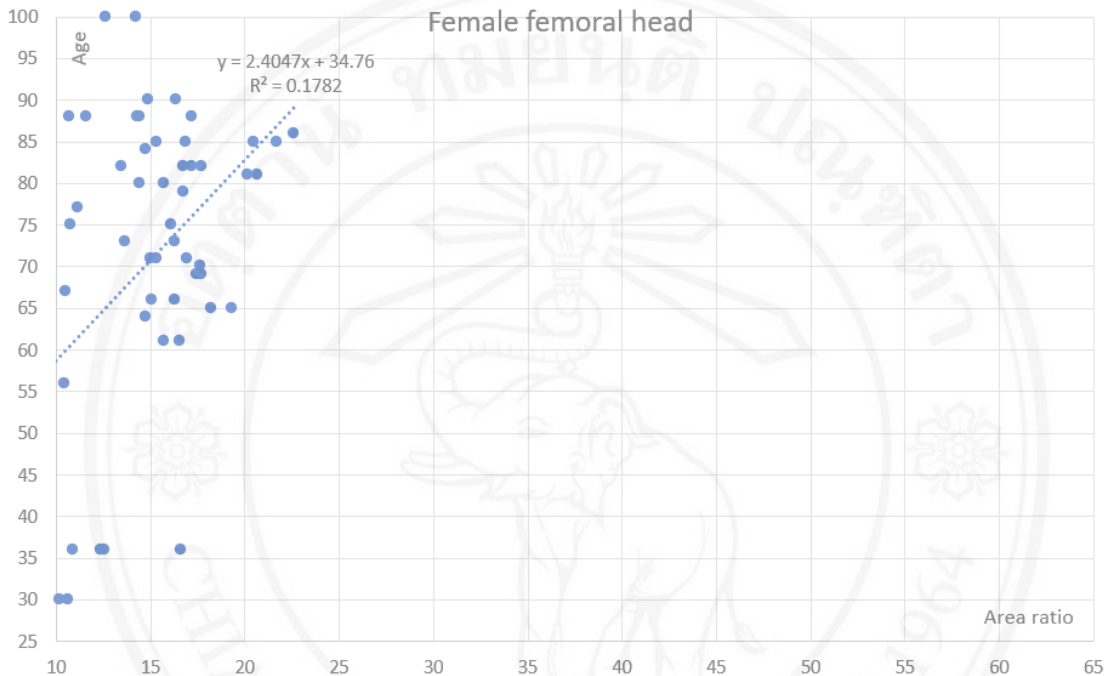


Figure 4.21 Area ratio and age of female femoral head both sides.

Table 4.21 Area ratio and age of female femoral head both sides.

Regression Statistics								
Multiple R	0.422127496							
R Square	0.178191623							
Adjusted R Square	0.161755455							
Standard Error	16.81337082							
Observations	52							
ANOVA								
	<i>df</i>	<i>SS</i>	<i>MS</i>	<i>F</i>	<i>Significance F</i>			
Regression	1	3064.758845	3064.758845	10.84143384	0.001826332			
Residual	50	14134.47192	282.6894385					
Total	51	17199.23077						
	<i>Coefficients</i>	<i>Standard Error</i>	<i>t Stat</i>	<i>P-value</i>	<i>Lower 95%</i>	<i>Upper 95%</i>	<i>Lower 90.0%</i>	<i>Upper 90.0%</i>
Intercept	34.76020347	11.31915452	3.070918716	0.003446597	12.02501251	57.49539443	15.79037553	53.73003142
X Variable 1	2.404654374	0.730313454	3.292633268	0.001826332	0.937776632	3.871532115	1.180718387	3.62859036

Male femoral head left side, the results of area ratio and age have shown as figure and table below. Number of bone sample (observations) is 48. The relationship equation is  $A = 0.9023R + 53.0514$  which A is age and R is area ratio. Regression ( $R^2$ ) = 0.0794. P-value is 0.0524.

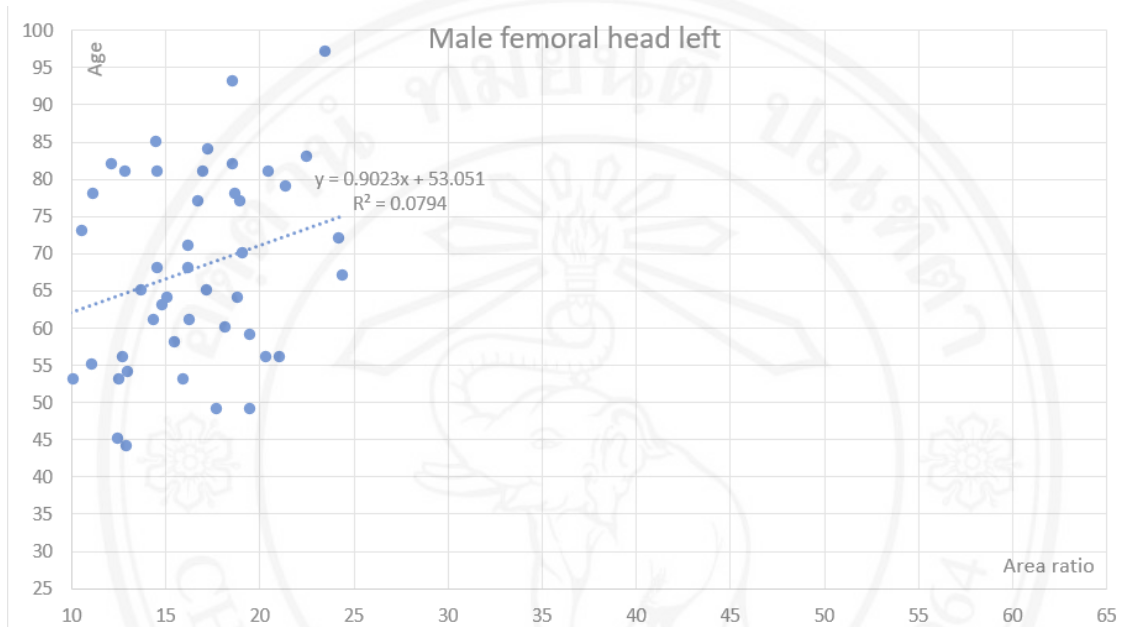


Figure 4.22 Area ratio and age of male femoral head left side.

Table 4.22 Area ratio and age of male femoral head left side.

SUMMARY OUTPUT								
Regression Statistics								
Multiple R	0.281713316							
R Square	0.079362392							
Adjusted R Square	0.059348531							
Standard Error	12.54009209							
Observations	48							
ANOVA								
	df	SS	MS	F	Significance F			
Regression	1	623.5701582	623.5701582	3.965371416	0.052403119			
Residual	46	7233.679842	157.2539096					
Total	47	7857.25						
	Coefficients	Standard Error	t Stat	P-value	Lower 95%	Upper 95%	Lower 90.0%	Upper 90.0%
Intercept	53.05138992	7.539054188	7.036876058	8.02276E-09	37.87606093	68.22671892	40.3958781	65.70690174
Percent	0.90225234	0.453091673	1.991324036	0.052403119	-0.009773896	1.814278575	0.141665284	1.662839396

Male femoral head right side, the results of area ratio and age have shown as figure and table below. Number of bone sample (observations) is 55. The relationship equation is  $A = 1.4185R + 47.3948$  which A is age and R is area ratio. Regression ( $R^2$ ) = 0.1628. P-value is 0.0022.

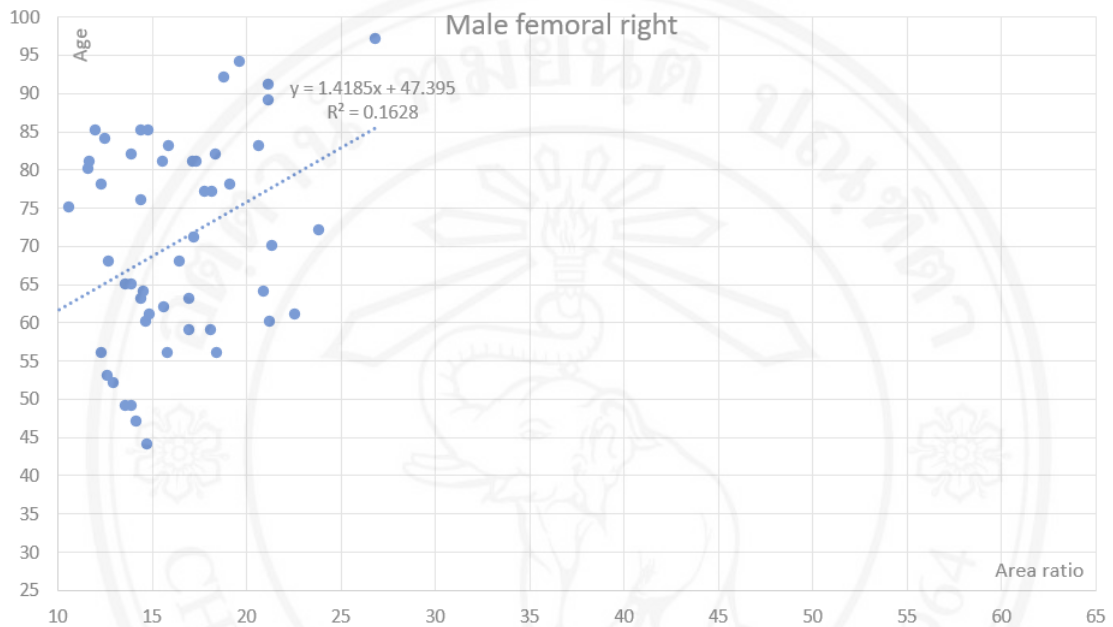


Figure 4.23 Area ratio and age of male femoral head right side.

Table 4.23 Area ratio and age of male femoral head right side.

SUMMARY OUTPUT								
Regression Statistics								
Multiple R	0.403431332							
R Square	0.16275684							
Adjusted R Square	0.146959799							
Standard Error	13.5583453							
Observations	55							
ANOVA								
	df	SS	MS	F	Significance F			
Regression	1	1893.98655	1893.98655	10.3029955	0.002256939			
Residual	53	9742.922541	183.8287272					
Total	54	11636.90909						
	Coefficients	Standard Error	t Stat	P-value	Lower 95%	Upper 95%	Lower 90.0%	Upper 90.0%
Intercept	47.39480291	7.193715644	6.588362017	2.07179E-08	32.96603657	61.82356926	35.35168675	59.43791908
Percent	1.418471516	0.441915123	3.209827955	0.002256939	0.532102028	2.304841005	0.678654233	2.158288799

Male femoral head both sides, the results of area ratio and age have shown as figure and table below. Number of bone sample (observations) is 103. The relationship equation is  $A = 1.1710R + 50.0877$  which A is age and R is area ratio. Regression ( $R^2$ ) = 0.1197. P-value is 0.0003.

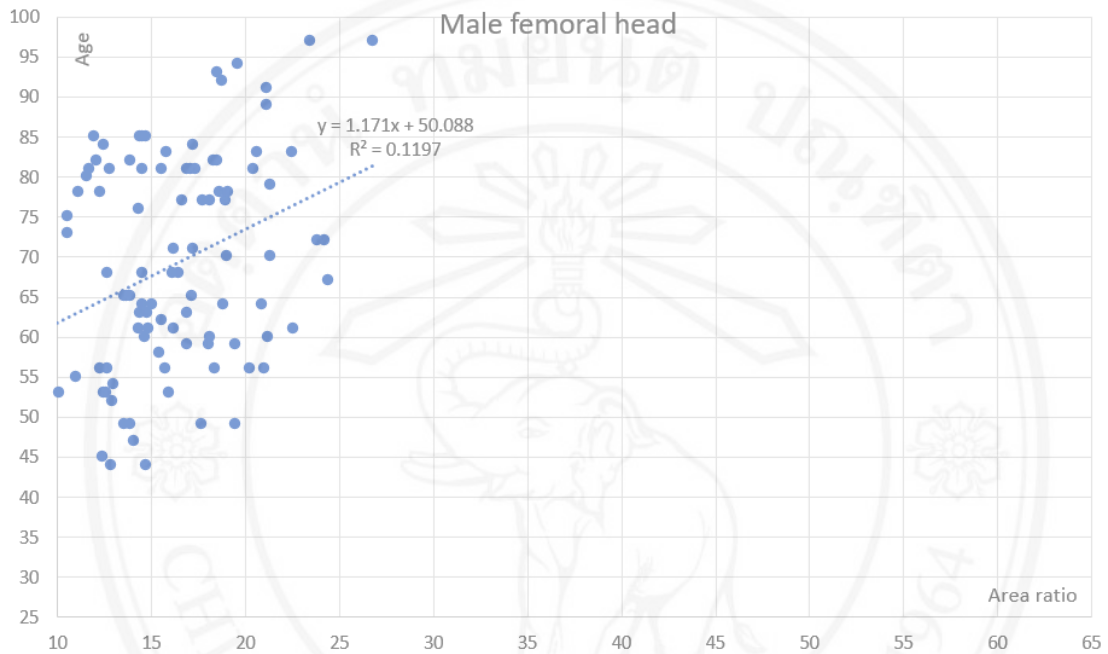


Figure 4.24 Area ratio and age of male femoral head both sides.

Table 4.24 Area ratio and age of male femoral head both sides.

Regression Statistics									
Multiple R	0.34598922								
R Square	0.11970854								
Adjusted R Square	0.110992783								
Standard Error	13.07263003								
Observations	103								
ANOVA									
		<i>df</i>	<i>SS</i>	<i>MS</i>	<i>F</i>	<i>Significance F</i>			
Regression		1	2347.177648	2347.177648	13.73472664	0.000343886			
Residual		101	17260.25924	170.8936559					
Total		102	19607.43689						
		<i>Coefficients</i>	<i>Standard Error</i>	<i>t Stat</i>	<i>P-value</i>	<i>Lower 95%</i>	<i>Upper 95%</i>	<i>Lower 90.0%</i>	<i>Upper 90.0%</i>
Intercept		50.08773626	5.19713326	9.637570128	5.64332E-16	39.77802189	60.39745063	41.460076	58.71539652
X Variable 1		1.171042626	0.315982255	3.706039212	0.000343886	0.544218831	1.797866421	0.646486606	1.695598647

## 4.2 Solutions of every group

Table 4.25 Percent porosity and age relationship.

	F/M	Part	L/R	Sample	Equation	R <sup>2</sup>	P-value	Relation
1	F	Ac	L	17	$A = 0.2316P + 67.072$	0.0069	0.7184	Non-Relate
2	F	Ac	R	23	$A = 0.7801P + 36.292$	0.0336	0.4022	Non-Relate
3	F	Ac	B	40	$A = 0.5004P + 51.475$	0.0160	0.4361	Non-Relate
4	M	Ac	L	35	$A = 2.2776P - 25.2553$	0.3317	0.0003	Relate
5	M	Ac	R	48	$A = 2.4259P - 35.2704$	0.2118	0.0010	Relate
6	M	Ac	B	83	$A = 2.2899P - 27.964$	0.2442	$2.0612 \times 10^{-6}$	Relate
7	F	Fh	L	25	$A = 2.7106P - 50.054$	0.0452	0.3077	Non-Relate
8	F	Fh	R	34	$A = 3.7040P - 91.5155$	0.0746	0.1180	Non-Relate
9	F	Fh	B	59	$A = 3.1768P - 69.413$	0.0585	0.0648	Relate
10	M	Fh	L	49	$A = 3.1073P - 65.1583$	0.0985	0.0281	Relate
11	M	Fh	R	59	$A = 4.9079P - 138.252$	0.1118	0.0096	Relate
12	M	Fh	B	108	$A = 3.8652P - 95.6029$	0.0972	0.0010	Relate

Table 4.25 presents the results of the relationship between percent porosity and age across all sample groups. The abbreviations F/M, F, and M represent female and male, respectively. The terms Part, Ac, and Fh refer to the acetabulum and femoral head parts. The abbreviations L/R, L, R, and B indicate the left side, right side, and both sides, respectively. The column labeled "Sample" refers to the number of bone samples in each group. Equation A and P represent the estimated age and percent porosity, respectively. The R<sup>2</sup> value denotes the coefficient of determination, while the P-value is used to test the statistical significance of the relationship. A significance level ( $\alpha$ ) of 0.10 corresponds to a confidence level of 90%. A P-value less than 0.10 indicates a significant relationship between percent porosity and estimated age.

Table 4.26 Area ratio and age relationship.

	F/M	Part	L/R	Sample	Equation	R <sup>2</sup>	P-value	Relation
1	F	Ac	L	21	$A = -0.5687R + 94.4611$	0.0354	0.4144	Non-Relate
2	F	Ac	R	28	$A = -1.0374R + 104.5570$	0.0642	0.1933	Non-Relate
3	F	Ac	B	49	$A = -0.8018R + 98.9409$	0.0473	0.1331	Non-Relate
4	M	Ac	L	44	$A = 0.1324R + 63.7569$	0.0033	0.7124	Non-Relate
5	M	Ac	R	57	$A = -0.6275R + 88.4590$	0.0306	0.1928	Non-Relate
6	M	Ac	B	101	$A = -0.1373R + 72.2740$	0.0023	0.6345	Non-Relate
7	F	Fh	L	21	$A = 2.5970R + 28.8814$	0.1877	0.0497	Relate
8	F	Fh	R	31	$A = 2.6049R + 33.7348$	0.2023	0.0111	Relate
9	F	Fh	B	52	$A = 2.4047R + 34.7602$	0.1782	0.0018	Relate
10	M	Fh	L	48	$A = 0.9023R + 53.0514$	0.0794	0.0524	Relate
11	M	Fh	R	55	$A = 1.4185R + 47.3948$	0.1628	0.0022	Relate
12	M	Fh	B	103	$A = 1.1710R + 50.0877$	0.1197	0.0003	Relate

Table 4.26 presents the results of the relationship between area ratio and age across all sample groups. The abbreviations F/M, F, and M represent female and male, respectively. The terms Part, Ac, and Fh refer to the acetabulum and femoral head parts. The abbreviations L/R, L, R, and B indicate the left side, right side, and both sides, respectively. The column labeled "Sample" refers to the number of bone samples in each group. Equation A and R represent the estimated age and area ratio, respectively. The R<sup>2</sup> value denotes the coefficient of determination, while the P-value is used to test the statistical significance of the relationship. A significance level ( $\alpha$ ) of 0.10 corresponds to a confidence level of 90%. A P-value less than 0.10 indicates a significant relationship between percent porosity and estimated age.

#### 4.3 Solution of equations audit

The relationship between percent porosity and age, as presented in Table 4.25, shows a correlation within the male group. This group includes the acetabulum and femoral head on both the left and right sides. The equations were validated using external subjects, with 10 test samples per group. The results are reported as average error, minimum error, and maximum error, with errors measured in years. M represent male.



Ac, and Fh refer to the acetabulum and femoral head parts. L and R indicate the left and right side.

Table 4.27 Equations audit of percent porosity and age relationship.

Group	Relation	Equation	Ave error (year)	Min error (year)	Max error (year)
M-Ac-L	Relate	$A = 2.2776P - 25.2553$	9	0	16
M-Ac-R	Relate	$A = 2.4259P - 35.2704$	6	0	11
M-Fh-L	Relate	$A = 3.1073P - 65.1583$	5	0	11
M-Fh-R	Relate	$A = 4.9079P - 138.2524$	9	3	16

The relationship between area ratio and age, as presented in Table 4.26, shows a correlation within the femoral head group. This group includes both female and male on both the left and right sides. The equations were validated using external subjects, with 10 test samples per group. The results are reported as average error, minimum error, and maximum error, with errors measured in years. F and M represent female and male. Fh refer to the femoral head parts. L and R indicate the left and right side.

Table 4.28 Equations audit of area ratio and age relationship.

Group	Relation	Equation	Ave error (year)	Min error (year)	Max error (year)
F-Fh-L	Relate	$A = 2.597R + 28.8814$	17	0	36
F-Fh-R	Relate	$A = 2.605R + 33.7348$	8	3	17
M-Fh-L	Relate	$A = 0.902R + 53.0514$	11	3	15
M-Fh-R	Relate	$A = 1.418R + 47.3948$	8	1	13

Copyright © by Chiang Mai University  
All rights reserved

## CHAPTER 5

### Conclusion and Suggestion

The conclusion is divided into three sections: the relationship between percent porosity and age, the relationship between area ratio and age, and the evaluation of the equations. Suggestions will be discussed thereafter.

Samples are captured from 167 skeletons, divided into 59 females aged 26 to 100 years and 108 males aged 26 to 97 years. The skeleton donations spanned from 2011 to 2019.

The resulting equations are linear, such as the equation for the relationship between percent porosity and age:  $A = 2.2776P - 25.2553$  where P represents percent porosity and A represents age. In applying this equation, bone images are used to determine the percent porosity (P), which is then substituted into the equation to estimate the age (A). Similarly, for the relationship between area ratio and age, the equation is  $A = 2.5970R + 28.8814$ , where R represents the area ratio. To apply this equation, bone images are used to calculate the area ratio (R), which is then used in the equation to estimate age (A).

#### 5.1 Percent porosity and age relationship

The relationship between percent porosity and age is presented in Table 4.25, with statistical analysis conducted at a significance level of  $\alpha = 0.10$ , corresponding to a 90% confidence level. A statistically significant relationship between percent porosity and estimated age is observed only in the male group, as shown in Table 5.1. In contrast, no significant relationship is found in the female group, as indicated in Table 5.2. The relationship in the male group is evident in both the acetabulum and femoral head regions, as well as on both the left and right sides. However, the regression values ( $R^2$ ) are relatively low, ranging from 0.0972 to 0.3317. The number of samples in the male group is 83 for the acetabulum and 108 for the femoral head, while in the female group, the sample sizes are 40 and 59 for the acetabulum and femoral head, respectively.

Table 5.1 Percent porosity and age relationship.

	F/M	Part	L/R	Sample	Equation	R <sup>2</sup>	P-value	Relation
1	M	Ac	L	35	$A = 2.2776P - 25.2553$	0.3317	0.0003	Relate
2	M	Ac	R	48	$A = 2.4259P - 35.2704$	0.2118	0.0010	Relate
3	M	Ac	B	83	$A = 2.2899P - 27.964$	0.2442	$2.0612 \times 10^{-6}$	Relate
4	M	Fh	L	49	$A = 3.1073P - 65.1583$	0.0985	0.0281	Relate
5	M	Fh	R	59	$A = 4.9079P - 138.252$	0.1118	0.0096	Relate
6	M	Fh	B	108	$A = 3.8652P - 95.6029$	0.0972	0.0010	Relate

Table 5.2 Percent porosity and age non-relationship.

	F/M	Part	L/R	Sample	Equation	R <sup>2</sup>	P-value	Relation
1	F	Ac	L	17	$A = 0.2316P + 67.072$	0.0069	0.7184	Non-Relate
2	F	Ac	R	23	$A = 0.7801P + 36.292$	0.0336	0.4022	Non-Relate
3	F	Ac	B	40	$A = 0.5004P + 51.475$	0.0160	0.4361	Non-Relate
7	F	Fh	L	25	$A = 2.7106P - 50.054$	0.0452	0.3077	Non-Relate
8	F	Fh	R	34	$A = 3.7040P - 91.5155$	0.0746	0.1180	Non-Relate
9	F	Fh	B	59	$A = 3.1768P - 69.413$	0.0585	0.0648	Relate

## 5.2 Area ratio and age relationship

The relationship between area ratio and age is presented in Table 4.26, with statistical analysis conducted at a significance level of  $\alpha = 0.10$ , corresponding to a 90% confidence level. A statistically significant relationship between area ratio and estimated age is observed only in the femoral head, as shown in Table 5.3. In contrast, no significant relationship is found in the acetabulum, as indicated in Table 5.4. The relationship in the femoral head group is evident in both female and male, as well as on both the left and right sides. However, the regression values (R<sup>2</sup>) are relatively low, ranging from 0.0794 to 0.2023.

Table 5.3 Area ratio and age relationship.

	F/M	Part	L/R	Sample	Equation	R <sup>2</sup>	P-value	Relation
1	F	Fh	L	21	$A = 2.5970R + 28.8814$	0.1877	0.0497	Relate
2	F	Fh	R	31	$A = 2.6049R + 33.7348$	0.2023	0.0111	Relate
3	F	Fh	B	52	$A = 2.4047R + 34.7602$	0.1782	0.0018	Relate
4	M	Fh	L	48	$A = 0.9023R + 53.0514$	0.0794	0.0524	Relate
5	M	Fh	R	55	$A = 1.4185R + 47.3948$	0.1628	0.0022	Relate
6	M	Fh	B	103	$A = 1.1710R + 50.0877$	0.1197	0.0003	Relate

Table 5.4 Area ratio and age non-relationship.

	F/M	Part	L/R	Sample	Equation	R <sup>2</sup>	P-value	Relation
1	F	Ac	L	21	$A = -0.5687R + 94.4611$	0.0354	0.4144	Non-Relate
2	F	Ac	R	28	$A = -1.0374R + 104.5570$	0.0642	0.1933	Non-Relate
3	F	Ac	B	49	$A = -0.8018R + 98.9409$	0.0473	0.1331	Non-Relate
4	M	Ac	L	44	$A = 0.1324R + 63.7569$	0.0033	0.7124	Non-Relate
5	M	Ac	R	57	$A = -0.6275R + 88.4590$	0.0306	0.1928	Non-Relate
6	M	Ac	B	101	$A = -0.1373R + 72.2740$	0.0023	0.6345	Non-Relate

### 5.3 Solution of equations audit

The evaluation of equations relating percent porosity to age is presented in Table 4.27. The errors range from 0 to 16 years, with average errors ranging from 5 to 9 years. The evaluation of equations relating area ratio to age is shown in Table 4.28, with errors ranging from 0 to 36 years and average errors ranging from 8 to 17 years.

### 5.4 Suggestion

The hip joint, especially the acetabulum, is particularly well-suited for examination in ancient and forensic remains because, as part of the central area of the os coxa, it is one of the most well-preserved skeletal elements [Rissech, 2006]. Beyond the acetabular fossa, other regions can also be analyzed. Several variables, including the shape of each area, are of interest, not just porosity.

The bone samples used in this study were obtained from body donations made between 2011 and 2019, and are therefore relatively old. If more recent bone donations could be acquired, the resulting relationship equations would be more current. Younger bone donors are difficult to find, which is why the bones used in this research are from individuals aged 30 years and older. Most donors passed away due to illness, which has led to reduced bone strength in many cases. A significant challenge is the cleanliness of the bones, as it directly affects pixel values, leading to potential inaccuracies. However, we are unable to clean the bones, as doing so could alter police evidence.

The acetabulum has a cup-like shape, while the femoral head is spherical. Imaging involves transforming the three-dimensional structure of the bone into a two-dimensional image. The camera plane should be aligned with the plane of the acetabulum during imaging. The first error arises at this point. Errors accumulate at each stage, leading to a progressive increase in overall error. The lighting conditions during imaging have minimal impact on error because the calculations are based on the ratio of porous area to the total area. An electronic flash was used to control the lighting conditions. The use of an electronic flash also allowed for a higher shutter speed, reducing camera shake and image blur.

The use of image processing techniques for image analysis involves multiple steps. If errors occur at each stage, they can accumulate. To minimize this accumulated error, it is crucial to design the image processing workflow appropriately. Initially, the goal was to automatically separate the acetabular fossa from the acetabulum area. However, not all bones were intact or clearly demarcated. Figure 5.1 (left) shows an acetabular fossa that is clearly separated from the lunate surface, while Figure 5.1 (right) illustrates an acetabular fossa where half of the edge is continuous with the lunate surface. As a result, manual selection of the region of interest (ROI) was employed.

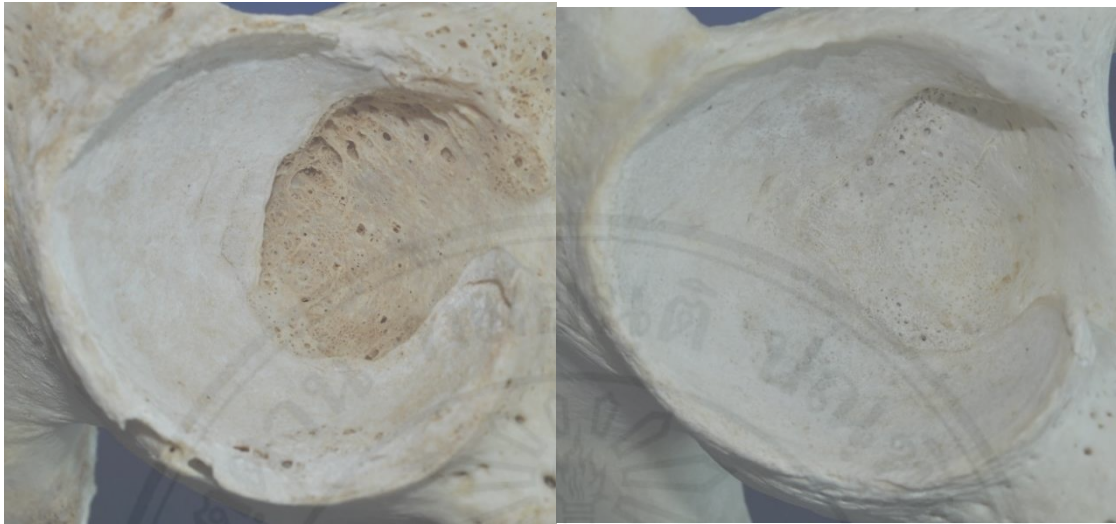


Figure 5.1 Clear acetabular fossa (left), Unclear acetabular fossa (right).

Most of the bones used in this study were donated by individuals who passed away due to illness. Human bones exhibit significant variability, even among individuals of the same age. As a result, the statistical outcomes yielded very low regression values, as shown in Tables 4.25 and 4.26. The quality of female bones differs from that of male bones, which may partly explain the lack of a significant relationship between percent porosity and estimated age in the female group. The male sample size was nearly double that of the female group, with 83 samples for the acetabulum and 108 for the femoral head in the male group, compared to 40 and 59 samples for the acetabulum and femoral head in the female group, respectively. Increasing the number of female samples might enhance the strength of the observed relationships.

As shown in Table 5.1, there is a relationship between percent porosity and estimated age in males, but the regression values are very low. No such relationship is observed in females. Khomkham (2017) reported statistically significant correlations with age at death: the left side of the acetabular groove in females ( $r = 0.61$ ), acetabular rim porosity ( $r = 0.59$ ), and apex activity score in the left-side male acetabulum ( $r = 0.62$ ) [Khomkham, 2017]. However, no significant correlation was found between the porosity of the acetabular fossa and age at death in Khomkham's study. The findings of this research align with Khomkham's results. Rissech (2006) demonstrated 89% accuracy in

10-year intervals, while the results of this study show errors ranging from 0 to 16 years, based on equations with a 90% confidence level.

The results indicate a correlation between bone porosity and age in males, but no such correlation was observed in females, both in the acetabulum and femoral head regions. Females exhibited greater variability in bone porosity compared to males, likely due to significant hormonal differences between the sexes. Additionally, the menstrual cycle in females may contribute to this variability in bone porosity.

In examining the association between area ratio and age, no statistically significant correlation was identified within the acetabulum, irrespective of sex or laterality. All p-values for comparisons in the acetabulum were greater than 0.10. San-Millan (2017) reported that both sex and age significantly influence variations in acetabular shape, with age-related changes evident in the acetabular structure of both sexes. These modifications are thought to be linked to bone formation associated with aging, impacting the entire margin of the lunate surface [San-Millan, 2017]. The findings of this study contrast with those of San-Millan. However, methodological differences between the studies should be noted. This study assessed the area ratio of the acetabular fossa relative to the acetabulum, whereas San-Millan's research concentrated on the shape of the acetabular fossa.

ลิขสิทธิ์มหาวิทยาลัยเชียงใหม่  
Copyright© by Chiang Mai University  
All rights reserved

## REFERENCES

- [Acar, 2017] Acar, N. et al, "Femoral head fovea capitis variant configurations and age-related changes- a radiological study," Iran J Radiol, April 2017.
- [Benazzi, 2009] Benazzi, S. et al, "Sex assessment from the sacral base by means of image processing," J Forensic Sci, Vol.54, No.2, March 2009, pp.249-254.
- [Bertsatos, 2018] Bertsatos, A. et al, "Morphological variation of the femoral head fovea capitis," Eur. J. Anat. 22 (5), 2018, pp.397-402.
- [Buikstra, 1994] Buikstra, J. E. and Ubelaker, D. H., "Standards for data collection from human skeletal remains," Proceedings of a Seminar at The Field Museum of Natural History, Arkansas Archeological Survey Research Series No.44, 1994.
- [Calce, 2011] Calce, E. S. and Rogers, T. L., "Evaluation of age estimation technique: testing traits of the acetabulum to estimate age at death in adult males," J. Forensic Sci. 56, 2011, pp.302–311.
- [Calce, 2012] Calce, E.S., "A new method to estimate adult age-at-death using the acetabulum," Am. J. Phys. Anthropol. 148, 2012, pp.11–23.
- [Cieszko, 2015] Cieszko, M. et al, "Determination of bone porosity based on histograms of 3D  $\mu$ CT images," J mater Sci, Vol.50, 2015, pp.948-959.
- [Daniel, 2010] Daniel, Wayne W., "Biostatistics; Basic Concepts and Methodology for the Health Sciences," 9<sup>th</sup> Ed., John Wiley & Sons Inc., 2010.
- [Evison, 2009] Evison, M.P., "Forensic anthropology and human identification," Handbook of Forensic Science, January 2009, pp.84-112.



- [Gonzalez, 2002] Gonzalez, Rafael C. and Woods, Richard E., "Digital Image Processing," 2<sup>nd</sup> Ed., Prentice-Hall Inc., 2002.
- [Khomkham, 2017] Khomkham, P. et al, "Association between age and acetabulum morphological changes in dry bones in the Thai population," Chiang Mai Med J, May 2017, 56(1), pp.21-28.
- [Kumar, 2019] Kumar Pal, A. et al, "Porosity Estimation by Digital Image Analysis," Researchgate Publication, January 2019.
- [Li, 2018] Li, Y. et al, "Forensic age estimation for pelvic x-ray images using deep learning," European Radiology, November 2018.
- [Lovejoy, 1985] Lovejoy, C. O. et al, "Multifactorial age determination of skeletal age at death: a method and blind tests of its accuracy," Am J Phys Anthropol;68, 1985, pp.1–14.
- [Martin, 2013] Martin III, William D. at al, "Using Image Analysis to Measure the Porosity distribution of a Porous Pavement," Construction and Building Materials 48, 2013, pp.210-217.
- [Navidi, 2008] Navidi, W., "Statistics for Engineers and Scientists," 2<sup>nd</sup> Ed., McGraw-Hill, 2008.
- [Otsu, 1979] Otsu, N., "Threshold selection method from gray-level histograms," IEEE Trans Syst Men Cybern SMC 9, 1979, pp.62–66.
- [Rajagopalan, 2004] Rajagopalan, S. et al, "Evaluation of thresholding techniques for segmenting scaffold images in tissue engineering," Proc SPIE 5370, 2004, pp.1456–1465.
- [Rissech, 2006] Rissech, C. et al, "Using the acetabulum to estimate age at death of adult males," J Forensic Sci, Vol.51, No.2, March 2006, pp.213-229.

- [Rosenfeld, 1983] Rosenfeld, A. and Torre, P., "Histogram concavity analysis as an aid in threshold selection," *IEEE Trans Syst Man Cybern SMC* 2, 1983, pp.231–235.
- [San-Millan, 2017] San-Millan, M. et al, "Shape variability of the adult human acetabulum and acetabular fossa related to sex and age by geometric morphometrics. Implications for adult age estimation," *Forensic Science International*, January 2017, pp.50-63.
- [Schmitt, 2002] Schmitt, A. et al, "Variability of the pattern of ageing on the human skeleton: evidence from bone indicators and implications on age at death estimation," *J Forensic Sci*;47, 2002, pp.348–476.
- [Sundari, 2021] Sundari, R. K., et al, "Age Related Anatomical Changes in Articular Cartilage of Femoral Head in Buffalo (*Bubalus bubalis*)," *Journal of Animal Research*: v.11 n.3, June 2021, pp.415-420.
- [Venara, 2013] Venara, A, et al, "Estimation of skeletal Age at Death in Adults Using the Acetabulum and the Auricular Surface," *Anthropol* 2: 113, 2013. doi:10.4172/2332-0915.1000113
- [Wang, 2003] Wang, X. and Ni, Q., "Determination of cortical bone porosity and pore size distribution using a low field pulsed NMR approach," *Journal of Orthopedic Research*, Vol.21, 2003, pp.312-319.
- [White, 2012] White, Tim D. et al, "Human Osteology," 3<sup>rd</sup> Ed., Elsevier Inc., 2012.
- [Whitmarsh, 2019] Whitmarsh, T. et al, "A cross-sectional study on the age-related cortical and trabecular bone changes at the femoral head in elderly female hip fracture patients," *Scientific Reports*, January 2019.

## CURRICULUM VITAE

Author's Name	Mr. Supachard Krudtong
Place of Birth	Chiang Mai, Thailand
Education	2014 Master of Science in Engineering (MSE), Minnesota State University, Mankato, Minnesota, USA. 2007 Master degree in Mechanical Engineering (M.Eng.), Chiang Mai University, Thailand. 2001 Bachelor degree in Agricultural Machinery Engineering (B.Eng.), Chiang Mai University, Thailand. 1996 High school diploma, Montfort College, Chiang Mai, Thailand.

ลิขสิทธิ์มหาวิทยาลัยเชียงใหม่  
Copyright© by Chiang Mai University  
All rights reserved